Aus dem Bereich Med. Physiologie

Theoretische Medizin und Biowissenschaften

der Medizinischen Fakultät

der Universität des Saarlandes, Homburg/Saar

Syntaxin11 serves as a t-SNARE for the final fusion step of lytic granules in human cytotoxic T lymphocytes

Dissertation zur Erlangung des Grades eines Doktors der Naturwissenschaften

der Medizinischen Fakultät

der UNIVERSITÄT DES SAARLANDES

2013

vorgelegt von: Mahantappa Halimani

geb.am: 01.06.1983 in Chinamagera, India

Tag des Promotionskolloquiums: _____

Dekan: _____

Vorsitzender: _____

Berichterstatter: _____

_____

_____

_____

To my beloved parents

ABBREVIATIONS

APC	Antigen presenting cell
BSA	Bovine serum albumin
CHS	Chediak-Higashi syndrome
CMP	Common myeloid progenitor
CLP	Common lymphoid progenitor
cSMAC	Central supra-molecular activation complex
CTL	Cytotoxic T lymphocyte
DCs	Dendritic cells
DEPC	Diethylpyrocarbonate
dNTPs	Deoxyribonucleotides
dSMAC	Distal supra-molecular activation complex
ELISA	Enzyme-linked immunosorbent assay
FCS	Fetal calf serum
FHL	Familial hemophagocytic lymphohistiocytosis
GFP	Green fluorescent protein
HBSS	Hank's balanced salt solution
HEPES	N-(2-hydroxyethyl)-piperazine-N'-2-ethanesulfonic acid,
HPS	Hermansky pudlak syndrome
HSCs	Hematopoietic stem cells
ICAM	Intracellular cellular adhesion molecules
ITAM	Immunoreceptor tyrosine-based activating motif
IS	Immunological synapse
LAMP	Lysosomal associated membrane protein
LDS	Lithium dodecyl sulphate
LFA-1	Lymphocyte function-associated antigen 1
LGs	Lytic granules
LRC	Leucocyte reduction chamber
LYST	Lysosomal trafficking regulator
MHC	Major histocompatibility complex

MTOC	Microtubule organizing center
PBMNCs	Peripheral blood mononuclear cells
PBS	Phosphate buffer saline
pSMAC	Peripheral supra-molecular activation complex
qRT-PCR	Quantitative real- time PCR
RNAi	RNA interference
SEA	Staphylococcal enterotoxin A
SNAP	Synaptosomal-associated protein
SNAREs	Soluble N-ethyl-maleimide-sensitive attachment protein receptor
STIM	Stromal interaction molecule
TCR	T-cell receptor
TFP	Teal fluorescent protein
TIRFM	Total internal reflection fluorescence microscope
TMD	Trans-membrane domain
UBC	Ubiquitin C
VAMP	Vesicle associated membrane protein
WAS	Wiskott aldrich syndrome

Acknowledgements

First and foremost, I would like to thank my supervisor Prof. Dr. Jens Rettig for his constant support, excellent guidance. Without his encouragement and consistent support and understanding, I would not have been able to complete my thesis. I would specially mention how he encouraged me during all ups and downs throughout my project, by taking his own examples. I would always be grateful to him for his constant advice regarding my scientific carrier.

I would also like to sincerely thank Prof. Dr. Markus Hoth for his valuable suggestion and inputs to improve my work. I extend my sincere thanks to Dr. Elmar Krause for helping me throughout my work. I also thank Dr. Varsha Pattu, for offering me great help, especially with my paper, thesis and presentations.

I would like to thank Dr. Ulf Matti for helping me with molecular biology, Dr. Ute Becherer and Hsin Fang Chang for TIRF analysis. I would like to thank Dr. Misty Marshall, Dr. Monika Maier-Peuschel, Quynh Nguyen Truong Cuc and Anneka Bost for their immense help for preparing talks and Ali Shaib for photoshop.

I would like to acknowledge members of Prof. Markus Hoth's lab, Dr. Eva C. Schwarz, Dr. Bin Qu, Christian Junker, Dr. Carsten Kummerow, Shruti Bhat for their valuable suggestions and assistance. I extend my sincere thanks to our lab members, Dr. David Stevens, Dr. Claudia Schirra, Prof. Olaf Pongs, Dr. Ulrike Hahn, Dr. Monika Dudenhöffer-Pfeifer, Dr. Sandra Hugo, Dr. Mathias Pasch, Lisa Weins, Moritz Ruben, Ming Min, Johannes Schneider and Hawraa Bzeih.

I would like to thank the graduate school GK-1326, Calcium-Signaling and Cellular Nanodomains, especially Prof. Dieter Bruns and Judith Wolf for financial support. I thank Anja Ludes, Katrin Sandmeier, Manuela Schneider, Anne Weinland, Margarete Klose, Reiko Trautmann and Caroline Bick for excellent technical help.

Lastly, I would like to thank my beloved family for their love and constant support. I also owe my sincere gratitude to all my friends, especially Jagdish Akki, Liza Swain, Rhisikesh Bergaje, Roshini Lakra and Soumyajit Dutta for always being there for me.

Zusammenfassung

In der vorliegenden Arbeit wird der molekulare Mechanismus der Fusion lytischer Granulen (LG) mit der Plasmamembran in cytotoxischen T Lymphocyten (CTL) untersucht. Im Speziellen habe ich mich mit der Funktion des SNARE-Proteins Syntaxin11 beschäftigt. Dazu wurde die Syntaxin11 Expression in humanen CTLs durch Transfektion einer spezifischen siRNA herunterreguliert. Anschließend wurde mit biochemischen, durchflusszytometrischen und mikroskopischen Techniken untersucht, welchen Einfluss die Entfernung von Syntaxin11 auf die Funktion der CTLs hatte.

In einem durchflusszytometrischen Degranulationsassay konnte ich zeigen, dass die Exozytose von Lysosomen, wovon LG eine Subpopulation sind, stark reduziert war. Außerdem konnte mit TIRFM nachgewiesen werden, dass die Verweilzeit (dwell time) von LG an der Immunologischen Synapse (IS) verlängert und die Zahl der Fusionsereignisse reduziert ist. Passend zu diesen Beobachtungen zeigte ein Zytotoxizitätsassay eine starke Beeinträchtigung der siRNA behandelten CTLs in ihrer Fähigkeit, Zielzellen zu töten. Zusammenfassend zeigen diese Experimente, dass siRNA behandelte humane CTLs einen Zytotoxizitäts-Defekt besitzen und sich phänotypisch wie CTLs aus Patienten verhalten, die an einer erblichen immunologischen Erkrankung leiden, bei der das Syntaxin11 Gen mutiert ist (FHL-4).

Um die zellbiologischen Prozesse zu identifizieren, an denen Syntaxin11 beteiligt ist und die zu dem beschriebenen Zytotoxizitäts-Defekt führen, wurden mikroskopische (Co-) lokalisationsstudien durchgeführt. Es zeigte sich, dass Syntaxin11 zusammen mit recycling TCR und Rab11a in sogenannten Recycling-Endosomen auftritt, aber nicht in den LGs selbst vorkommt. Diese Beobachtung führte zu der Hypothese, dass Syntaxin11 bei der Etablierung der IS möglicherweise über Recycling-Endosomen an die Plasmamembran transportiert wird und nach Fusion als Target-SNARE für LGs dient. Zur Überprüfung dieser Hypothese wurde die Etablierung der IS in lebenden Zellen, bei denen sowohl die LGs als auch die Recycling-Endosomen markiert waren, mikroskopisch beobachtet. Es konnte eindeutig die erwartete zeitliche Abfolge von Ereignissen gefunden werden. Nachdem die CTLs Kontakt mit ihren Zielzellen aufgenommen hatte, wanderten zunächst die Syntaxin11 tragenden Vesikel an die Membran. Erst nachfolgend trafen die LGs ein. Diese Beobachtungen wurden mit

TIRFM bestätigt. Auch mit dieser Technik konnte zunächst das Eintreffen der Syntaxin11 tragenden Vesikel an der IS gezeigt werden. Erst später trafen die LGs ein. Wir interpretieren dese Daten in der Weise, dass der Aufbau der IS zunächst durch den Antransport von Syntaxin11 und möglicherweise weiterer molekularer Komponenten durch Recycling-Endosomen erfolgt. Erst nachdem die molekularen Komponenten eingetroffen sind, werden die LGs antransportiert und können fusionieren. Syntaxin11 ist dabei wahrscheinlich das Target-SNARE für die Fusion von LGs. Anders als in der verfügbaren Literatur vorgeschlagen, gehen wir nicht davon aus, das Syntaxin11 bei der Reifung von LGs eine Rolle spielt, da LGs nicht mit Syntaxin11 kolokalisiert sind und, wie in der vorliegenden Arbeit auch gezeigt, die Gesamtzahl der LGs in einer CTL und an der IS nicht von Syntaxin11 abhängig ist. Allein der Fusionsprozess ist Syntaxin11 abhängig.

Die vorliegende Arbeit beschreibt erstmals einen exozytotischen Weg in CTLs der Bausteine der IS transportiert. Dieser Weg ist unabhängig von Reifung und Transport der LGs selbst, ist aber eine Voraussetzung für deren Fusion. Diese Daten tragen zum Verständnis der cytotoxischen Funktion von CTLs bei und helfen, das pathophysiologische Geschehen bei FHL-4 besser zu verstehen.

1. INTRODUCTION

1.1 Human cell defense systems – the immune system

The immune system functions to protect our body from bacteria, viruses, fungi and parasites, collectively known as pathogens, as well as environmental pollutants. The immune system provides three lines of defense that are dependent upon severity of the infection. The first line of defense includes non-specific barriers, such as physical and chemical barriers. The second line of defense consists of polymorphonuclear (granulocytes) and mononuclear (agranulocytes) leukocytes. Granulocytes include neutrophils for phagocytosis, eosinophils for destruction of parasitic worms and antigen-antibody complexes and basophils which release heparin and histamine. Furthermore, monocytes are later converted into macrophages in various tissues. Agranulocytes include B and T lymphocytes which mediate antigen-specific immune responses. (Abbas, 2007; Goldsby, 2000).

1.2 Innate and adaptive immune systems

The innate immune system provides non-specific immune responses which occur rapidly and do not confer the long term protection. In contrast, the adaptive immune system responses are both specific and long lasting. In vertebrates, this provides the immune system with the ability to specifically recognize and remember a pathogen, allowing a more rapid and robust response if the pathogen is encountered again. Hence the name adaptive since the body adapts after challenge. Recent advances in basic immunology provide more evidence for extensive interdependence and cross-talk between the innate and adaptive immune systems, which provides more stable and constant protection from foreign pathogens (Eisenbarth and Flavell, 2009; Tipping, 2006).

1.3 Development and differentiation of immune cell lineages

Immune cells originate in bone marrow from $CD34^+$ hematopoietic stem cells (HSCs) and differentiate based on requirements of the immune system and the availability of specific growth factors for differentiation. The turnover of the cells of the hematopoietic system in a man weighing 70 kg can be estimated to be approximately 1 trillion cells per
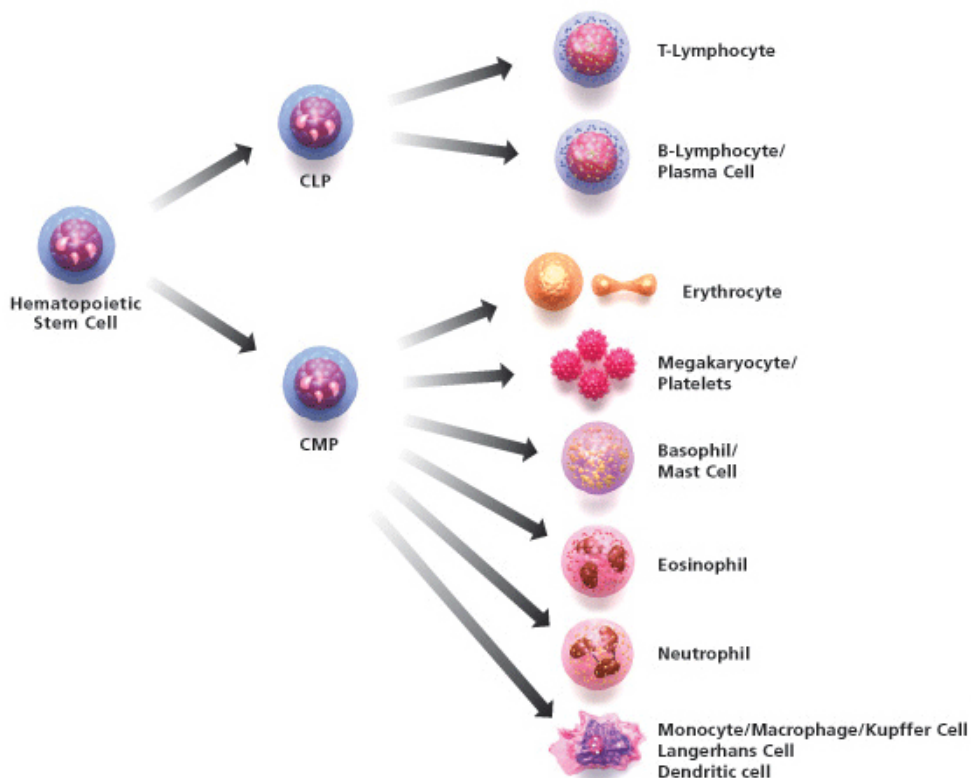
Figure 1: Differentiation of T lymphocytes from progenitor stem cell

Differentiation of hematopoietic progenitor stem cells into all other blood cell types from common lymphoid progenitor cells (CLP) and common myeloid progenitor cells (CMP). CLP cells differentiate into T and B lymphocytes and CMP cells differentiate into erythrocytes, platelets, basophils or mast cells, eosinophils, neutrophils, monocytes and macrophages (Ref: figure modified from Stem cell resources, Sigma Aldrich).

day, including 200 billion erythrocytes and 70 billion neutrophilic leukocytes. This remarkable cell renewal process is supported by a small population of bone marrow cells termed as hematopoietic stem cells (Ogawa, 1993). The process of hematopoiesis is the production of blood cells from HSCs in the presence of growth factors and cytokines like G-CSF, GM-CSF, M-CSF, IL-1, 6, 7, 8, 10, 11, SCF, LIF, MP 1α, β, TGF-β and TNF- α, etc., as depicted in a hierarchical fashion (Figure 1). HSCs first give rise to the two progenitors, the common myeloid progenitor (CMP) and the common lymphoid progenitor (CLP). CMPs produce erythrocytes, thrombocytes, neutrophils, monocyte/macrophages, eosinophil, basophils and mast cells, whereas CLPs generate

B cells, NK cells and T cells (CD4$^+$ and CD8$^+$). A flow chart for differentiation of the HSC into different lineages is depicted in figure 1 (Orkin, 2000).

1.4 Lymphocytes

Lymphocytes consist mainly of T cells, B cells and NK-cells. T lymphocytes and B lymphocytes are the major cellular components of the adaptive immune system where T lymphocytes function in cell mediated immunity and B lymphocytes contribute to humoral immunity. The interaction between T lymphocytes and antigen presenting cells (APCs) is the basis of the adaptive immune system (Goldsby, 2000). Unlike T cells and B cells, NK cells are critical to the innate immune system and consist of large, granular lymphocytes that do not express the same set of surface markers as B or T cells. Naïve T and B lymphocytes are small (Bromley and Dustin, 2002). But once they are exposed to an antigen, they proliferate, producing blasts called lymphoblasts. These cells have a higher cytoplasm to nucleus ratio and more organellar complexity than naïve lymphocytes. Lymphoblasts ultimately proliferate and become effector cells or memory cells. Effector cells consist of two types of cells, T helper cells (CD4$^+$) and cytotoxic T lymphocytes (CTLs/CD8$^+$).

1.4.1 Early activation

CD8$^+$ cells mature and migrate from the thymus to the lymph nodes, where they recognize specific antigen presenting cells (APCs) via T cell receptors (TCRs) and major histocompatibility complexes (MHC) that are found on the surface of APCs such as dendritic cells (DCs), macrophages and B cells (Gay, 1987). T cell and DC interactions have three different phases. The first step of T cell activation occurs in the thymus, where T cells and DCs engage in an initial recognition and conjugation lasting for 8 hours (h). This interaction results in several short encounters between migratory T cells and DCs, which are independent of antigen interactions and contribute to the maintenance of the T cell repertoire in the absence of T cell activation (Tanchot, 1995). Specific recognition of DCs by naïve T cells via the MHC molecules results in a mature synapse that lasts for 30 min (Huppa and Davis, 2003) and leads to the expression of the early activation markers CD44 and CD69. The second phase of naïve T cell

activation lasts ~ 24 h after T cell migration and is associated with upregulation of the surface marker for the IL-2 receptor (CD25), considered as an activation marker for lymphocytes. Prolonged stable contact between lymphocytes and DCs in the thymus elicits an increase in CD8 clusters on the surface of lymphocytes in contact with the DCs, indicating the final phase of T cell activation, the establishment of a mature synapse through MHC:TCR mediated signaling (Hurez et al., 2003; Bousso, 2004).

1.4.2 Naïve to activated cytotoxic T lymphocytes (CTLs)

The naïve T cell pool is not stable in number, diversity or function in the absence of a strong stimulus, in contrast to the maintenance of the T cell repertoire in the absence of activation. Mature naïve T cells can survive for many days without proliferation, after they migrate from thymus. In order to recognize a variety of foreign antigens, naïve T cells maintain a large number of clones with unique receptors within the thymus. Hence, not only the numbers but also the diversity and functional competence of the naïve T cell population must be maintained. The signals for naïve T cell homeostasis involve T cell receptor (TCR) engagement using self-peptide-MHC complexes and interleukin-7 receptor (IL-7R) stimulation by IL-7 (Takada and Jameson, 2009). During the initial and late activation of naïve T cells, they undergo drastic rearrangements of their molecular and cellular components in order to reach an activated state. CD3 molecules play an important role in this process by initiating calcium signaling, which ultimately results in the activation of a complex signaling pathway allowing naïve T cells to become CTLs (killing competent). TCR recognition, followed by downstream calcium signaling, which includes key components like Src kinases, ITAMs, ZAP-70, PLCγ, IP3 and DAG in association with STIM/ORAI calcium channels, lead to the T cell activation (Garvin et al., 2009; Kummerow et al., 2009). Activated T cells are now capable of conjugating with specific target cells through TCR-CD3 molecules and establishing a firm contact zone called the Immunological synapse (IS). During this time, the cell is actively producing the components required for the killing process. There are two independent pathways which lead to target cell death; the first one is calcium dependent, in which cytotoxic granules are required for lytic function (Becherer et al., 2012); The second one is calcium independent and involves components of the FAS ligand signaling (CD95; a

member of the tumor-necrosis factor receptor family of death receptors) pathway and does not require perforin (Helgason et al., 1992; Barry and Bleackley, 2002).

1.5 Cytotoxic T lymphocytes

Naïve CD8$^+$ T cells acquire killing competence after activation by producing the lytic substances required for killing. Three important aspects of the conversion from naïve to activated CTLs include; IL-2 expression or IL-2 receptor expression, proliferation and the gain of cytotoxic ability. In the case of CD4$^+$ cells, only Th1 (T helper cell subset 1) cells are cytotoxic (Hahn et al., 1995). After activation, naïve CD4$^+$ T cells undergo vigorous clonal expansion and differentiation. This massive proliferative response, accompanied by clonal selection for the immune function of CD4$^+$ T cells in the periphery, allows CD4$^+$ cells to differentiate into mature T$_H$1, T$_H$2 or T$_H$17 cells (Reiner, 2009). These T$_H$-subsets help other immune cells to activate, providing them direction by engaging in B cell antibody class switching, the activation and growth of CTLs and the activation of macrophages to fight against bacterial infection.

After antigen-specific recognition, the integrin receptor LFA-1 on the CTL membrane binds to ICAMs on the target cell membrane, resulting in the formation of a conjugate. Antigen-mediated CTL activation converts LFA-1 from a low-avidity state to a high-avidity state. Because of this phenomenon, CTLs adhere to and form conjugates only with specific target cells that display the antigenic MHC complex. CTLs then engage in TCR/CD3 mediated recognition of target cells followed by sequential induction of calcium signaling that leads to polarization of CTL towards its target cell. Initially, CTLs crawl and move in search of an APC with the help of flagella like structures called uropods (Fais and Malorni, 2003). These uropods enable CTLs to move and sense the presence of MHC class I molecules with an antigenic peptide on the surface of APCs. Stable IS formation depends on the strength of TCR accumulation. This TCR signaling strength also influences target cell death, as TCR signaling controls centrosome polarization to the cSMAC followed by delivery of LGs (Jenkins et al., 2009; Krammer, 2000; Peter and Krammert, 1998). TCR dependent stable IS formation results in killing of the target cell through three pathways. Killing occurs by lytic granule release (O'Keefe and Gajewski, 2005), cytokine release (Andersen et al., 2006) and Fas ligand mediated apoptosis (Nagata, 1996). Nevertheless, one major disadvantage of active CTL function

is an autoimmune disease (Section 1.8) in which CTLs recognize the organisms own (self)-cells as a target cell and destroy these cells or tissues, ultimately resulting in death. Hence, the alternate description of CTL function is that 'all roads lead to death' (Barry and Bleackley, 2002).

1.6 Immunological synapse (IS)

As a result of CTL recognition of target cells harboring a cognate MHC-bound peptide antigen, a dynamic reorganization of membrane and cytosolic molecules occurs at the CTL-APC contact zone. This interaction results in the formation of a stable and highly organized IS, where the CTL prepares a zone of close contact with the target cell for release of its cytotoxic components to kill the target cell. The term 'synapse', which means junction, was initially used for neuronal connections. The term 'immune synapse' was first proposed by Norcross and Paul to describe the CTL-APC conjugation. CTL and NK cell synapses have a high degree of similarity. However, NK cells actively secrete LGs without having APC contact, unlike CTLs which synthesize LGs only after APC interaction (Huppa and Davis, 2003; Finetti et al., 2009). IS formation is a dynamic process that includes the rearrangement and polarization of components within CTL towards the contact zone with the target cell. Signaling molecules of IS formation include the TCR/CD3 complexes (cSMAC), which induce downstream calcium signaling and involve PKC-θ. Activation of this pathway is rapidly followed by migration of cell adhesion molecules such as ICAMs, LFA1 (pSMAC) and the cytoskeleton linker talin, along with CD43 and CD45 (dSMAC) as depicted in figure 2 (Delon et al., 2001). The process of mature synapse formation is divided into three major steps which include several smaller steps (Orange, 2008). Briefly, the initial stage is the recognition of membrane bound receptors that lead to cell to cell interaction and anchor the CTL to its target cell. This step depends on cell adhesion molecules which establish a firm contact zone that causes the CTL to stop migrating, allowing it to form an increasingly stable contact with the target cell. The next step is the effector stage that occurs after a stable IS has formed, creating the interface between CTLs and target cells to which lytic granules are recruited.
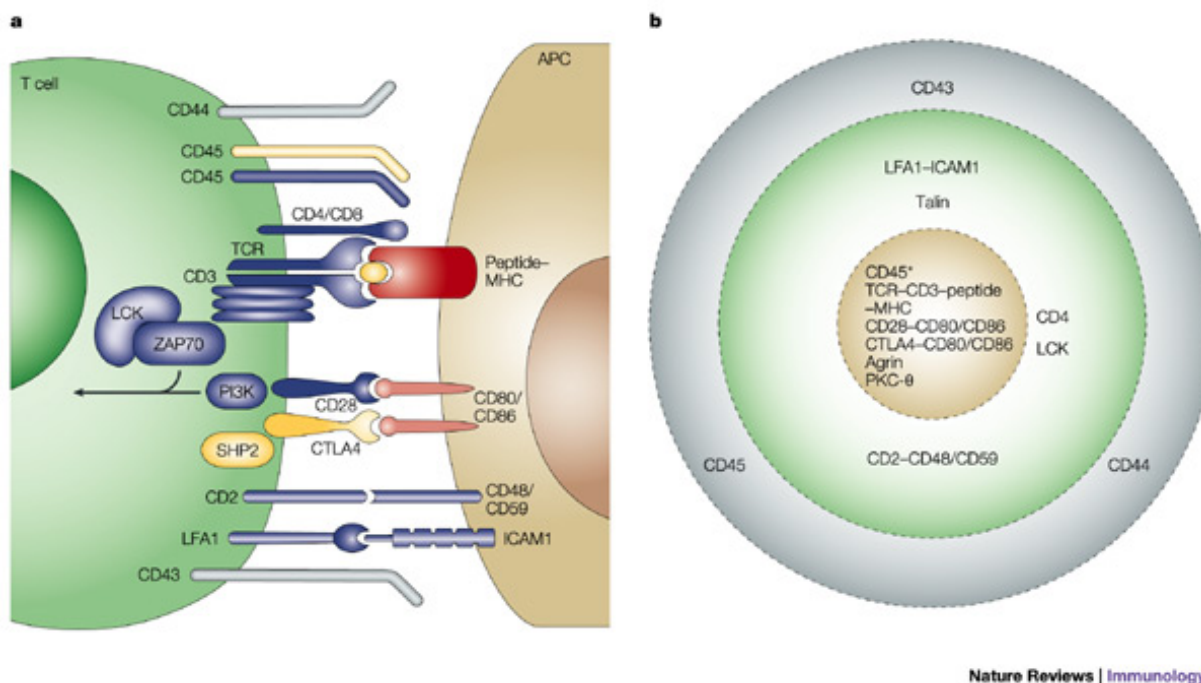
Nature Reviews | Immunology

Figure 2: Cell to cell contact zone for lytic granule release: The immunological synapse
(a) TCR/CD3 complexes and the MHC-I complex mediate conjugation between effector cells (T cell) and target cells
(APC) leading to formation of a mature synapse (the IS) for release of lytic components into the target cell cleft. (b)
Organization of a mature synapse showing the central, peripheral and distal rings of its components (Huppa and
Davis, 2003).

LG maturation, polarization and fusion processes are tightly controlled by the MTOC
(microtubule organizing center) and SNARE proteins. The MTOC directed movement of
lytic granules is directly dependent on the motor function of dynein and kinesin-1. The
mature synapse required for LG arrival and fusion includes several complexes that form
an association at the CTL:APC interface. Initial recognition and early events mainly
include CD8, along with TCR/CD3:MHC complex, CD44/45 and the LFA1:ICAM1
complexes that strengthen adhesion. Additionally, CD28 binds to CD48/59 on APCs
involved in stimulating IL-2 expression and production. CD2, in association with CD48,
supports adhesion as depicted in figure 2 (Mentlik et al., 2010; Stow et al., 2006). In the
final phase after the maturation of the synapse, recycling endosomes deliver key
components of vesicle fusion, such as priming factors, proteins that mediate docking
and various components of the fusion machinery soluble N-ethyl-maleimide-sensitive
attachment protein receptor (SNAREs), required for LG exocytosis (de Saint Basile et

al., 2010; Stow et al., 2006). After killing, the CTLA4 (CD-152):CD86 complex functions to aid the dissociation of the CTL:target cell complex.

1.7 Soluble N-ethyl-maleimide-sensitive attachment protein receptors (SNAREs)

SNARE proteins are the mediators of intracellular membrane fusion events and play a crucial role in exocytosis by allowing release of vesicular contents. Generally, trafficking is an exchange of materials between two intracellular compartments or the release of contents from a vesicle membrane to a target membrane (Chen and Scheller, 2001; Jahn et al., 2003). The mechanism of SNAREs and SNARE associated proteins are well studied in neuronal synapses (Fasshauer et al., 1998a), neuroendocrine cells (Kesavan et al., 2007), cytotoxic T lymphocytes (Stow et al., 2006), pancreatic beta cells (Jewell et al., 2010), etc. SNAREs have a characteristic domain structure called the SNARE motif or the coiled-coil domain, containing an evolutionarily conserved stretch of 60–70 amino acids that are arranged in heptad repeats. Most of the SNARE proteins have single transmembrane domains at their C-terminus that connects to the SNARE motif by a short linker (Kesavan et al., 2007). These proteins also have N-terminal domains that vary between the subgroups of SNAREs. However, the current classifications of SNAREs are based on either their localization or composition. SNARE proteins are classified based on their localization to vesicular or target membrane, v-SNAREs for SNAREs associated with vesicles and t-SNAREs for those associated with target membranes (Sollner et al., 1993). However, these classifications were confusing when it comes to the homotypic fusion of vacuoles. Thus, an alternative classification has evolved which is based on the residue at the center of the zero ionic layers in the coiled-coil domain. R-SNAREs contain an arginine and Q-SNAREs contain a glutamine at this position. Q-SNAREs are farther divided into Qa, Qb and Qc SNAREs and a functional SNARE complex consists of a four helix from each Qa, Qb, Qc and R-SNARE (Fasshauer et al., 1998b). Together these four helices constitute a functionally stable SNARE complex that lowers the activation threshold for membrane fusion and induces fusion between vesicular and target membranes (Bock et al., 2001). The crystal structure of SNARE complexes revealed that a SNARE complex consists of four helical bundles and zero ionic layers which consists of leucine, isoleucine and valine residues in heptad repeats (Sutton et al., 1998). The glutamine residues from Syntaxins and

SNAPs and the arginine from VAMPs, forms a central ionic interaction layer (the zero layer) or hydrophobic core of the SNARE complex (Figure 3). Thus, four coiled-coil domains collectively create an electrostatic potential which results in membrane fusion. These SNARE complexes are thermally stable and can withstand temperatures up to 90°C (Hayashi et al., 1994). Following a successful fusion event, SNARE complexes are disassembled by *N*-ethylmaleimide-sensitive fusion protein (NSF) and alpha-SNAP proteins (Barnard et al., 1996).

Recent studies (Stow et al., 2006) have highlighted the importance of SNARE and SNARE associated proteins in membrane fusion and trafficking in almost all aspects of immune cells, including CTLs. A number of inherited diseases of the immune system in humans are associated with defective membrane fusion in immune cells. For example, mutations in Munc13-4 (Feldmann et al., 2003), Syntaxin11 (Bryceson et al., 2007) and Munc18-2 (zur Stadt et al., 2009) all result in an inheritable genetic defect called familial hemophagocytic lymphohistiocytosis (FHL).
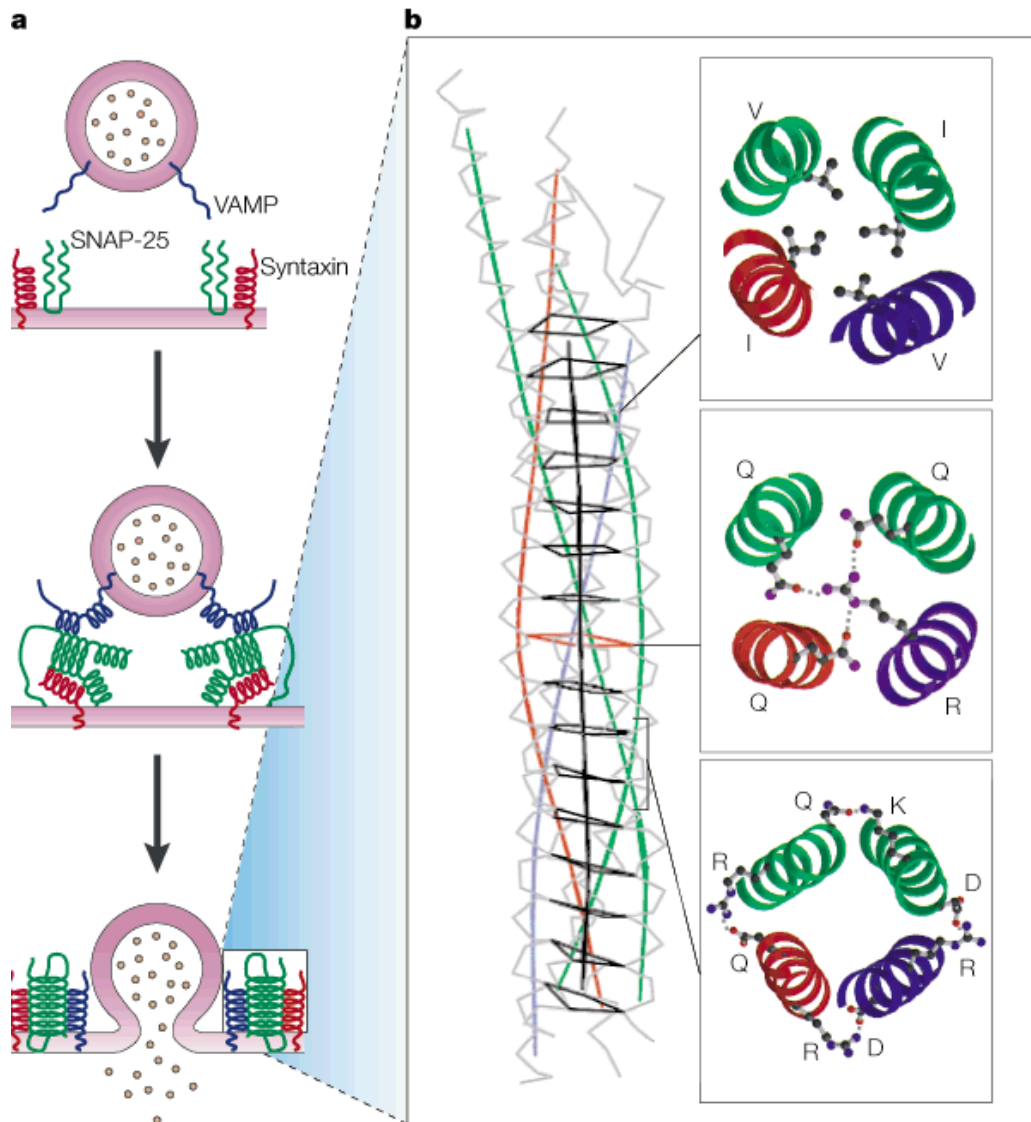
Nature Reviews | Molecular Cell Biology

Figure 3: SNARE proteins, regulators of membrane fusion

A model for zippering of four SNARE helices (a), v-SNARE protein VAMP (in blue) on the vesicle along with target SNAREs on the plasma membrane. The Qa-SNARE Syntaxin (in red) and Qbc SNARE, SNAP-25 (in green) before and after formation of the four-helix bundle, including the zero ionic layer. (b) The backbone of the SNARE complex with Q-SNAREs and R-SNAREs are characterized by a glutamine (Q) or arginine (R) residue, respectively, in the central layer of the SNARE complex (Chen and Scheller, 2001).

1.8 Genetic disorders associated with CTL function

There are several diseases associated with immune dysfunction which develop due to defective CTL function resulting in severe clinical manifestations. *Wiskott-Aldrich Syndrome* (WAS) is an immunodeficiency disease that originates from mutations in the gene encoding WASP (Wiskott-Aldrich syndrome protein), a key actin regulator of immune cells (Li et al., 2003). WAS deficient CTL cell lines show normal numbers of LGs and normal exocytosis. However, WAS CTLs also show clear defects in the polarization of LGs to the IS. *Hermansky-Pudlak syndrome* (HPS mutations in the paladin protein) is a genetically heterogeneous disorder characterized by oculocutaneous albinism, prolonged bleeding and pulmonary fibrosis due to abnormal vesicle trafficking of lysosomes and related organelles in melanosomes and of dense granules in platelets (Li et al., 2003). *Griscelli syndrome* is an autosomal recessive disorder resulting in albinism because of pigmentation loss in skin and hair, primarily due to vesicular trafficking defects in melanocytes (Schmid et al., 2008). Interestingly, mutations within the Rab27a gene are directly associated with Griscelli syndrome. Moreover, Rab27a deficient CTLs exhibit a hemophagocytic syndrome caused by defective CTL cytotoxicity and Rab27a knockout mice (ashen mice) display defects in the granule mediated killing pathway (Menasche et al., 2000).

Chediak–Higashi syndrome (CHS) is characterized by mutations in the lysosomal trafficking regulator protein (LYST) leading to a rare autosomal recessive defect associated with the CTL granule-mediated killing pathway. CHS is characterized in its classical form by albinism, a bleeding diathesis; infections mediated by defective neutrophil and natural killer cell function and an eventual progression to hemophagocytosis. CHS typically results in death due to infection (Baetz et al., 1995). Lastly, mutations in a transcript variant of VAMP8 gene which is involved in platelet degranulation is associated with early-onset myocardial infarction (Shiffman et al., 2006). In summary, SNAREs and SNARE associated proteins along with LYST and WASP proteins are required for normal LG fusion and defects in this pathway lead to a profound disturbances in lymphocyte homeostasis in humans.

1.8.1 Familial hemophagocytic lymphohistiocytosis

Familial hemophagocytic lymphohistiocytosis (FHL) is an autosomal recessive disorder featuring hyperactivated immune cells resulting from an excessive production of cytokines from CTLs. This excessive cytokine production leads to over activation of a variety of immune cells, such as macrophages, which then infiltrate into organs, causing organ failure and eventually death. Early symptoms include prolonged fever, hepatosplenomegaly, cytopenia and hyperferritinemia. Neurologic abnormalities include increased intracranial pressure, neck stiffness, irritability, cranial nerve palsies, ataxia, coma, blindness, hemiplegia, quadriplegia, rashes and lymphadenopathy (Henter et al., 1998; Janka, 2007). The average survival rate of children with typical FHL, if left untreated, is less than two months and the majority of deaths in untreated children are due to infection.

A mutation within the coding region of the *PRF-1* gene (Perforin: pore forming protein) was originally identified as the cause of FHL-2. Perforin is a key molecule in CTLs that functions at the IS to form pores on the target cell membrane, allowing the contents of LGs to enter the target cell in order to induce apoptosis. Mice lacking perforin show a reduced but not abolished killing activity of CTLs, even though perforin is crucial for effector T cell and NK cell mediated cytolysis (Lowin et al., 1994). Similarly, mutations within the coding region of human Munc13-4 cause FHL-3. The Munc13 protein family is a family of specialized proteins well studied as priming factors in neuronal synapses. Initially, there were only 3 recognized isoforms of Munc13s; Munc13-1, 2 and 3 (Brose et al., 1995). Deletion of these proteins leads to a complete loss of synaptic transmission. Munc13-2 is reported to be expressed in hippocampal synapses. A fourth member of the Munc13 family, Munc13-4, has recently generated interest due to its function in human CTLs. Mutations in the coding region of Munc13-4 are directly associated with FHL-3, a form of FHL which is fatal. Human Munc13-4 is localized to cytotoxic granules at the IS and its loss in humans (FHL-3 patients) leads to defective priming but not docking of secretory vesicles at the IS (Feldmann et al., 2003). Recently two more genes have been reported to have direct association with FHL, i.e. FHL-4 and FHL-5, which code the proteins Syntaxin11 and Munc18-2 respectively. However, the molecular mechanism behind these functional consequences is not clear.

1.9 Syntaxin11

Syntaxins have a carboxy-terminal transmembrane domain for membrane anchoring and a coiled-coil region for SNARE complex formation. 15 members of the human Syntaxin family members have been reported. Syntaxin1-4 are primarily present on the plasma membrane (Bennett et al., 1993); Syntaxin3 is involved in the regulation of apical membrane transport in epithelial cells (Riento et al., 1998); Syntaxin4 is localized to dendritic spines (Kennedy et al., 2010); Syntaxin5 and Syntaxin16 are on the Golgi apparatus (Bennett et al., 1993; Tang et al., 1998b); Syntaxin6, 10, 12 and 16 are distributed on the trans-Golgi apparatus (Wang et al., 2005); Syntaxin7 is localized to early endosomes (Pattu et al., 2011; Wong et al., 1998); Syntaxin17, 18 are present on ER-Golgi intermediate compartments (Hatsuzawa et al., 2000; Muppirala et al., 2011) and Syntaxin8 is localized to both early and late endosomes (Prekeris et al., 1999).

Syntaxin11 has an N-terminal Habc domain, followed by linker region connecting to coiled-coil domain. Unlike other Syntaxins, Syntaxin11 lacks a transmembrane domain (TMD) (Tang et al., 1998a), which is a characteristic feature of the Syntaxin family members. Not all SNARE proteins harbor TMD and some SNAREs such as neuronal SNAP-25 (Ravichandran et al., 1996) have a palmitoylation region allowing fatty acids such as palmitic acid to interact with cysteine residues allowing membrane association. The C-terminal carboxyl tail of Syntaxin11 has five cysteine residues enabling it to interact with plasma membrane via palmitoylation.

A wide variety of mutations in Syntaxin11 have been reported in patients suffering from FHL-4, which include complete loss of protein (Marsh et al., 2010), point mutations (Rudd et al., 2006), exon deletions (zur Stadt et al., 2005) and frame shift mutations (Macartney et al., 2011). *Stx11* gene mutations are reported to be independent of associated FHL subtypes i.e., FHL-2 and FHL-3.

It has been proposed that Syntaxin11 is the target SNARE for lytic granules (de Saint Basile et al., 2010; Hong, 2005). However several other predictions which are mainly based on the localization have been reported in a variety of cell types. Syntaxin11 is expressed in CTLs and NK cells and is localized to membrane-associated structures in the cytoplasm and is required for cytotoxic function (Arneson et al., 2007; Bryceson et al., 2007). In monocytes or macrophages, Syntaxin11 is required for platelet secretion (Ye et al., 2012). It is localized to the cation-dependent mannose-6-phosphate receptor

(M6PR) containing compartment and Rab27a positive vesicles and likely mediating the fusion of these vesicles with cytotoxic granules (Dabrazhynetskaya et al., 2012). Syntaxin11 interacts with Vti1b and mediates fusion between late endosomes and lysosomes in macrophages (Offenhauser et al., 2011). Furthermore, it is localized to the TGN (Trans-Golgi network) and late endosomes in HeLa cells (Valdez et al., 1999), TGN and cis-Golgi complex (Prekeris et al., 2000), distinct cytoplasmic granules in neutrophils (Xie et al., 2009), growth hormone (GH) containing granules in GH producing cell line MtT/S cells (Kawashima et al., 2010), post-Golgi complex in normal rat kidney cells (NRK cells) (Advani et al., 1998) and the plasma membrane in macrophages and many other cell types (Zhang et al., 2008).

Cognate interacting partners for Syntaxin11 were also suggested based on in-vivo, in-vitro studies and based on its localization. In HeLa cells and B lymphocytes, it is associated with VAMP and SNAP-25 on late endosomes (Valdez et al., 1999). Recently, two independent groups have identified mutations within gene encoding for Munc18-2, proposed to be a close interacting partner for Syntaxin11, as another cause of FHL, FHL-5. Moreover, interaction studies with mutant forms of Munc18-2, result in reduced steady state levels of endogenous Syntaxin11 protein, causing a severe defect in secretion of LGs (Cote et al., 2009; Lopez and Voskoboinik, 2013; zur Stadt et al., 2009).

1.10 Aim of the work

Cellular trafficking is the fundamental process underlying all the subcellular and intercellular exchange of material. For instance, proteins produced by de-novo synthesis leave the ER for further processing in the Golgi apparatus. Many of these proteins will be inserted into lipid membrane bound organelles which are then transported actively to their target regions. Cell membrane targeted protein will reach the membrane via fusion of their transport organelle with the cell membrane. This final fusion step is mediated by SNARE proteins, as are all membrane fusion processes in cells. Cytotoxic T lymphocytes are not an exception and SNARE proteins have been extensively studied as major regulators of CTL function. The killing function of CTL involves several processes that include intercellular interactions, one of which is the formation of the functional IS. The release of lytic granules via exocytosis to specific target cells also requires SNARE complex driven fusion. Mutations in many of the candidate genes or proteins, for example *PRF1* (FHL-2), *Munc13-4* (FHL-3), *Stx11* (FHL-4), *Stxbp2* (FHL-5), *Rab27a* (GS) etc., involved in this highly orchestrated pathway lead to severe consequences including death.

The specific contributions of modulatory proteins such as Munc13-4 and Rab27a to lytic granule fusion have been studied and are well understood. However, the contributions of some of the other players, such as Syntaxin11 and Munc18-2, need to be elucidated. The complete cataloging of the cognate SNARE partners and the key SNARE modulatory proteins required for the final fusion of lytic granules is required to understand the underlying molecular mechanism behind the CTL mediated target cell killing process.

In this study, our aim is to understand the importance of SNARE proteins for the final fusion of lytic granules at the IS. Syntaxin11, a Qa-SNARE is implicated in the release of lytic granules. However, its precise role has not been characterized in FHL-4 patients in whom Syntaxin11 function is lacking. CTLs and NK cells show a severe defect in LAMP1a positive vesicle degranulation, an indirect measure of LG exocytosis. We aim to provide a detailed functional analysis of Syntaxin11 in human CTL.

2. MATERIALS AND METHODS

2.1 Materials

2.1.1 Reagents

Agarose	Roth
Bovine serum albumin (BSA)	Sigma
Chloroform	Roth
Diethylpyrocarbonate (DEPC)	Sigma
Dithiothreitol (DTT)	Sigma
ECL reagent	GE Healthcare
EDTA (Ethylene diamine tetra-acetate)	Sigma
Ethanol	Roth
Ethidium Bromide	Life technologies
Fetal Calf Serum (FCS)	Life technologies
Formaldehyde (16%)	Polysciences
Glucose	Merck
Glycine	Roth
H_2O	Sigma
Nitrocellulose membrane	Roth
Phosphate Buffered Saline (PBS)	GIBCO
Propanol	Roth
Skimmed milk powder	Roth
TritonX100	Roth
Tween20	Roth
TRIzol® reagent	Life technologies

All other chemicals, if not specified otherwise, obtained were from Sigma.

2.1.2 Plasmids

Plasmid coding for pmTFP-N1 (Teal fluorescence protein), pmTFP-C1 and pmCherry-N1 and pmCherry-C1 were generated by replacing GFP in pEGFP-C1 and pEGFP-N1 clones (Clontech) with mTFP (Allele Biotech) and mCherry (gift from Roger Tsien) using *Age I* and *Bgl II* restriction digest sites.

Syntaxin11 was amplified using cDNA obtained from human CTLs with following primers: 5'-TAT AAA GCT TCC ATG AAA GAC CGG CTA GCA GAA and 5'-TAT AGG ATC CCT ACT TGA GGC AGG GAC AGC A to add *Hind III* and *BamH I* restriction sites. After digestion with *Hind III* and *BamH I*, Syntaxin11 was ligated to vectors containing the fluorescent tags GFP- C1, TFP-C1 and mCherry-C1 at the N terminal end of Syntaxin11.

Rab11a was amplified using cDNA obtained from CTLs, using primers 5'-TAT ATG AAT TCT ATG GGC ACC CGC GAC GAC and 5'-TAT ATA GGA TCC TTA GAT GTT CTG ACA GCA CTG to add *EcoR I* and *BamH I* restriction sites at each end. After digestion with *EcoR I* and *BamH I*, Rab11a was ligated to vectors containing fluorescent tags GFP- C1 and mCherry-C1 at the N-terminal end of Rab11a.

Granzyme B was amplified using cDNA obtained from human CTLs, using the primers: 5' TAT ACT CGA GCC ACC ATG CAA CCA ATC CTG CTT CTG and 5' ATA TAT CCG CGG GTA GCG TTT CAT GGT TTT CTT T to add *Xho I* and *Sac II* restriction sites. After digestion with *Xho I* and *Sac II*, Granzyme B was ligated to vectors containing the fluorescent tags, TFP-N1 and mCherry-N1 at the C-terminal end of Granzyme B. CD3e (epsilon) was amplified by PCR from clone NM_000733 (Origene technologies) with forward primer 5'-TAT AAA GCT TCC ACC ATG CAG TCG GGC ACT CAC TG-3' and reverse primer 5'-TAT AGG ATC CCC GAT GCG TCT CTG ATT CAG GC-3' to remove the stop codon and then ligated to both TFP-N1 and mCherry-N. All constructs used in this study were sequenced and their specificity confirmed either with a specific antibody or upregulation upon transfection using quantitative real-time PCR (qRT-PCR).

The siRNAs specific to Syntaxin11 were purchased from Qiagen. Sequences for all siRNAs are given below. Control siRNA: UUC UCC GAA CGU GUC ACG U, Syntaxin11 siRNA 1: CCA GGU UCA AGA AUU GCA A, Syntaxin11 siRNA 2: CAC UCA AAU UGA AGU AUC A. Syntaxin11 siRNA 6: GCA UCA AGC GCG ACA CCA A. For TIRFM and degranulation assay, CD8$^+$ cells were stimulated with anti-CD3/CD28 ab

coated beads for 48 h and then transfected using a nucleofector kit (LONZA) with both control and Syntaxin11 specific siRNAs (20 μM) along with a marker of lytic granule. Cells were washed 12 h after transfection and replaced with fresh AIMV supplemented with 10% FCS medium containing no IL-2. Cells were used for experiments 36 h after siRNA transfection. Syntaxin11 knock down was verified using qRT-PCR and immunoblotting.

2.1.3 Media and solutions

2.1.3.1 Solutions for CTL preparation

- Ficoll
- Hank's Balanced Salt Solution (HBSS)
- Erythrocyte lysis buffer:

    155 mM NH_4Cl

    10 mM $KHCO_3$

    0.1 mM EDTA

    pH 7.3

- Buffer 1: PBS (GIBCO) supplemented with 0.5% BSA
- Buffer 2: RPMI medium (Life technologies) with 0.1% FCS
- AIMV medium supplemented with 10% FCS (Life technologies)

2.1.3.2 Solutions for TIRFM experiments

10 mM extracellular Calcium solution	0 mM extracellular Calcium solution
140 mM NaCl	140 mM NaCl
4.5 mM KCl	4.5 mM KCl
5 mM HEPES	5 mM HEPES
2 mM $MgCl_2$	2 mM $MgCl_2$
10 mM $CaCl_2$	pH: 7.4 and Osmolarity:
pH: 7.4 and Osmolarity: 300-310 mOsm.	300-310 mOsm.

2.1.3.2 Solutions for ELISA

Coating buffer:

100 mM - Na_2CO_3

100 mM - $NaHCO_3$

Bring the volume to 1 L with distilled water (pH 9.6).

Blocking solution:

5x Assay diluent buffer (Biolegend: 421203) diluted to 1x with PBS before use.

Wash solution:

PBS + 0.05% (v/v) Tween20 (TBST).

Stop solution:

2N H_2SO_4

Substrate: 3.3' 5.5' Tetramethylbenzidine (TMB) (Sigma: T0440).

2.2 Methods

2.2.1 Peripheral blood mononuclear cell (PBMNCs) isolation

The starting material for the isolation of PBMNCs was leukocyte reduction chambers (LRCs) containing whole blood obtained from the clinic of the Department of Haematology and Transfusion medicine, University of Saarland. All isolation steps were carried out at room temperature (RT). 15-17 ml of Ficoll was added to special leukocyte separation tubes and the tubes were spun at 1000 g for 30 s. Shown in figure 4 is a picture of the cone shaped LRC containing blood from a healthy donor. The hose was cut at the two points marked by 1 and 2 in figure 4a using sterile scissors cleaned with 70% ethanol. First, the lower hose was cut and made to point to the inside of the leukocyte separation tube as shown in figure 4. Then the top tube was cut to allow the flow of blood through the cone. A 20 ml syringe containing HBSS was used to rinse the cone into the LRC as shown in figure 4b.
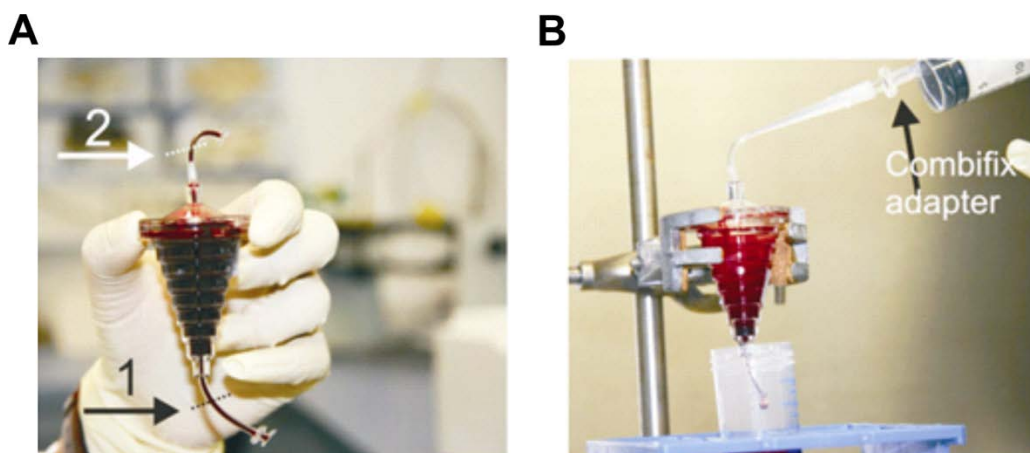
Figure 4: Isolation of PBMNCs

Shown above is the cone shaped leukocyte reduction chambers used for PBMNCs isolation. See text for details.

The leukocyte separation tubes were then spun at 450 g for 30 min at RT without any brake or special settings. The leukocyte containing ring that was obtained after centrifugation was removed carefully with a 5 ml pipette and transferred to a 50 ml tube and then filled with HBSS. This step was followed by centrifugation at 250 g for 15 min at RT. The red pellet obtained after centrifugation was resuspended in 1-3 ml erythrocyte lysis buffer (Section 2.1.3.1) for the erythrocyte lysis process. After 60-120

s, 50 ml of HBSS was added to the pellet to stop the lysis process and the tubes were spun at 200 g for 10 min.

The white pellet obtained was devoid of erythrocytes and was resuspended in 20 ml of cold PBS containing 0.5 % BSA. A small amount of cells were taken to make a 1:10 dilution in PBS. Trypan blue staining was used to assess the viability of purified PBMNCs before using them for isolation of naïve CD8$^+$ T cells or for stimulation with Staphylococcal enterotoxin A (SEA).

2.2.2 Isolation of CD8$^+$ cells

2.2.2.1 Positive isolation

CD8$^+$ T cells were positively isolated from PBMNCs using a CD8 positive cell isolation kit (Life technologies). PBMNCs were resuspended at a concentration of 10x10^6 cells/ml in a Ca^{2+} and Mg^{2+} free phosphate buffer (supplemented with 0.1% BSA and 2 mM EDTA), along with 25 µl of prewashed beads per 10x10^6 cells. Suspended PBMNCs and dynabeads were subjected to constant rotation at 4°C for 20 min in order to bind CD8$^+$ cells to the beads. Using a magnet, all the beads were collected and rest of the unbound cells were discarded to obtain a pure population of CD8$^+$ cells. Bead bound cells were resuspended in RPMI with 1% FCS in a ratio of 250x10^6 beads per ml of RPMI along with the detach beads solution provided in the kit (100 µl/ml of RPMI). Bead bound cells were allowed to rotate constantly for 45 min at RT and then beads were separated from cells by using the magnet. The supernatant contained the positively isolated naïve CD8$^+$ T cells. The cells were stained with trypan blue to assess the viability of purified CD8$^+$ T cells. Cells were then centrifuged at 200 g for 5 min at RT and the pellet was resuspended in, pre-warmed AIMV medium containing 10% FCS with 100 U/ml of IL-2 at a density of 1.5x10^6 cells/ml.

2.2.2.2 Negative isolation

Naïve CD8$^+$ T cells were negatively isolated from PBMNCs with a CD8 negative isolation kit (Life technologies) as depicted in figure 5. The percentage of CD8$^+$ T cells obtained by this method from PBMNCs was approximately 10-15% and the initial number of PBMNCs for all the isolations varied according to the number of CD8$^+$ T cells

required. PBMNCs were resuspended at a concentration of 100×10^6 cells/ml in a Ca^{2+} and Mg^{2+} free phosphate buffer (supplemented with 0.1% BSA and 2 mM EDTA), as the starting material for the negative isolation. Heat inactivated FCS and the antibody mix that was provided in the kit were mixed in a 1:1 ratio and added to the PBMNCs for incubation at 4°C by gentle rotation for 20 min. The volume of the antibody mix was 20 µl per the starting material of 100×10^6 PBMNCs. For isolating from a large volume of PBMNCs the volumes of all the reagents were scaled accordingly for every step of the isolation. The cells were then washed by adding 2 ml of the isolation buffer and centrifuged at 300 g for 8 min at 4°C. The pellet was resuspended in 800 µl of the isolation buffer and then 200 µl of the pre-washed depletion dynabeads (supplied in the kit) were added. For prewashing, 200 µl of the depletion dynabeads were transferred to a fresh tube and the same volume of isolation buffer, or at least 1 ml, was added and mixed. The tube was placed in a magnet for 1 min and then the supernatant was discarded. The beads were then resuspended in 200 µl of isolation buffer. Subsequently, the cells and beads were mixed and incubated for 15 min at 18-25°C by gentle tilting and rotation. The tube was then placed in the magnet for 2 min. The supernatant contained the negatively isolated naïve $CD8^+$ T cells and was transferred to a new tube. The cells were stained with trypan blue to assess the viability of the purified $CD8^+$ T cells. Cells were centrifuged at 200 g for 5 min at RT and the pellet was resuspended in pre-warmed AIMV medium (Life technologies) containing 10% FCS at a density of 3×10^6 cells/ml.

Add Fetal Calf Serum and antibody mix to PBMNCs

Mix and incubate for 20 min at 2-8°C

Wash cells and add depletion Dynabeads

Incubate for 15 min at 18-25°C

Resuspend and increase volume

Place in magnet for 2 min

Transfer supernatant to fresh tube

Discard beads with unwanted cells

Pure and untouched target cells
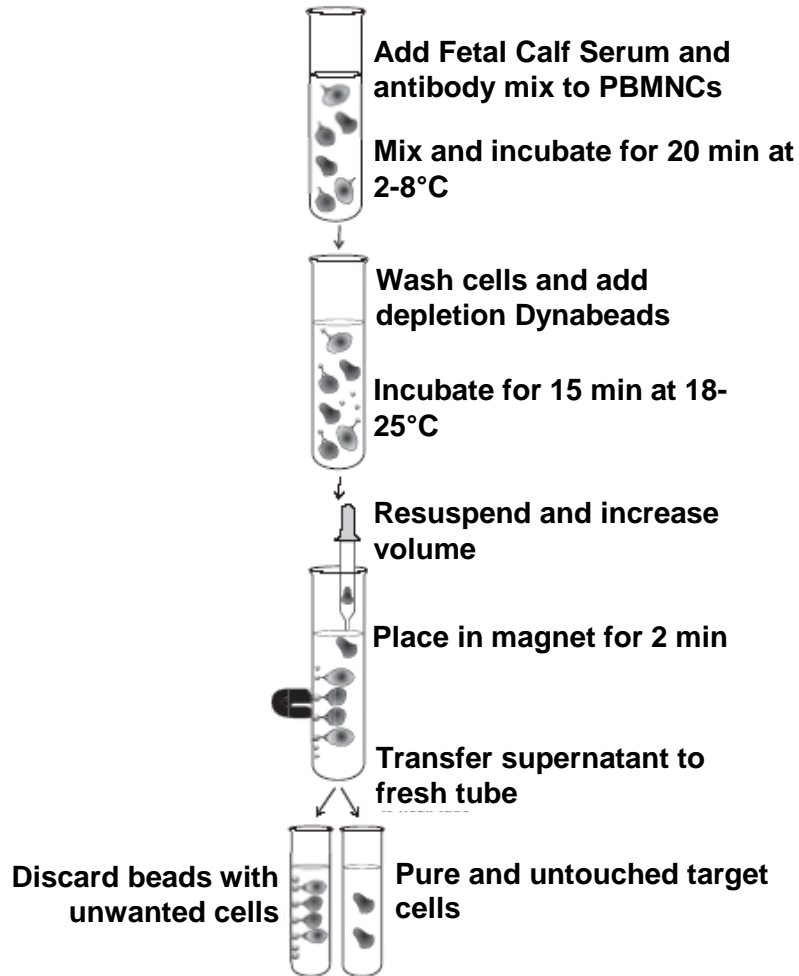
Figure 5: Schematic outline of the negative isolation of naïve CD8+ T cells

The isolation of naïve CD8+ T cells from PBMNCs using dynabeads (See text for details).

2.2.3 Activation of naïve to effector cells (CTLs)

2.2.3.1 Activation using anti-CD3/CD28 antibody (ab) coated beads

CD8+ T cells after positive/negative isolation were activated using CD3/CD28 T cell expander beads (Life technologies) at a 1:0.7 ratio. The appropriate volume of expander beads were prewashed and suspended in initial volume of buffer 1 (PBS supplemented with 0.1% BSA, pH 7.4). The beads were then added to the cells and plated at a concentration of 2×10^6 cells/ml for 3 days in AIMV medium with 10% FCS.

2.2.3.2 Activation using Staphylococcal enterotoxin A (SEA-superantigen)

Whole blood samples obtained from healthy donors were subjected to RBC lysis in order to obtain a pure population of lymphocytes (PBMNCs). PBMNCs were stimulated with 0.1 µg/ml of SEA at a density of $100x10^6$ cells/ml in AIMV medium (Life technologies), supplemented with 10% FCS and 100 U/ml of recombinant human IL-2. After 5 days, SEA-specific CTLs were positively isolated as described above (Section 2.2.2.1).

2.2.4 Quantitative real time PCR (qRT-PCR)

2.2.4.1 RNA isolation

RNA was isolated from $5x10^6$ naïve $CD8^+$ cells from healthy donors. Briefly, whole blood samples were subjected to RBCs lysis, followed by negative isolation of $CD8^+$ cells from PBMNCs and then cells were lysed immediately in 1 ml of trizol. The remaining cells from the same donor were then stimulated with anti-CD3/CD28 expander beads. After three days of stimulation, $CD8^+$ cells were treated the same way as naïve $CD8^+$ T cells for RNA isolation.

RNA was then isolated according to manufacturer's protocol provided with trizol Reagent. Briefly, the protocol is rescaled based on 1 ml of trizol as starting material for isolation. The samples were spun at 11,400 g for 10 min at 4°C. The supernatant was transferred to a fresh tube and then incubated at RT for 5 min. 200 µl of chloroform was added to 1 ml of trizol and the contents of the tubes were mixed and incubated at RT for 2 or 3 min. The tubes were spun at 11,400 g for 10 min at 4°C. The aqueous phase was carefully collected and transferred to a new tube and then 500 µl of isopropanol was added for precipitation of RNA. Samples were incubated at RT for 10 min. The tubes were then spun at 11,400 g for 10 min at 4°C. The supernatant was then removed and 1 ml 75% ethanol prepared in diethyl-pyrocarbonate (DEPC) water was added to the pellet. The tubes were spun at 11,400 g for 10 min at 4°C. The supernatant was removed and the pellet was air dried at RT. When the colour of the pellet changed from white to transparent, 30 µl of DEPC treated water was added to dissolve the pellet.

2.2.4.2 RNA quantification

Isolated RNA was quantified using UV absorbance for concentration and an agarose gel for quality. RNA was diluted to 1:100 using RNase free water and absorbance was calculated at 260 nm and 260/280 nm. Water was used as blank control. The absorbance at E260 was used for calculating concentration of RNA using the following formula:

RNA concentration = 40 × E_{260} × 100

Where 40 stands for OD = 1 corresponds to 40 µg per ml of RNA, E_{260} absorbance and 100 is dilution factor.

$$= 40 \times E_{260} \times 100 = 40 \times 0.100 \times 100$$
$$= 400 \text{ µg/ml}$$
$$= 400 \times 0.030 \text{ (30 µl final volume)}$$
$$= 12 \text{ µg in 30 µl}$$
$$= 0.4 \text{ µg/µl final concentration of RNA.}$$

Pure preparations of RNA will have OD_{260}/OD_{280} values of 1.8 to 2.0. If this value is < 2 or 1.8 then there is possibility of protein or phenol contamination.

An alternate way to examine the quality/integrity of RNA is to analyze samples on an agarose gel. Pure RNA has a band intensity for 28 S which is two times stronger than 18 S (Figure 6), on the other hand degraded RNA shows only smear on the gel instead of two clear bands.
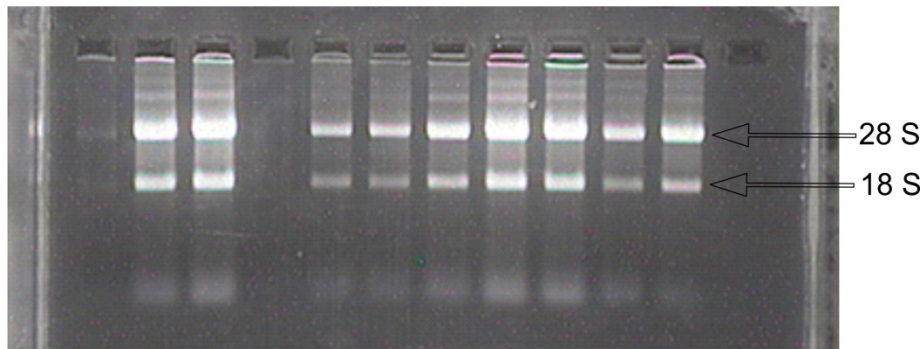
RNA gel eletrophoresis

28 S

18 S

Figure 6: RNA quality assessment using agarose gel electrophoresis

Total RNA was loaded on 1% gel agarose gel for determining RNA quality. From left to right: naïve (column 1) followed by stimulated CTLs (column 2 and 3). Similarly, naïve (column 4) followed by 1-7 days stimulated CTLs.

2.2.4.3 cDNA synthesis

Using reverse transcription, cDNA (Complementary DNA) was synthesized from 1 µg RNA at 42°C for 1 h using SuperScript™ II reverse transcriptase (Life technologies) in 20 µl reaction mix. Initially, total RNA along with random hexamers and dNTPs were boiled at 65°C for 5 min to linearize the RNA secondary structure followed by addition of 5x first strand synthesis buffer, 0.1 M DTT, RNaseOUT (RNase inhibitor) and SuperScript™ II reverse transcriptase followed by incubation at 42°C for 1 h.

2.2.4.4 PCR

The mRNA expression level of Syntaxin11 (GenBank accession number NM_003764.3) and the housekeeping gene ubiquitin C (UBC) were analyzed using quantitative real-time PCR assay with the following forward and reverse primers designed using NCBI primer blast (http://www.ncbi.nlm.nih.gov/tools/primer-blast/): Syntaxin11 (Forward primer) 5'-ACT CTC GCT CCC AGT CCA GGC AA and (Reverse primer) 5'- ATG TCC TCG TGG GGC GAG TCA A, UBC (GenBank accession number: NM_021009.5) (Forward primer) 5'- ATT TGG GTC GCG GTT CTT G and (Reverse primer) 5'- TGC CTT GAC ATT CTC GAT GGT.

PCR reactions were carried out in 96-well plates in 25 µl reaction volume with the QuantiTect SYBR green PCR master mix (QIAGEN). The reaction conditions are as follows: 15 min of heat activation of HotStart Taq DNA Polymerase enzyme at 95°C,

followed by 35 cycles of denaturation (15 s at 95°C), annealing (15 s at 60°C) and amplification (30 s at 72°C). At the end of the PCR reaction, a melting curve analysis was carried out in order to examine the specificity of the primers to their transcripts. Reactions were performed in duplicates for 3 independent experiments using the MaxPro-Mx300P Real Time PCR System (Stratagene).

2.2.4.5 Data analysis

Raw data obtained from PCR reactions were analyzed using MaxPro 3000P software (Stratagene). The Threshold Cycle (Ct) value for the gene of interest was normalized to the Ct value obtained for the housekeeping gene. The relative level of transcripts obtained for naïve cells was normalized to one in order to analyze the fold change in activated cells.

2.2.5 Syntaxin11 antibody

2.2.5.1 Selection of epitopes

Antigenic regions or epitopes for Syntaxin11 antibody within the Syntaxin11 full length protein were selected using online tool '**predicted antigenic peptides**' from 'universidad complutense de madrid' (http://imed.med.ucm.es/Tools/antigenic.pl). The epitope regions selected were aligned with all other Syntaxin isoforms from Syntaxin1 to Syntaxin15 to ensure the epitope selected for Syntaxin11 was unique and did not overlap with any other Syntaxin family members to avoid cross reactivity. Selected epitopes showed 100% overlap with murine Syntaxin11, hence the antibody could be used in murine assays. Two epitopes were chosen that fulfill all of the above defined criteria, one epitope within the N-terminal end and the other close to the C-terminal end of Syntaxin11.

2.2.5.2 Immunization

Rabbits were immunized with a short fragment of a synthetic peptide corresponding to the N-terminal (amino acid 30 to 46; EDIVFETDHILESLYR-C) and C-terminal (amino acid 30 to 46; AKAQVRKAVQY-C) region of Syntaxin11. Synthetic peptides were coupled to maleimide-activated keyhole limpet hemocyanin using a carboxy-terminal

cysteine. The keyhole limpet hemocyanin-peptide complex was emulsified in complete Freund's adjuvant immediately before injection into rabbits. Booster doses were given every alternate week using the same antigen emulsified in incomplete Freund's adjuvant. The rabbits were bled 1 week after each immunization and bleeds were screened by ELISA for the highest antibody titer using the epitope peptide.

2.2.5.3 Testing antibody titers using the ELISA

ELISAs were performed to measure the antibody titer across bleeds allowing the selection of a high titer bleed for antibody purification. The initial aim of the experiment was to find out the optimal concentration of peptide to which crude sera (antibody) can bind that is not too low to react with sera or too high leading to saturation. The ELISA includes ten steps listed as follows:

Coating peptide: The desired amount of peptide (from 1 pg to 100 μg) was dissolved in 100 μl of coating buffer and used to coat a flat bottomed 96 well plate by incubation overnight at 4°C. Unbound peptides were washed using 220 μl/well of wash buffer (PBS + 0.05% Tween20).

Blocking: Peptide coated 96 well plates were blocked using 200 μl/well of 1x assay diluent buffer.

Primary antibody incubation (crude sera): Different dilutions (1:500/1000/2500) of crude sera were prepared in 1x assay diluent buffer and added to a 96 well plate followed by incubation for 1 h at RT. After 1 h incubation well was washed 5 times with wash buffer and incubated with secondary antibody.

Secondary antibody incubation: Secondary antibody (horse radish peroxidase donkey anti-rabbit from Amersham) was diluted to 1:50,000 in 1x assay diluent buffer then added to plates and incubated for 45 min at RT. Plates were washed 5 times with wash buffer and 100 μl of substrate solution was added to each well and plates incubated for 15 min at RT in dark. The reaction was stopped immediately by adding 50 μl of stop solution (2 N H_2SO_4).

The absorbance was measured at 465 nm with a GENios pro plate reader (TECAN).

The rabbit sera containing highest antibody titer was selected for affinity purification.

2.2.5.4 Affinity purification

Affinity purification of rabbit polyclonal anti-human Syntaxin11 antibody was carried out using column chromatography with sepharose beads as matrix. Purification included the following steps:

Swelling of sepharose beads: Sepharose beads were activated in 100 mM HCl using gentle rotation at 4°C overnight. Beads are washed using a glass funnel with 100 mM HCl before being coupled to the epitope region peptides.

Coupling: Sepharose beads were resuspended in 10 ml of coupling buffer containing 5 mg of peptide, followed by overnight rotation at 4°C. Unbound peptide was washed away and peptide-linked beads were blocked using 10 ml of blocking buffer (0.1 M Tris HCl, pH 8.0) for 2 h. The blocking step was followed by a series of acidic (Sodium acetate 0.1 M pH 4.0 + 0.5 M NaCl) and basic (0.1 M Tris HCl+ 0.5 M NaCl) washes, followed by a final neutralizing wash using coupling buffer.

Primary antibody incubation: Crude serum along with previously activated/peptide coupled beads were mixed in an affinity purification column and followed by overnight rotation at 4°C. Sera was eluted to rinse all unbound components from the column and washed with an excess amount of cold 10 mM Tris + 0.5 M NaCl pH 7.5.

Elution: Matrix bound antibodies were eluted using 100 mM glycine pH 2.5, to break all acidic interactions between matrix bound antibodies and elute was collected in a tube containing 1 M Tris, pH 8.0.

After glycine elution, the column was washed thoroughly with 10 mM Tris pH 8.8 and followed by a second antibody elution using 3.5 M $MgCl_2$ to elute any remaining antibodies bound to the column. Flow through from all of above elution was subjected to a concentration step using centricon tubes (Millipore: UFC901008).

2.2.5.5 Evaluation of antibody specificity

2.2.5.5.1 Western blot

2.2.5.5.1.1 Lysate preparation

SEA stimulated human CTLs were washed in ice cold PBS and lysed in freshly prepared chilled lysis buffer (1 mM EDTA, 1 mM DTT, 50 mM Tris-Cl (pH 7.4), 1% TX-100, 1 mM Deoxycholate, 100 mM NaCl and protease inhibitors). CTLs were

homogenized using a syringe five times manually in lysis buffer on ice. Lysates were rotated for 30 min at 4°C and insoluble material and cell debris were removed by high speed centrifugation. All extracts contained the protease inhibitors pepstatin A (1 µM), benzamidine (100 µM), leupeptin (1 µM), aprotinin (0.3 µM), phenylmethanesulfonyl fluoride (25 mM), trypsin inhibitor (20 µg/ml) and PefBloc SC (1 mM).

2.2.5.5.1.2 Blotting

Lysates were boiled for 10 min in 1x LDS (Lithium dodecyl sulphate) sample buffer (Life technologies) with 4% β-mercaptoethanol and then loaded onto a denaturing 4-12% Bis-tris gel. Proteins were then transferred onto nitrocellulose membrane (0.2 µm pore diameter). Blots were blocked using 5% skim milk powder in 1x TBS (20 mM Tris, 0.15 M NaCl, pH 7.4) for 2 h at RT or overnight at 4°C. Blots were incubated with affinity-purified anti-human Syntaxin11 antibody (1:500) and anti-GAPDH ab in 5% skim milk (1:5000). The blots were washed with TBS containing 0.05% Tween-20 (TBST) (five changes) followed by 1 h incubation with horseradish peroxidase donkey anti-rabbit secondary antibody (Amersham), diluted to 1:50,000 in SM-TBST, washed 6 times with TBST and developed with ECL reagent (Pierce).

2.2.5.5.1.3 Western blot quantification (Densitometry)

Quantification of Western blot was performed using ImageJ 4.16r software. TIF images generated out of blots were used for analysis. For measurements of pixel density, we multiplied the mean fluorescence value by the pixel value for each band. Normalized data was obtained by dividing the relative intensity over our standard as the common point of comparison according to standard analysis procedures. Measurements were then analyzed using Sigmaplot.

2.2.6 Electroporation

2.2.6.1 Plasmid electroporation

SEA stimulated or anti-CD3/CD28 bead stimulated CTLs were used for electroporation of plasmid DNA (TFP-Syntaxin11, Granzyme B-mCherry and mCherry-Rab11a) was

carried out using nucleofection kit (LONZA). Using PBS, 5×10^6 cells were washed with PBS and resuspended in 100 µl of nucleofection solution provided with kit along with 2 µg of plasmid DNA each for double transfection or 4 µg in case of single transfection. Cells were cultured without IL-2 for up to 12 h and then cells were washed and replaced with fresh in AIMV + 10% FCS containing 100 U/ml of human recombinant IL-2.

2.2.6.2 siRNA electroporation

Anti-CD3/CD28 bead stimulated CTLs were used for electroporation of siRNA (control and Syntaxin11 siRNAs) and all electroporations were carried out using a 6×10^6 cells and the human T cell nucleofection kit (LONZA). Cells were washed with PBS and resuspended in 100 µl of nucleofection solution provided with kit along with 20 µM siRNA for eletroporation. Cells were cultured for 12 h and then washed and media replaced with fresh AIMV + 10% FCS.

2.2.7 Degranulation assay

Degranulation assay was performed using CTLs transfected with either control or Syntaxin11 siRNAs. Briefly, anti-CD3/CD28 bead stimulated CTLs were transfected with control and Syntaxin11 specific siRNAs. 36 h after transfection, equal numbers of cells from control and Syntaxin11 siRNA transfected CTLs (0.5×10^6 cells) were plated in duplicates using flat bottomed 96 well plates that were previously coated with or without anti-CD3/CD28 ab for stimulated degranulation along with Golgi-stop monensin (BD Biosciences). Cells were incubated for 4 h at 37^oC, then washed and resuspended in FACS buffer (PBS with 0.1% BSA and 5% FCS) before acquisition. Degranulation was measured using a PE conjugated-CD107a ab (Clone H4A3 from BD Pharmingen) which binds to LAMP1a containing vesicles that have fused with the plasma membrane. PE-IgG1, κ Isotype was used as control in same experiments. Cells were acquired in FACS Canto II analyzer (BD Pharmingen). Data were analyzed using FlowJo software. Gates were set based on no antibody controls (constitutive secretion).

2.2.8 Cytotoxicity assay

To analyze the killing efficiency of CTLs in control and Syntaxin11 siRNA treated cells, the CytoTox 96 non-radioactive cytotoxicity kit (Promega) was used. In brief, effector cells (SEA stimulated CTLs; E) were co-cultured with target cells (SEA pulsed Raji cells; T) at various effector:target cell (E:T) ratios at 37° C for 4 h in a 96 well plate in RPMI medium containing 2% FCS, but without phenol red. After 4 h, cells were pelleted by centrifugation and 50 µl of supernatant was used to measure the amount of lactate dehydrogenase released into the supernatant. The supernatant was incubated with a suitable substrate for 30 min at RT and the reaction was stopped using 1 M acetic acid. The absorbance was measured at 490 nm with GENios pro plate reader (TECAN). Cytotoxicity was calculated by subtracting LDH release from effector cells alone and target cells alone to effector + target cells using the following equation: % Cytotoxicity = (experimental – effector spontaneous – target spontaneous)/(target maximum – target spontaneous) x 100. All experiments were performed in triplicate.

2.2.9 Total internal reflection fluorescence microscopy (TIRFM)

2.2.9.1 TIRFM setup

The TIRFM setup used in this study consists of an inverted Olympus IX70 microscope with the following components: a solid-state laser 85 YCA emitting at 561 nm (Melles Griot, Carlsbad, CA, USA), a Micromax 512 BFT camera (Princeton instruments Inc., Trenton NJ, USA) controlled by Metamorph (Visitron, Puchheim, Germany), a TIRF condenser (T.I.L.L Photonics, Grafeling, Germany) and an Acousto Optical tunable filter (AOTF)-nC (AA optoelectronic, St Remy-les Chevreuses, France), a dual band FITC/Texas red filter set (# 51006, AHF Analysen technik AG, Tübingen, Germany), a dual-view camera splitter (Visitron, Puchheim, Germany) to separate the red and green channels, a Visichrome Monochromator (Visitron, Puchheim, Germany) to acquire images in epifluorescence. A 100x Olympus objective with a N.A of 1.45 was used for all TIRFM experiments. The object size which is represented in one pixel size was 130 nm.

2.2.9.2 Coating of coverslips

For artificial stimulation that mimics real antigen presenting cells, glass coverslips coated with anti-CD3/CD28 ab, were used. Briefly, glass coverslips (25 mm) were precleaned with 70% ethanol and coated with 0.1 mg/ml poly-ornithine for 30 min at RT. The anti-CD3 monoclonal ab (1 mg/ml) and anti-CD28 ab (1 mg/ml) antibodies that were used for coating were diluted in PBS to obtain concentration 30 µg/ml (CD3) and 90 µg/ml (CD28). The maximum volume of antibody solution that was used for coating one coverslip was 30 µl. Coverslips were incubated with an antibody solution for 2:30 h in a 37°C humidified tissue culture incubator. The solution was aspirated after the incubation period and coverslips were then used for TIRFM.

2.2.9.3 Experimental protocol for TIRFM

CTLs used in TIRFM experiments were cotransfected with GFP-Syntaxin11 and either the lytic granule marker Granzyme B-mCherry or the recycling endosome marker mCherry-Rab11a. For all knockdown studies, CTLs were cotransfected with siRNA and Granzyme B-mCherry. Cells were spun down for 5 min and resuspended in 50 µl extracellular solution containing 0 mM Ca^{2+} and allowed to settle for 2 min on anti-CD3/CD28 ab coated coverslips. The cells were then perfused with an extracellular solution containing 10 mM Ca^{2+} to optimize Ca^{2+} influx during secretion. Cells were imaged for 20 min by TIRFM at 488 nm and 561 nm. The acquisition speed was set to 10 Hz and the exposure time was 100 ms. All experiments were carried out at RT. The analysis of accumulation was performed with ImageJ software.

Syntaxin11 and LGs: For simultaneous visualization of Syntaxin11 and LGs in TIRFM, CTLs were cotransfected with mCherry-Syntaxin11 and Granzyme B-TFP plasmids. The cells were allowed to settle for 3-4 min on anti-CD3/CD28 ab coated coverslips and acquisition in TIRF mode was performed using 488 nm and 561 nm. The acquisition speed was 10 Hz and the exposure time was 100 ms. All experiments were performed at RT.

Syntaxin11 and recycling endosomes (Rab11a): For simultaneous visualization of Syntaxin11 and recycling endosomes (Rab11a) in TIRFM, CTLs were cotransfected with GFP-Syntaxin11 and mCherry-Rab11a plasmids. The cells were allowed to settle for 3-4 min on anti-CD3/CD28 ab coated coverslips and acquisition in TIRF mode was

performed using 488 nm and 561 nm. The acquisition speed was 10 Hz and the exposure time was 100 ms. All experiments were performed at RT.

2.2.10 Lytic granule fusion analysis

Fusion analysis was carried out using ImageJ software with the plugin Time Series V3_2 analyzer. Fusion was analyzed as a measure of total fluorescence of all pixels over a selected region of interest (ROI) for single vesicle in the form of graph showing a sudden drop in the fluorescence of the vesicle in less than 300 ms. Each individual vesicle was tracked manually over time to see whether the LG (Granzyme B-mCherry) moves back into the cell or it fuses at the IS. Movement of the vesicle back into the cell can be distinguished from fusion by delayed or gradual loss of fluorescence which is much longer than typical fusion events.

2.2.11 Dwell time analysis of lytic granules

Dwell time is defined as the time spent by a vesicle at the plasma membrane (TIRF plane). Dwell time of the vesicle is calculated by tracking a single vesicle over time before it fuses or moves back into the cell.

2.2.12 Mean fluorescence analysis

Average number of vesicles or total fluorescence corresponding to Syntaxin11, Rab11a and LGs at the TIRF plane was measured using a defined threshold in ImageJ software (http://rsbweb.nih.gov/ij/).

2.2.13 Colocalization analysis

For TIRFM and live cell imaging data, Mander's colocalization analysis between Syntaxin11, Rab11a and LGs were carried out using JACoP plugin in ImageJ. For line scans, ZEN2011 software (Carl Ziess) was used to draw lines and fluorescence values for individual pixels were exported to sigma plot.

2.2.14 Confocal ELYRA set up

LSM 780 (Carl Zeiss) is regular confocal laser scanning microscope with a highly sophisticated light detection system composed by a 32 channel spectra GaAsP array and two standard alkali PMTs in positions for blue and far-red detection and a transmitted light detector. The confocal setup is equipped with both a 37ºC incubator and a 5% CO_2 supply. A 40x oil objective with numerical aperture (N.A) of 1.3 was used for image acquisition. For acquisition, ZEN software was used with a frame size 512 x 512 and a pinhole size of 5 (A.U). Laser light of wavelengths 488 nm, 561 nm and 647 nm were used for excitation using a multiple band beam splitter for 488/561/633 nm. The laser power used was 1-2% of maximal power to avoid bleaching. Simultaneous confocal z-sections were taken at 1 µm intervals for whole cell analysis. In the z-direction, a total of 6 slices were acquired with a speed of 400 ms per slice. All 6 slices were merged to create the maximum intensity projection from the acquired images and compressed to 50 frames per second using the ImageJ movie compression.

2.2.15 Live cell imaging

For live cell imaging experiments, SEA specific CTLs were cotransfected with TFP-Syntaxin11 and with either a marker for LGs (Granzyme B-mCherry) or a marker for recycling endosomes (mCherry-Rab11a).

Raji cells (target cells) were pulsed with SEA for 30 min prior to live cell imaging. CTLs and target cells were observed in AIMV medium at 37°C and 5% CO_2 to study the dynamics of cells in real time. Movies were acquired using a LSM780 Carl Zeiss microscope. CTLs and target cells were imaged simultaneously in 3 channels with the following lasers; 488 nm for TFP, 561 nm for mCherry and DIC images. Images of cells were acquired at 1 µm intervals in the z-direction for all 3 channels simultaneously.

3. RESULTS

3.1 Syntaxin11 is expressed in CTLs and up regulated upon activation

We analyzed the expression of Syntaxin11 at the mRNA level in naïve CD8$^+$ cells (day 0) and after stimulation of CD8$^+$ cells (CTLs) for three days with anti-CD3/CD28 antibody coated activator beads, using quantitative real time PCR (qRT-PCR; figure 7). We found that the expression of Syntaxin11 is increased 3.19 ± 0.002 fold (n=4) upon stimulation for 3 days, in contrast to un-stimulated cells (naïve cells). CD8$^+$ cells were also stimulated using super-antigen (SEA) and positively or negatively isolated CD8$^+$ cell populations were quantified using FACS and were about 99% pure for CD8$^+$ cells (Pattu et al., 2011).
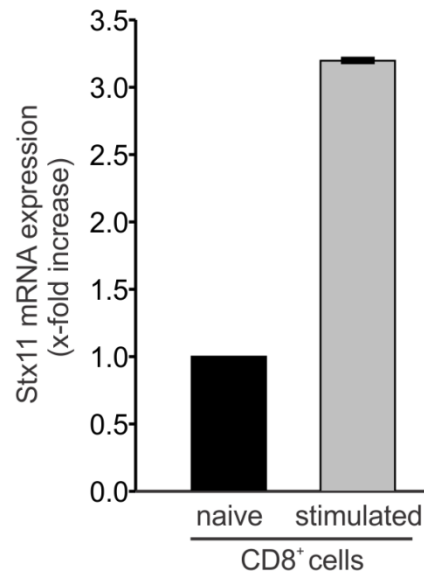

Figure 7: Syntaxin11 is upregulated upon activation of CD8$^+$ cells

Expression studies of Syntaxin11 at mRNA level using qRT-PCR in naïve CD8$^+$ cells and three day anti-CD3/CD28 expander bead stimulated CTLs. Expression of Syntaxin11 in naïve cells is normalized to one in order to study the fold change upon activation. Upon activation expression of Syntaxin11 is upregulated. Data normalized to the housekeeping gene ubiquitin-C (UBC). Error bars show standard error of the mean (SEM).

We produced a rabbit polyclonal antibody specific for Syntaxin11 and affinity purified (Section 2.2.5). The epitope was a peptide corresponding to the N-terminal region of Syntaxin11. Western blot analysis was performed using antibody by loading varying amounts of CTL lysates (5 µg, 10 µg, 15 µg and 20 µg; figure 8 A). The affinity purified

Syntaxin11 antibody detected a single band at the expected molecular weight of 33.3 kDa. Having verified the sensitivity of the antibody to endogenous Syntaxin11, we next used siRNAs directed against Syntaxin11 as a confirmation for sensitivity and specificity. CTLs were transfected with three different siRNAs 1, 2 and 6 (Section 2.2.5.2) against Syntaxin11 to knockdown the expression of endogenous Syntaxin11. The amount of knockdown was quantified using qRT-PCR (Figure 8 C) and western blot (Figure 8 B). The reduction of Syntaxin11 mRNA was found to be for siRNAs 1, 2 and 6 was reduced to 40%, 45 % and 20% of control value which is normalized to 100%, respectively (n=3) (Figure 8 C).

Knockdown of Syntaxin11 was also verified using Western blot analysis (Figure 8 B) which detects the protein and quantified using densitometry (Figure 8D). We found a strong reduction in the protein levels (by 75%, 80% and 85% for siRNAs 1, 2 and 6 respectively). The reproducibility of the knockdown for Syntaxin11 was confirmed with cells from 3 independent human donors.

Based on these positive and negative controls, the Syntaxin11 antibody is specific and sensitive. All three siRNAs directed against Syntaxin11, were effective in reducing Syntaxin11 protein levels significantly. Thus the antibody and siRNAs are suitable for functional studies.
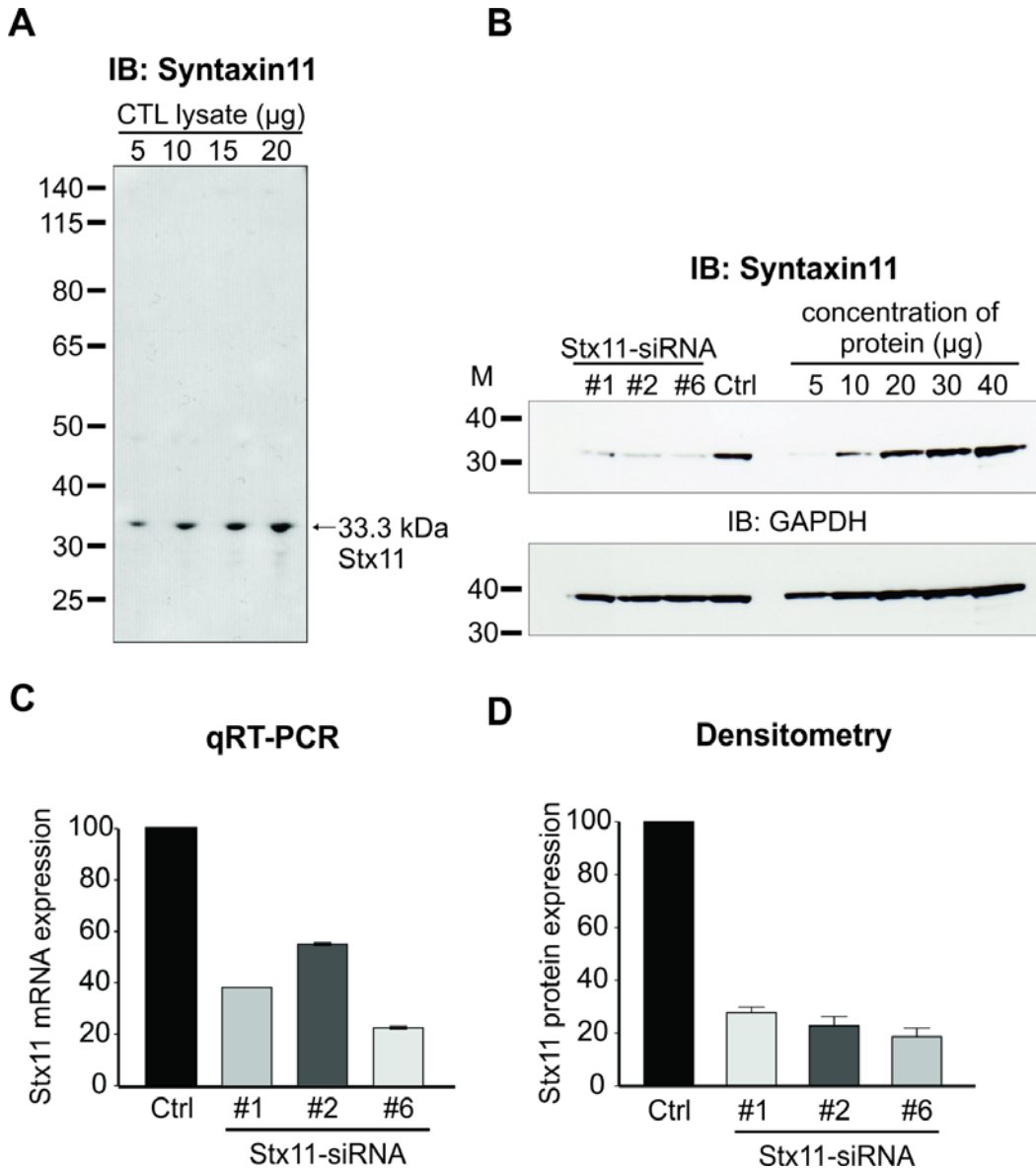
A

IB: Syntaxin11

CTL lysate (µg)

5 10 15 20

140—
115—

80—

65—

50—

40—

30— ←33.3 kDa
Stx11

25—

B

IB: Syntaxin11

concentration of
protein (µg)

Stx11-siRNA

M   #1 #2 #6 Ctrl   5 10 20 30 40

40—

30—

IB: GAPDH

40—

30—

C

qRT-PCR

Stx11 mRNA expression

100
80
60
40
20
0

Ctrl   #1   #2   #6

Stx11-siRNA

D

Densitometry

Stx11 protein expression

100
80
60
40
20
0

Ctrl   #1   #2   #6

Stx11-siRNA

Figure 8: Affinity purified antibody is specific for Syntaxin11 in Western blot

Antibody specificity test using Western blot (A) in which CTL lysate blotted with a polyclonal anti-Syntaxin11 antibody shows a single band at the predicted molecular weight of 33.3 kDa. (B) Control and Syntaxin11 siRNA transfected CTL lysates blotted for Syntaxin11 (upper panel) and GAPDH (lower panel) as loading control shows reduced protein amount in all three siRNA treated CTLs compared to control siRNA treated CTLs. (C) Quantification of Syntaxin11 mRNA downregulation by transfection of three different siRNAs specific for Syntaxin11 using qRT-PCR shows that all three siRNA treated groups show reduced amount of transcript level compared to control which is normalized to 100%. (D) Quantification of Syntaxin11 protein reduction (densitometry) from three independent experiments with a calibration curve derived from the right part of (D) shows that there is significant reduction in the protein level compared to control which is normalized to 100%. Error bars are SEM.

3.2 Downregulation of Syntaxin11 leads to a strong reduction in degranulation and a reduction in CTL mediated target cell killing

To confirm the functional contribution of Syntaxin11 in LG exocytosis, we performed a FACS based LAMP1a degranulation assay (Section 2.2.6). siRNA 2 was used for all further functional experiments. Cells were stimulated with anti-CD3/CD28 ab for 4 h and labeled with LAMP1a (Lysosomal Associated Membrane Protein 1a) CD107a. Upon stimulation, LAMP1a is exposed to the cell surface after LAMP1a positive compartments (lytic granules) fuse with the plasma membrane. The surface LAMP1a expression can be quantified, using a LAMP1a specific antibody by FACS and serves as an indicator of exocytosis. Gating was performed based on the negative control (no antibody control). Degranulation was calculated as the percentage of cells that showed an increase in CD107a membrane fluorescence upon stimulation in contrast to their respective unstimulated counterparts. CTLs transfected with Syntaxin11 siRNA (Figure 9 A) showed, a strong decrease in LAMP1a surface expression degranulation (Figure 9 B), in surface expression of CD107a (LAMP1a), in contrast to control (inactive) siRNA (6.83% vs 28.6% respectively) indicating a defect in degranulation (76.12 ± 0.84%, n=3; ***p < 0.001, figure 9 C). Knockdown for Syntaxin11 was confirmed for each experiment and was comparable to the knockdown shown in figure 8 D. Thus, Syntaxin11 is functional in CTLs and is required for LAMP1a degranulation.
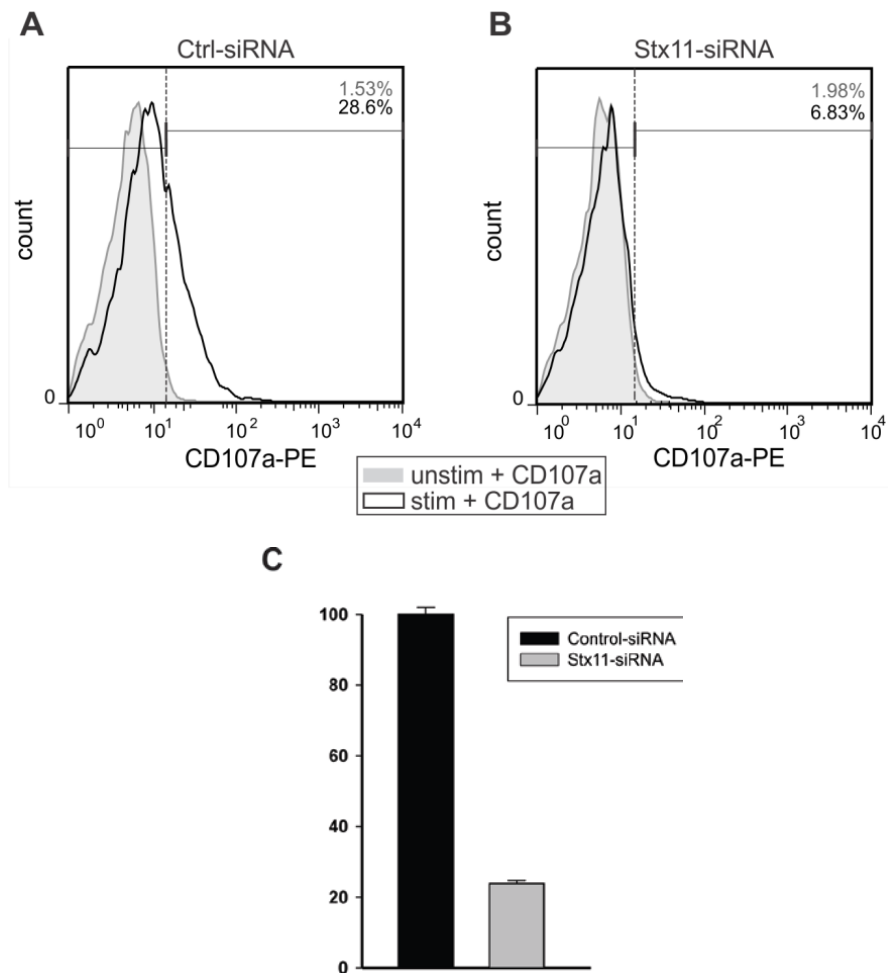
Figure 9: Downregulation of Syntaxin11 leads to a strong reduction in LAMP1a degranulation

 LAMP1a degranulation of CTLs treated with control (A) and Syntaxin11 siRNA (B). Syntaxin11 siRNA treated cells show reduced degranulation compared to control siRNA. Shown are representative histograms from 3 independent experiments. Gray area represents constitutive secretion and black line represents stimulated secretion. Quantification of degranulation (C) shows a reduction in degranulation by approximately 76%. Error bars are SEM.

In order to study the function of Syntaxin11 in CTL mediated cytotoxicity, we performed a population based killing assay to test the function of CTLs that were downregulated with Syntaxin11 siRNA and control siRNA. We used a non-radioactive, colorimetric based assay which recognizes lactate dehydrogenase (LDH) released into the extracellular space. LDH is involved in the interconversion of pyruvate and lactate. As a result of CTL mediated killing, the target cell membrane becomes leaky and thus releases its cytoplasmic contents into the medium. The percentage of target cell lysis was measured as the amount of LDH that was released, at various effector:target cells ratios (Section 2.2.1). We found a significant reduction in the ability of Syntaxin11

siRNA treated cells to kill target cells in contrast to control siRNA treated cells at effector: target cell ratios of 20:1 (63.0 ± 2.2% vs. 30.1 ± 7.1%; **p < 0.004) and 30:1 (100% vs. 52.5 ± 6.4%; **p < 0.003, figure 10, n=3). Our results demonstrate that reduction of Syntaxin11 expression in human primary CTLs by siRNA mimics the phenotype of FHL-4 patients and can thus be used to study the function of Syntaxin11 with high resolution imaging.
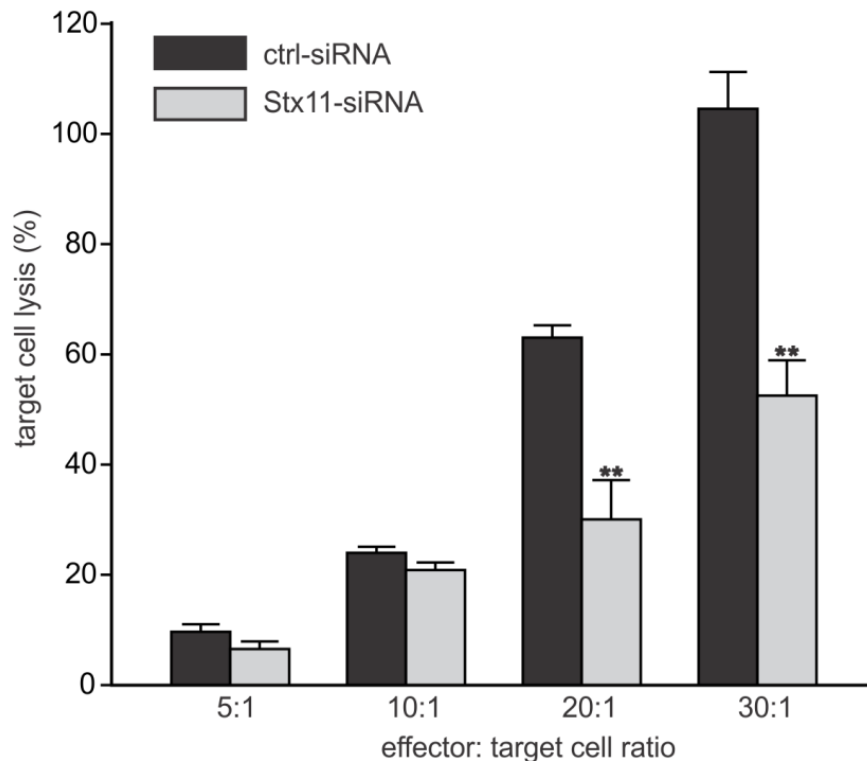

Figure 10: Downregulation of Syntaxin11 leads to reduced cytotoxicity of CTL

CTL mediated cytotoxicity is reduced upon downregulation of Syntaxin11. SEA pulsed Raji cells and SEA-specific CTLs were co-cultured for 4 h at the indicated effector to target cell ratios. Experiments were performed in triplicates. Syntaxin11 siRNA treated CTLs show a reduced killing ability when compared to cells treated with control siRNA. Error bars are SEM.

The defect in cytotoxicity is specifically due to the knockdown of Syntaxin11 and not because of other Syntaxin isoforms (Qu et al., 2011).

Thus, we conclude that Syntaxin11 is needed for CTL effector function since knockdown of Syntaxin11 results in a dramatic reduction of LAMP1a degranulation and CTL mediated target cell killing.

3.3 Syntaxin11 downregulation results in a complete ablation of LG fusion at the IS

Having confirmed a role for Syntaxin11 in CTL mediated cytotoxicity by LAMP1a degranulation and cytotoxicity assay, we aimed to identify the mechanism of Syntaxin11 function in CTLs. For this purpose we used high resolution TIRF microscopy to study the behavior of individual LGs at the IS upon Sxntaxin11 downregulation. CTLs were transfected with Syntaxin11-siRNA or control-siRNA as described earlier. The cells were then transfected with Granzyme B-mCherry to mark the LGs. Previous reports have shown that Syntaxin11 is involved in the maturation of the LGs, meaning Syntaxin11 functions at a step upstream of LG fusion (Dabrazhynetskaya et al., 2012). Thus, one would expect to see either fewer LGs at the IS, or LGs of a different size and morphology accumulating at the IS. However we found no difference in the LG size or morphology at the IS. There was also no difference in the number of LGs at the IS. These results rule out an effect of Syntaxin11 upstream of LG fusion at the IS. CTLs that were transfected with either control siRNA or Syntaxin11 siRNA were allowed to settle on coverslips coated with anti-CD3/CD28 ab for 3 min in an extracellular solution containing 0 mM Ca^{2+}. The cells were imaged in TIRF and then perfused with extracellular solution containing 10 mM Ca^{2+}. CTLs were analyzed for the number of LG fusion events in TIRFM. Out of ten cells analyzed for control-siRNA treated CTLs, an average of 2.4 vesicle fusion events per cell were observed with a total of 24 fusion events (Figure 11 A; upper panel) as highlighted using red and yellow arrowheads. However, in Syntaxin11 siRNA treated CTLs, there was a dramatic reduction in the number of LG fusion events with only a total of 3 fusion events from 10 cells analyzed (an average of 0.3 fusion events per cell) (Figure 11 A; lower panel). Therefore in Syntaxin11 siRNA treated cells, there was 87.5% reduction in the number of LG fusion events in contrast to control siRNA treated cells (Figure 11 B). These results clearly implicate the direct involvement of Syntaxin11 in LG fusion.
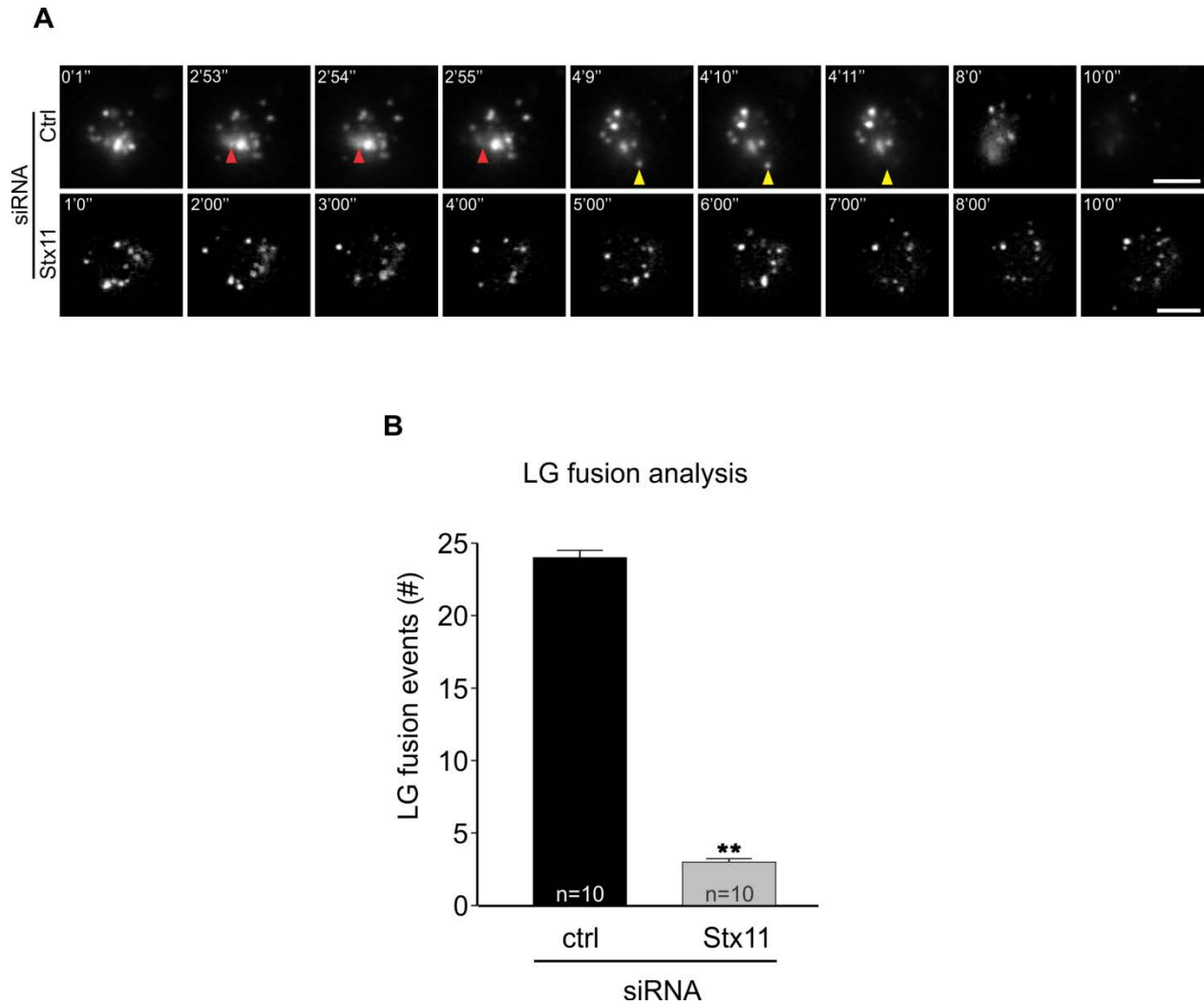
A

B

LG fusion analysis

Figure 11: Knockdown of endogenous Syntaxin11 results in a significant reduction in the number of LG fusion events

Visualization of LGs in real time using TIRF microscopy in Syntaxin11 downregulated cells. Shown are TIRFM images of control siRNA transfected CTL (A- upper panel) demonstrating accumulation and decrease in number of LG over the time. Arrowheads indicate LG fusion. In contrast, TIRFM images of Syntaxin11 siRNA treated CTL (A-lower panel) show no fusion events over the entire recording time. (B) Quantification of the average fusion events of LG at the IS in control and Syntaxin11 siRNA transfected cells reveal a drastic reduction in the number of fusion events upon Syntaxin11 knockdown (n=10; **p < 0.01). Scale bars: 5 μm. Error bars are SEM.

3.4 Syntaxin11 knockdown reduces dwell time of LGs at the IS

Having established a reduction in the number of LG fusion events in CTLs treated with Syntaxin11 siRNA, we examined LG behavior at the IS in more detail, in particular those LGs that do not fuse at the IS. The predicted role for Syntaxin11 is that of a t-SNARE, therefore we analyzed the dwell time of LGs at the IS. Dwell time can be defined as the amount of time spent by an LG at the IS before it fuses or moves away from the evanescent field. We analyzed the dwell time of LGs in CTLs treated with Syntaxin11 siRNA and control siRNA and found that there is a significant decrease in the dwell time of LGs from 1.3 min (control siRNA; Figure 12 A; upper panel) to 0.4 min (Syntaxin11 siRNA, figure 12 A; lower panel) (p < 0.001). However, when we analyzed the number of LGs in control and Syntaxin11 siRNA treated cells, we found that there is no significant difference in the number of LGs between the two groups when the extracellular solution contained 0 mM Ca^{2+}. However, when the cells are perfused with extracellular solution containing 10 mM Ca^{2+}, there is a significant reduction in the number of LGs at the IS in control siRNA treated cells in contrast to Syntaxin11 siRNA treated cells.

In control siRNA treated CTLs, the number of LGs at the IS declines over time from about 6-7 LGs to ~1-2, over the course of the experiment. The reduction is the result of ~2 fusion events and movement of most of the remaining granules from the TIRF field (Figure 13). This is expected since CTLs release very few granules at a single target cell. One or two granules are sufficient to kill a target cells and after release occurs, the CTL detaches from the target cell and moves on to the next target. On the other hand, in Syntaxin11 siRNA treated cells, there is a dramatic reduction in LG fusion and a significant increase in the number of LGs at the IS. These LGs are more mobile, showing active movement throughout the acquisition time. The inability of LGs to fuse at the IS leads to accumulation of LGs in Syntaxin11 siRNA treated cells. Thus, Syntaxin11 serves as the t-SNARE for the final fusion of LG at the IS.
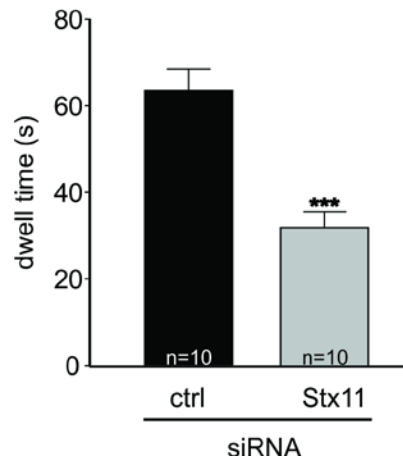
A
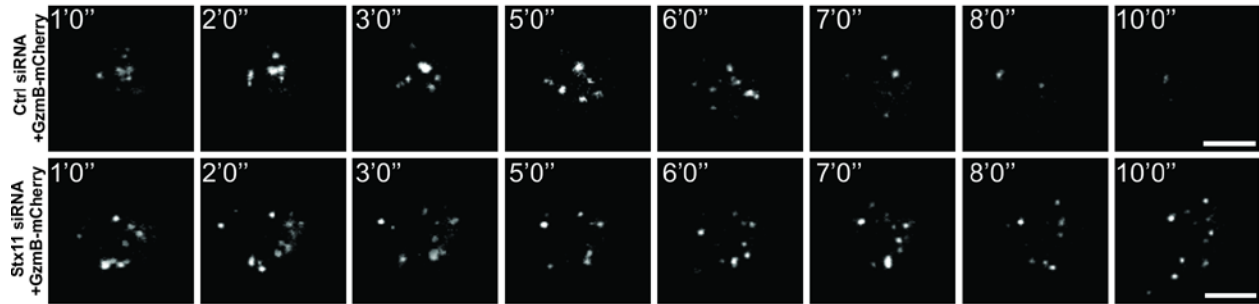
B

LG dwell time analysis

Figure 12: Knockdown of endogenous Syntaxin11 in CTLs results in a reduction of LG dwell time

Exemplary TIRFM images showing (A) the accumulation of LG over time in control siRNA treated cells (upper panel) and Syntaxin11 siRNA treated cells (lower panel). (B) Quantification of LG dwell time in control siRNA and Syntaxin11 siRNA transfected cells. Syntaxin11 siRNA treated cells show a 50% reduction in LG dwell time (31.87 ± 3.6 s) in comparison to cells treated with control siRNA (63.58 ± 4.8 s) (n=10; ***p < 0.001). Scale bars: 5 μm. Error bars are SEM.
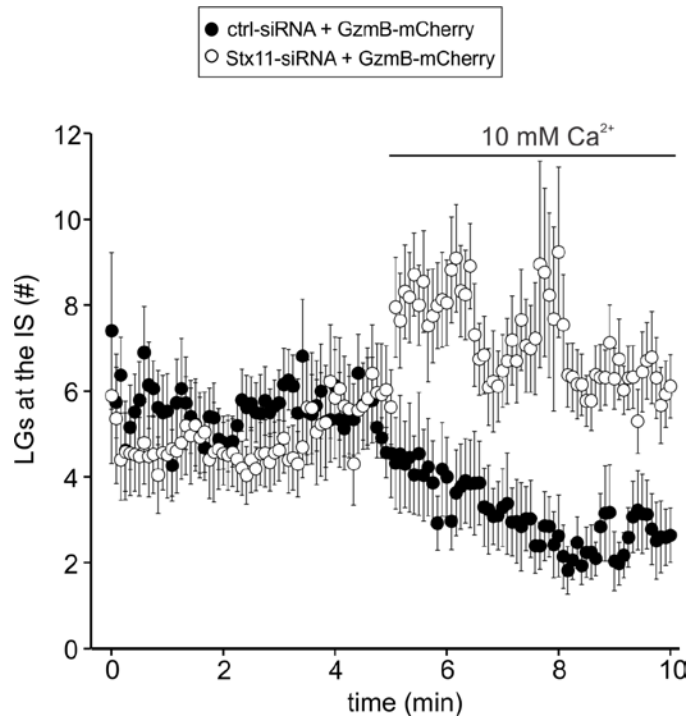
Figure 13: Knockdown of endogenous Syntaxin11 in CTLs results in an increased number of LGs over time

Analysis of the average number of LGs over time in Syntaxin11 siRNA treated cells and control siRNA treated cells. There was no change in the number of LGs over time in Syntaxin11 siRNA treated cells, however in control siRNA treated cells there was a significant reduction in the number of LGs towards the end of the movie (n = 10). Error bars are SEM.

3.5 LG and Syntaxin11 clusters associate with each other at the IS

Our results provide evidence that Syntaxin11 serves as a t-SNARE for the fusion of LGs at the IS. Next, we investigated the temporal and spatial organization of Syntaxin11 molecules at the IS and compared this to the localization of LGs. CTLs overexpressing full length Syntaxin11 protein fused to mCherry (mCherry-Syntaxin11, see section 2.2.5.1) were used. To mark LGs we expressed Granzyme B-TFP by electroporation. The cells were then examined using TIRFM. Briefly, the transfected CTLs were allowed to settle on coverslips coated with anti-CD3/CD28 ab in extracellular solution containing 0 mM Ca^{2+} followed by perfusion with extracellular solution containing 10 mM Ca^{2+}. CTLs were then analyzed for the fluorescence intensity of Syntaxin11 (Figure 14 A; upper panel) and LGs (Figure 14 B; panel in the middle) in the TIRF field over time. The mCherry-Syntaxin11 fluorescence appears in the TIRF plane first, almost as soon as the CTL settles and forms an IS. The fluorescence of Syntaxin11 initially appears to be membrane associated as expected of a plasma membrane associated t-SNARE,

however later there is an aggregation of Syntaxin11 to form clusters or hotspots (Figure 14) (Bar-On et al., 2009; Barg et al., 2010; Sieber et al., 2006). Over time several hotspots or clusters of Syntaxin11 appear on the plasma membrane as visualized in the TIRF plane. The formation of Syntaxin11 hotspots is followed by the subsequent accumulation of LGs in the TIRF plane (Figure 14C; lower panel) which is followed by fusion. CTLs transfected with control mCherry vector showed no clusters and no association with LGs (Figure15). Thus, LG arrival at the IS is always associated with Syntaxin11 hotspots and since there is a strong overlap of LG with Syntaxin11 clusters, we conclude that Syntaxin11 is the plasma membrane t-SNARE needed for LG fusion at the IS.
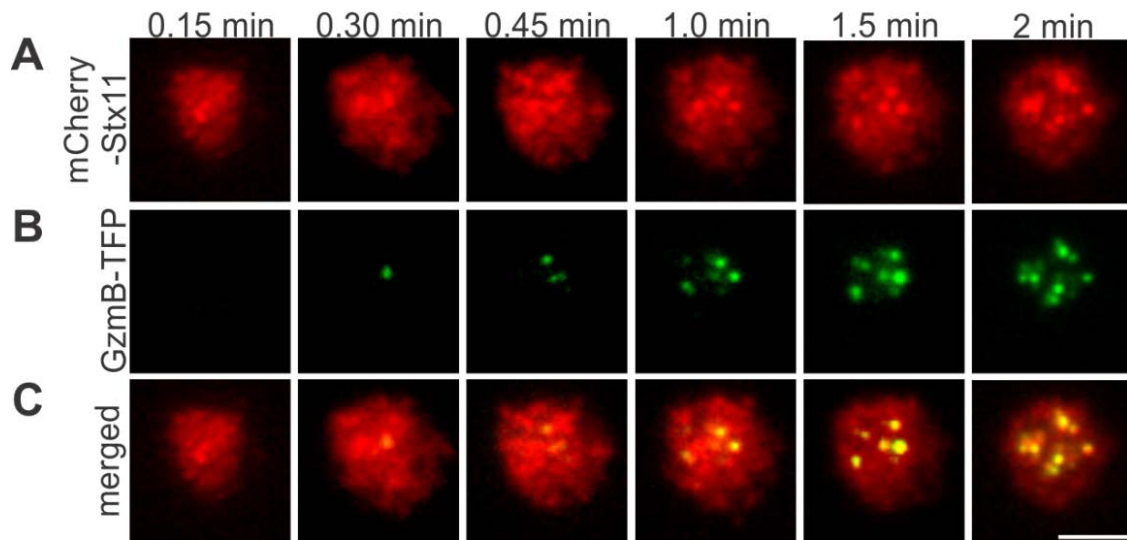

Figure 14: Syntaxin11 forms hotspots at the IS and this is followed by LG arrival at the IS

(A) Real time visualization of Syntaxin11 cluster formation at the IS (TIRF) (B) followed by sequential arrival of LGs

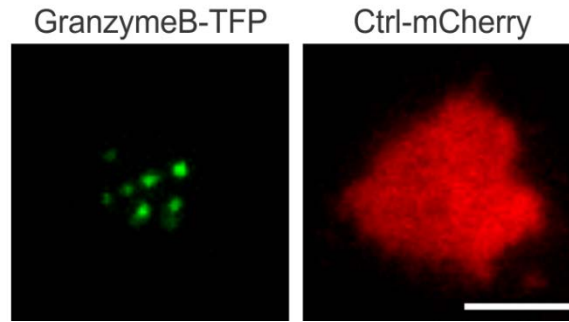(C) demonstrating LGs arrive at the hotspots formed by Syntaxin11 clusters at the IS. Scale bar: 5 μm.

GranzymeB-TFP   Ctrl-mCherry

Figure 15: mCherry encoding vector and lytic granules at the IS

CTLs were transfected with vector encoding for mCherry (instead of mCherry-Syntaxin11) and the LG marker Granzyme B-TFP. There was no cluster formation in case of mCherry; instead the fluorescence appears to be cytoplasmic. Scale bar: 5 µm.

Quantification of the overall fluorescence at the TIRFM for Syntaxin11 and LGs (Figure 16) shows that fluorescence of Syntaxin11 was always more intense than that of the LGs, indicating that the clusters of Syntaxin11 generate a platform for landing of LGs in preparation for fusion at the IS.
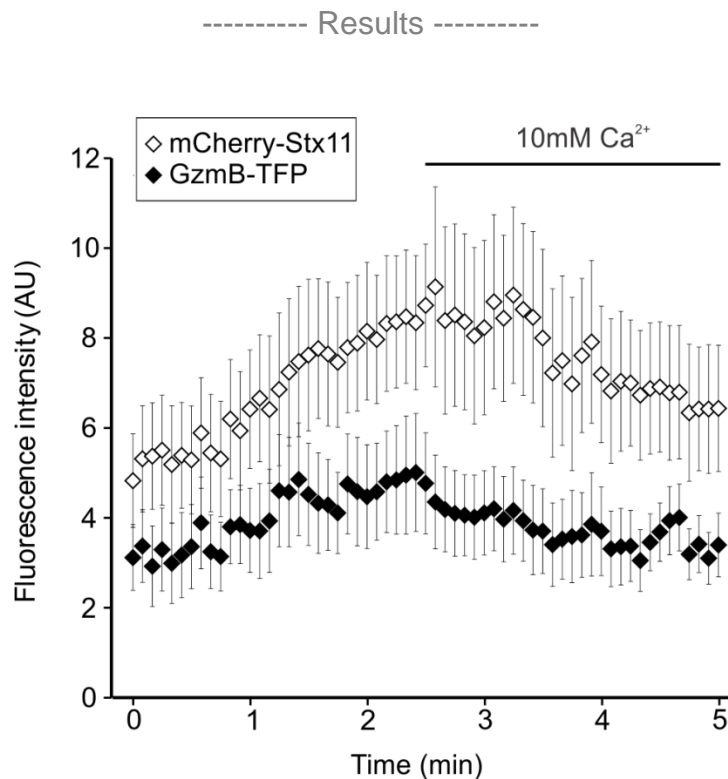
Figure 16: Syntaxin11 fluorescence remains higher than LGs at the IS

Quantification of the overall fluorescence of Syntaxin11 and LGs at the TIRF plane (n=10). The fluorescence of Syntaxin11 is always higher than that of LGs indicating that Syntaxin11 provides a platform for arriving LGs. Error bars are SEM.

3.6 Syntaxin11 polarizes before the arrival of lytic granules at the IS

Our results strongly support the evidence that Syntaxin11 is not involved in the maturation of LGs (Figure 11 and 12); we examined specifically early events at the IS. TIRF microscopy is limited to fluorescence imaging in the area of the cell that is in the vicinity of the plasma membrane, we sought to analyze fluorescence signals in the entire cell. We performed live imaging of CTLs and target cells before and after contact (Methods section 2.2.15) in order to visualize the dynamics of Syntaxin11 and Granzyme B (LGs) in the entire cell. For that purpose we used CTLs expressing TFP vector as a control (Figure 18) and TFP-Syntaxin11 with Granzyme B-mCherry. We found that Syntaxin11 positive compartments are distinct from LGs and are randomly distributed in CTLs when not in contact with target cells (resting phase, figure 17). As CTLs polarize towards the target cell (polarization phase, figure 17), there is still a clear distinction between Syntaxin11 and LGs, more importantly Syntaxin11 compartments appear to polarize first. After CTLs and target cell conjugate (Figure 17), Syntaxin11 accumulates at the IS, followed by accumulation of LGs at the IS. The quantification of

colocalization between Syntaxin11 and LGs at different stages of IS formation is described in figure 19 (n=10) and shows a high degree of overlap between Syntaxin11 and LGs after formation of the IS in comparison to the resting state.

Thus, we conclude that Syntaxin11 containing vesicles polarize to the IS, delivering Syntaxin11 to the plasma membrane to serve as the t-SNARE for LG fusion.
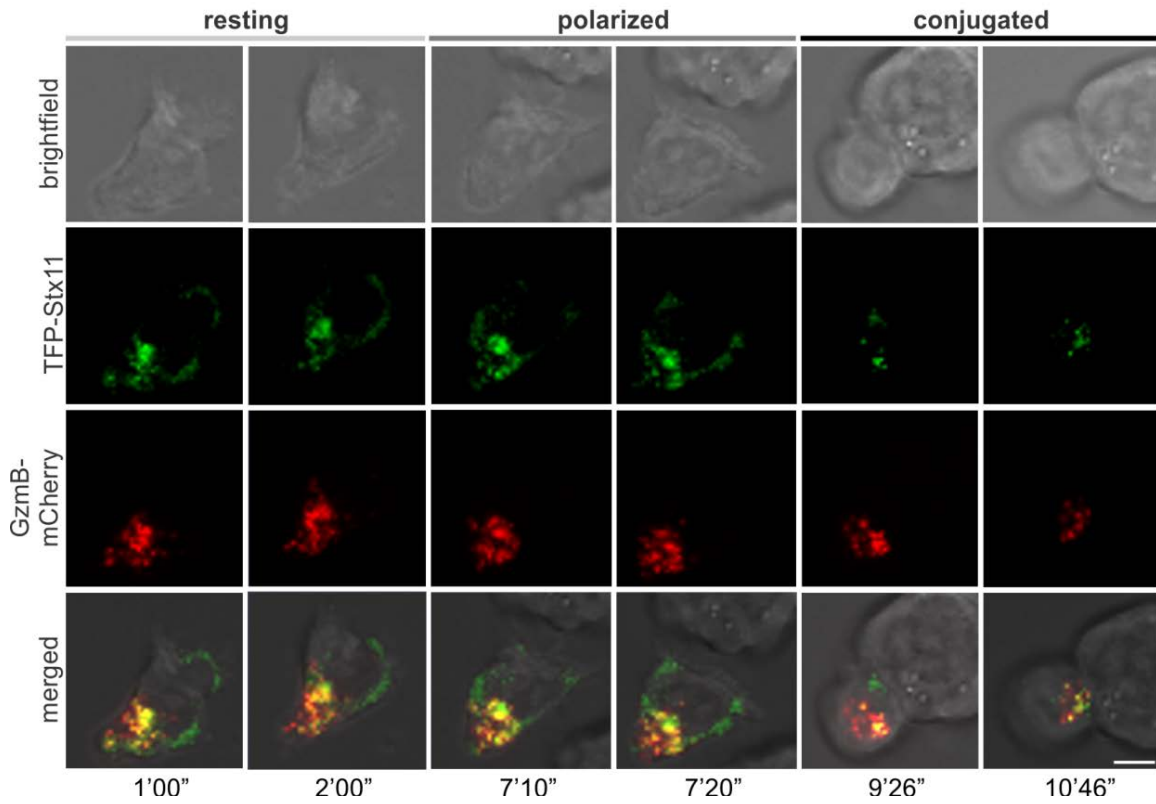

Figure 17: Syntaxin11 polarizes to the IS before LG accumulation
Dynamic imaging of TFP-Syntaxin11 (second panel, green) and Granzyme B-mCherry (third panel, red) in CTLs before and during IS formation. The merged images in the lower panel show that Syntaxin11 accumulates first at the cell-cell interface after conjugation while LGs arrive later. Scale bar: 5 µm.
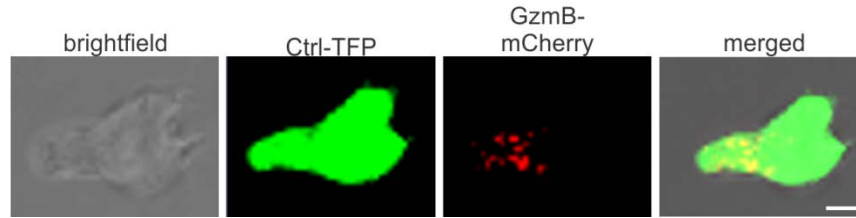
Figure 18: TFP plasmid and LGs in CTLs

Vector encoding for TFP was transfected along with LG marker Granzyme B-mCherry. TFP appears to be cytoplasmic compared to vesicular TFP-Syntaxin11. Scale bar: 5 μm.
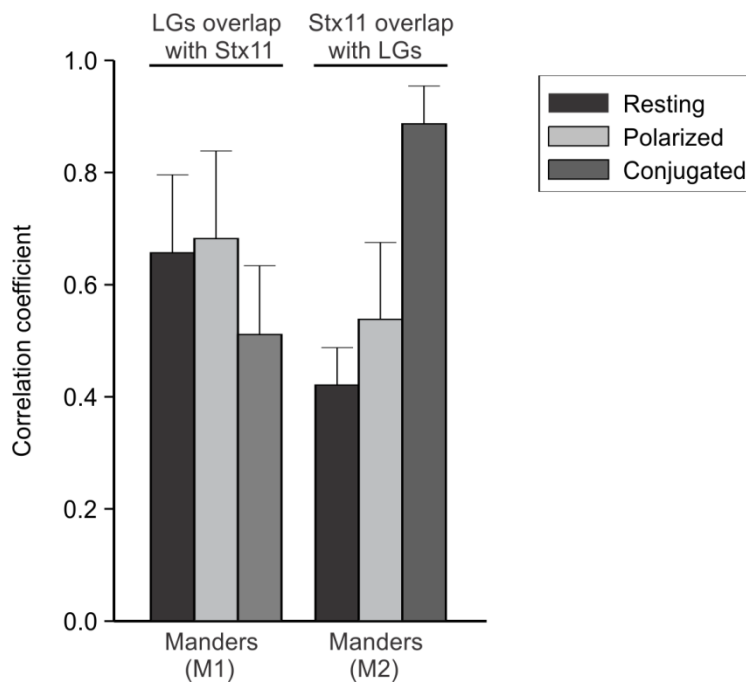
Figure 19: Syntaxin11 overlaps with LGs at the IS

Quantification of colocalization by Mander's coefficient for Syntaxin11 positive compartments and LGs in resting polarized and conjugated CTLs. The degree of Syntaxin11 and LG overlap increases upon conjugation of CTL with the target cell (n=10). Error bars are SEM.

3.7 Rab11a containing TCR positive recycling endosomes deliver Syntaxin11 to the IS

Rab GTPases are known for their association with endosomal compartments and play a major role in subcellular trafficking (Menager et al., 2007; Seabra and Wasmeier, 2004). Rab proteins such as Rab5a, Rab7a and Rab11a mark early, late and recycling endosomes respectively and mediate endosomal trafficking (Stenmark, 2009).

The next question we addressed was how do the Syntaxin11 vesicles get to the IS. Recycling endosomes (Rab11a positive compartments) play an important role in CTLs and are associated with key players required for LG release since they are required for transport of components for building the IS (Unpublished data), including the priming factor Munc13-4 (Menager et al., 2007). Therefore, we compared the temporal and spatial organization of Syntaxin11, to that of Rab11a containing recycling endosomes at the IS. Rab11a was overexpressed in CTLs (Figure 20; upper panel) to specifically label recycling endosomes along with TFP-Syntaxin11 (Figure 20; panel in the middle) or TFP vector as a control (Figure 21). The CTLs were added to coverslips coated with anti-CD3/CD28 ab to induce the formation of an IS and images were acquired in TIRFM.

We observed an early accumulation of Rab11a vesicles in the TIRF plane (at the IS) after the addition of CTLs to ab coated glass coverslips. Since recycling endosomes are involved in the early events that are necessary for the formation of an IS. We also observed a clear overlap between Rab11a compartments and Syntaxin11 compartments (Figure 23 A, 24 A). However, at later time points there were more Rab11a vesicles than Syntaxin11 positives vesicles, as depicted in figure 22. A possible explanation is that, the number of Syntaxin11 (t-SNARE) molecules are highly regulated and this intern controls the number of LG fusion events which are required for subsequent killing function.
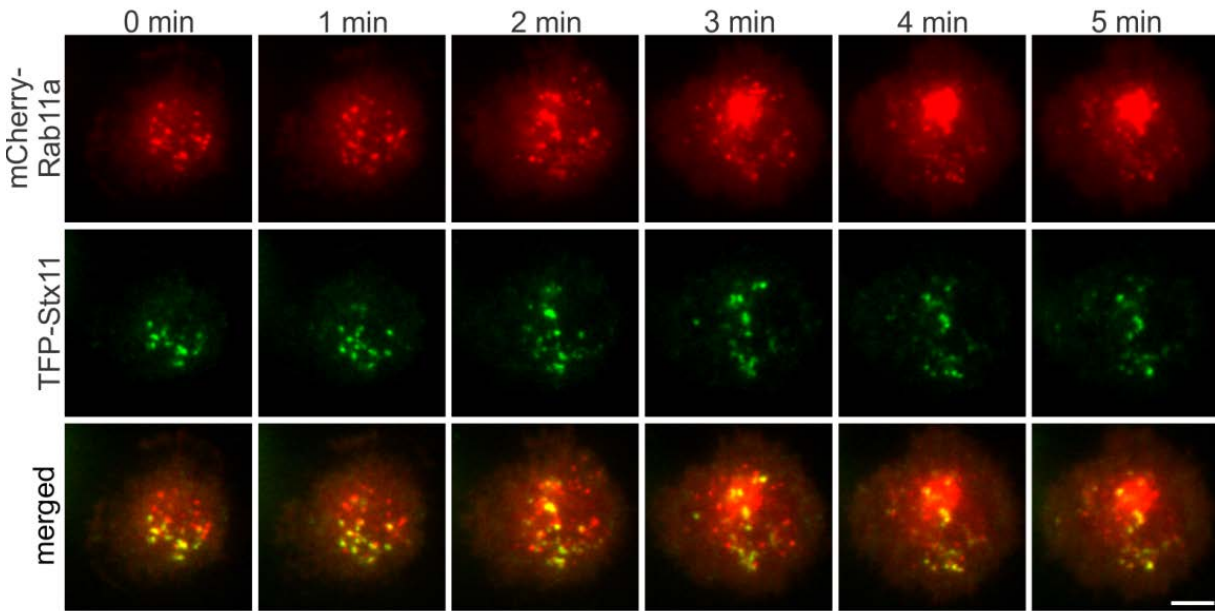
Figure 20: Recycling endosomes mediate the transport of Syntaxin11 to the IS

TIRFM images of CTLs transfected with TFP-Syntaxin11 (Green) and mCherry-Rab11a (Upper panel) at the IS (TIRFM plane). Images are acquired initially in extracellular solution without Ca^{2+}, after 3 min cells were perfused with extracellular solution containing 10 mM Ca^{2+}. Rab11a containing recycling endosomes deliver Syntaxin11, a target SNARE to the plasma membrane. Scale bar: 5 µm.
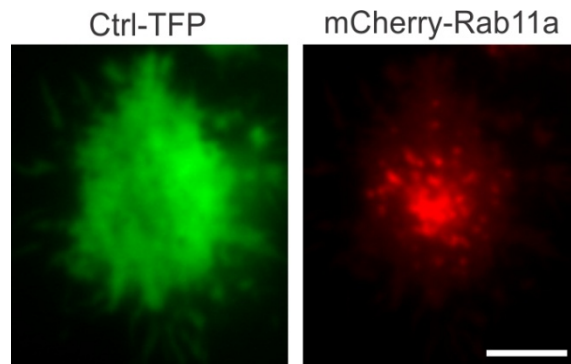
Figure 21: TFP encoding vector and recycling endosomes at the IS

TIRFM images of the CTL transfected with vector encoding for TFP (instead of TFP-Syntaxin11) and mCherry-Rab11a at the IS. Scale bar: 5 µm.

Colocalization of Syntaxin11 and Rab11a were tested using two independent approaches. We used line scans followed by graphical representation as shown in figure 23 and also applied the Mander's correlation as shown in figure 24. Fluorescence quantification of mCherry-Rab11a and TFP-Syntaxin11 at the IS over time shows that

(Figure 22), initial accumulation of Rab11a containing vesicles at the IS shows a strong overlap with Syntaxin11 fluorescence (Figure 23 A, 24 A). However, there is a continued steep increase in the number of Rab11a vesicles that is not associated with an increase in Syntaxin11; implicating Rab11a in trafficking of additional unidentified components to the IS.
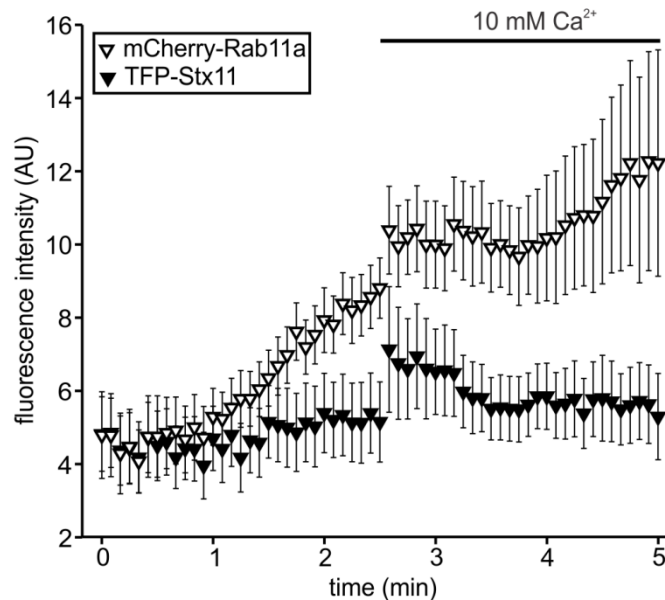
Figure 22: Quantification of recycling endosomes and Syntaxin11 vesicles/fluorescence at the IS
Quantification of the average fluorescence of Syntaxin11 and Rab11a at the TIRF plane shows that the fluorescence of Rab11a constantly increases overtime, whereas Syntaxin11 fluorescence remains more or less steady implying that the initial recycling endosomes bring Syntaxin11 to the IS (n=10). Error bars are SEM.

Syntaxin11 positive recycling endosomes are a small fraction within the recycling endosomes. To better define these Rab11a/Syntaxin11 positive compartments, we compared the colocalization of Rab11a to Syntaxin11 and then the colocaliaztion of Syntaxin11 to Rab11a, using the Mander's colocalization coefficient. We observed complete overlap of Syntaxin11 to Rab11a; Mander's colocalization coefficient = 0.8 ± 0.006 (n=26) and partial overlap of the Rab11a to that of Syntaxin11; Mander's colocalization coefficient = 0.2 ± 0.006 (n=26) as shown in figure 24 A.

We then searched for a subpopulation of recycling endosomes which might be essential for an IS formation. TCR/CD3 complexes play a crucial role in the initial recognition of MHC peptide on antigen presenting cells (Section 1.8). TCR/CD3 complex trafficking

occurs in three different ways. TCR/CD3 complexes are constantly recycled between the Golgi apparatus and cell membrane as a part of constitutive process to keep a CTL in an active state for target cell recognition. Upon recognition, the membrane associated TCR/CD3 complexes are transported to contact zone (IS) to stabilize the IS. Most TCR/CD3 aggregates via lateral diffusion to the IS. TCR/CD3 complexes are also delivered to the IS actively along microtubules. Polarization of the microtubule organizing center (MTOC) depends on TCR signaling by microtubule motor proteins in a dynein dependent manner. Hence MTOC and TCR trafficking is an interdependent process (Billadeau et al., 2007). Another way to deliver the TCR/CD3 is via Rab11a positive recycling endosomes (Cemerski and Shaw, 2006). Membrane associated TCR/CD3 complexes are constitutively endocytosed generating recycling endosomes and this process depends on the di-leucine-based (diL) receptor-sorting motif in the TCR subunit CD3γ (Geisler, 2004).

To define the Syntaxin11-positive vesicle subpopulation among the recycling endosomes, we transfected CTLs with CD3e-TFP along with Syntaxin11. There is a striking colocalization between Syntaxin11 and TCR/CD3 recycling compartments yielding a colocalization coefficient of 0.69, n = 15 (Figure 23 C, 24 C). Based on this result, we examined TCR and Rab11a association. To do so, we overexpressed CTLs with CD3e and Rab11a and carried out TIRF analysis on these cells. Overlap between TCR/CDe and Rab11a endosomes is comparable to that of Syntaxin11 and Rab11a (Mander's colocalization coefficient is 0.72 (n=8) (Figure 23 B, 24 B).
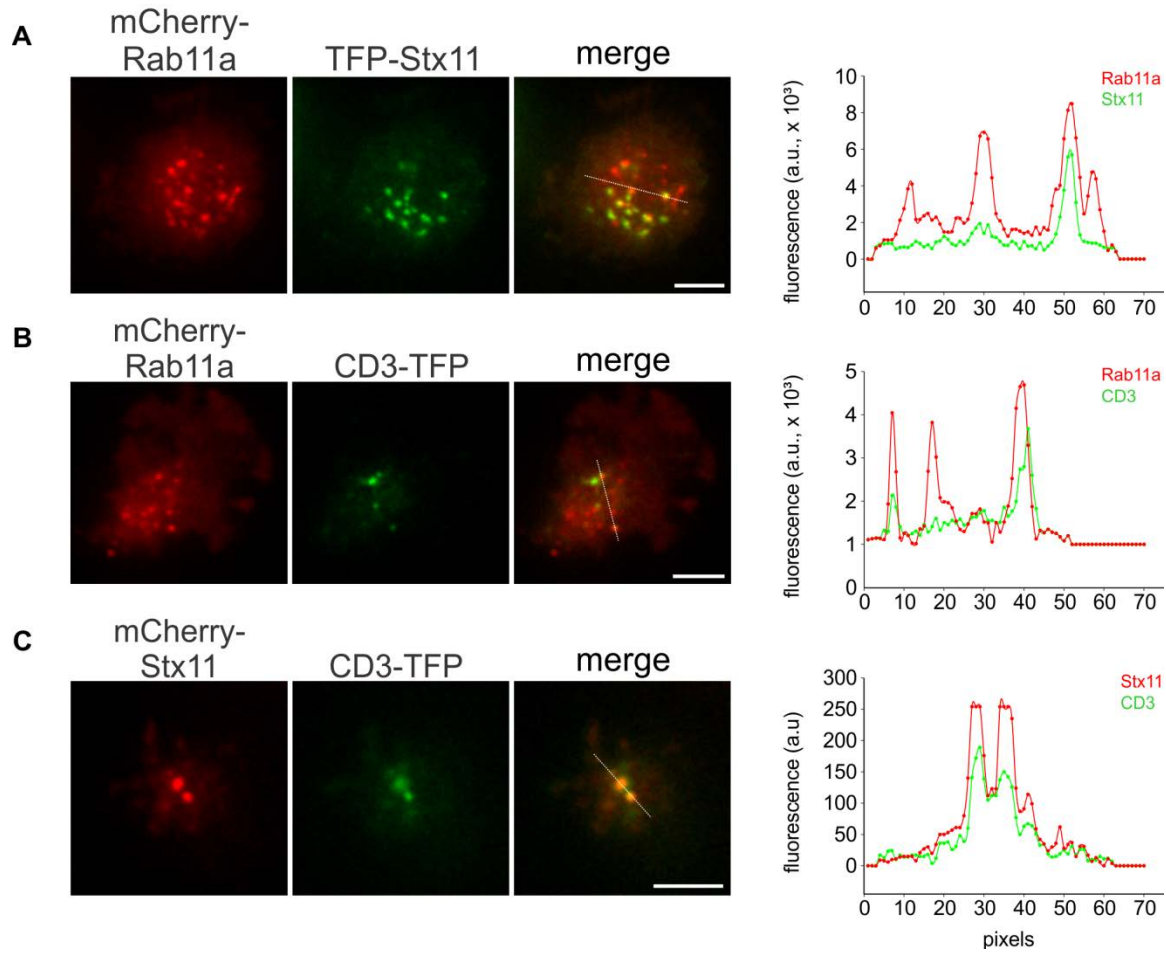
Figure 23: Recycling endosomes mediate the transport of TCR positive Syntaxin11 vesicles to the IS

TIRF images of CTLs transfected with mCherry-Rab11a along with TFP-Syntaxin11 (A) and CD3e-TFP (B) and CTLs co-transfected with mCherry-Syntaxin11 and CD3-TFP (C). Line scans along the stippled line on the merged images give rise to the fluorescence profiles (colocalization) of Syntaxin11 to Rab11a, CD3 to Rab11a and Syntaxin11 to CD3 shown on the right. Scale bar: 5 µm.

A

Stx11 and Rab11 colocalization analysis

M1: Stx11 overlap with Rab11 = 0.6;n=26
M2: Rab11 overlap with Stx11 = 0.21;n=26

B

CD3 and Rab11 colocalization analysis

M1: CD3 overlap with Rab11 = 0.72;n=8
M2: Rab11 overlap with CD3 = 0.17;n=8

C

CD3 and Stx11 colocalization analysis

M1: CD3 overlap with Stx11 = 0.69;n=15
M2: Stx11overlap with CD3 = 0.66;n=15

Figure 24: Colocalization analysis of recycling endosomes, Syntaxin11 and TCR

Quantification of the overlap between recycling endosomes, Syntaxin11 and TCR, using Mander's coefficient of colocalization. Bar graphs represent the strong overlap between (A) Syntaxin11 to Rab11a, (B) CD3 to Rab11a and (C) CD3 to Syntaxin11. Error bars are SEM.

4. DISCUSSION

We have examined the role of the protein Syntaxin11 in CTL function. Mutations within Syntaxin11 result in a disease called FHL that is the result of CTL dysfunction. We show that Syntaxin11 is the t-SNARE that is required for the final step of LG fusion at the IS. Downregulation of Syntaxin11 expression by RNA interference (RNAi) led to a dramatic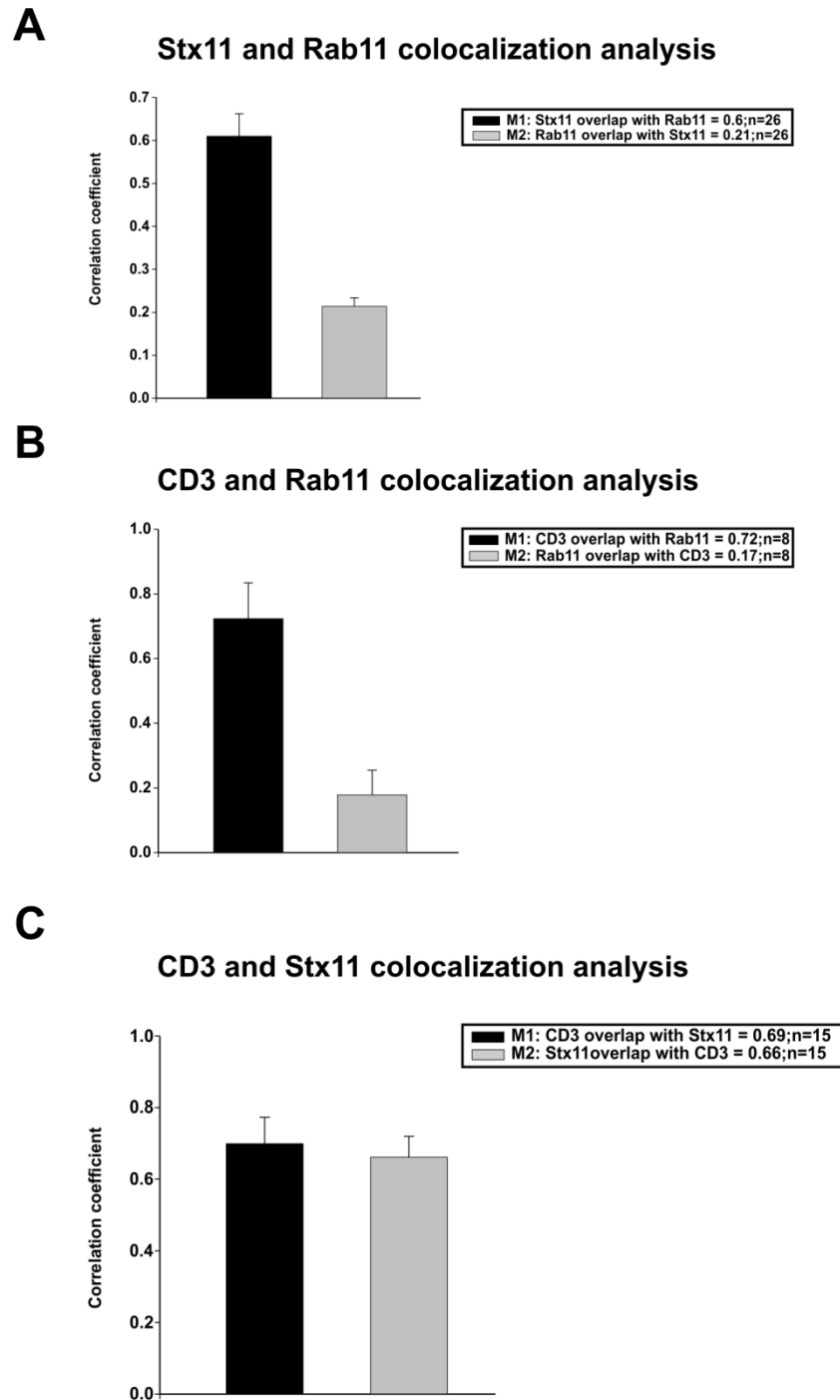 reduction in LG fusion at the IS concomitant with reduction in LG dwell time. RNAi treatment of primary human CTLs is a reliable method to study the mechanism of CTL function, since the phenotype is associated with FHL-4: reduced LAMP1a degranulation and CTL mediated target cell cytotoxicity.

We finally show that Syntaxin11 is colocalized with TCR/CD3 containing endosomal compartments which are delivered to the IS through Rab11a containing recycling endosomes (Figure 25 A, B and C).

4.1 SNARE proteins and the immune system

A newly synthesized protein must be transported to its respective target destination by intracellular trafficking processes. In immune cells, which are primarily secretory in function, release of proteins as messengers or effectors is also intimately tied to trafficking. SNARE proteins are the main players of intracellular trafficking since they are required for fusion of compartments which generates storage organelles and allows newly synthesized proteins to reach secretory vesicles (Stow et al., 2006). There are several other protein families that are also involved in trafficking and vesicle transport, such as the Rab GTPases, tethering factors and escort proteins

Loss of Syntaxin11 causes FHL-4, an immune disease with severe clinical manifestations (Bryceson et al., 2007; Danielian et al., 2010; zur Stadt et al., 2005). Other subtypes of FHL include FHL-2 (Feldmann et al., 2002; Horne et al., 2008) , FHL-3 (Feldmann et al., 2003) and recently identified FHL-5 (Cetica et al., 2010; Cote et al., 2009; zur Stadt et al., 2009). Major clinical symptoms (Section 1.9) include high levels of soluble IL-2 receptor in blood, less frequent central nervous system involvement; over activated macrophages, histiocytes and T cells with defective CTL and NK cell cytotoxicity, hemophagocytosis in bone marrow, cerebrospinal fluid or lymphonodes by

activated histiocytes and coagulopathy (Zhang et al., 1993; Zhizhuo et al., 2012; Zur Stadt et al., 2006).

FHL is due to uncontrolled activation or proliferation of effector cells (NK cell and CTLs), macrophages and histiocytes, due to inefficient eradication of pathogens or infections. This leads to an over production of cytokines resulting in hyperactivation of macrophages, which in turn leads to infiltration of tissues or organs by macrophages and eventual destruction of organs such as the liver and spleen (Horne et al., 2008; Janka, 1983).

Patients suffering from FHL have high serum levels of IFN-γ, TNF-α, interleukin IL-6, IL-8, IL-10, IL-12, IL-18 and macrophage inflammatory protein (MIP)-1α. Cytokines may also infiltrate tissues and promoting necrosis and organ failure. Fever and cytopenias are prominent in FHL and may be induced by several cytokines, such as TNF, IL-6 and IFN-γ. TNF also has a procoagulant activity, which accounts for hypofibrinogenaemia. Hypertriglyceridaemia is associated with reduced lipoprotein lipase (Janka, 2007; Osugi et al., 1997).

Identification of the molecular defects associated with FHL gives insight into the mechanisms by which pathology occurs. Congenital defects associated with either impaired perforin synthesis or any defect in perforin function results in FHL-2. Perforin is a 67 kDa protein stored in conjunction with Granzymes (a group of serine proteases) in secretory lysosomes or mature LGs in NK cells and CTLs. These proteins are released simultaneously at the IS through exocytosis. Upon release, perforin polymerizes and generates transmembrane pores in target cell membrane of about 10-20 nm in diameter through which granyzmes can enter the target cell in order to induce apoptosis (Voskoboinik et al., 2006). Some of the missense mutations in *PRF1* gene result in a conformational change within the perforin molecule which prevents proteolytic cleavage of perforin precursors into functional perforin. As a result, the functional form of the protein is absent, resulting in serious consequences (Risma et al., 2006).

Another form of FHL, FHL-3 is due to mutations of Munc13-4, thought to be the priming factor for LGs in NK cells and CTLs. FHL-3 accounts for 20% - 30% of all FHL cases (Janka, 2007). The Munc13 protein family includes Munc13-1, Munc13-2, Munc13-3 and Munc13-4. Munc13s have characteristic C2 domains and MHD domains, required for vesicle priming. Munc13-4 is believed to be an effector for Rab27a, a protein directly

associated with Griscelli syndrome type 2 (GS2) (See section 1.9). Mutations within Munc13-4 and Rab27a can disrupt the interaction between the two proteins and this disrupts their ability to promote fusion. The Munc13-4*Rab27a complex interaction is not required for maturation of secretory lysosomes (LGs) rather it is necessary for tethering of the LGs to plasma membrane. Moreover, the Munc13-4*Rab27a complex enhances the stability the SNARE complex required for the fusion of the LGs (Elstak et al., 2012; Elstak et al., 2011; Neeft et al., 2005). Elevated levels of perforin molecules have been reported in the CTLs of FHL-3 patients, consistent with LG priming defects (Bryceson et al., 2007). In vitro studies have shown that Munc13-4 promotes Ca^{2+}-dependent SNARE complex formation and SNARE-mediated liposome fusion. These properties of Munc13-4 led to the suggestion that it functions as a Ca^{2+} sensor which modulates priming, the rate-limiting step in granule exocytosis (Boswell et al., 2012).

Recently another form of FHL (FHL-5) has been associated with mutations in *STXBP2* encoding Syntaxin binding protein 2 (Munc18-2) a protein involved in the regulation of intracellular trafficking which also controls SNARE complex assembly. Studies with FHL-5 patient samples showed that mutations within Munc18-2, completely disrupt its ability to interact with Syntaxin11, thus leading to a defect at the final step of cytotoxic granule secretion (Cote et al., 2009; zur Stadt et al., 2009).

Involvement of Syntaxin11 in FHL-4 is well established on the basis of defective degranulation and cytotoxicity in patients carrying mutations within the coding region of *Stx11* gene. However, degranulation and cytotoxicity can be partially reconstituted using high doses of recombinant IL-2 treatment in FHL-3 and FHL-4 patient samples (Bryceson et al., 2007; Horne et al., 2008; Schneider et al., 2002).

4.2 Syntaxin11 and LGs: direct or indirect interaction

Inherited defects in immune function associated with mutations within the coding region of Syntaxin11 indicate an important role in immune cells. Syntaxin11 is expressed in neutrophils and is upregulated when neutrophils differentiate. This has been shown using the neutrophil differentiation marker CD11b at both the mRNA and protein levels (Xie et al., 2009), Syntaxin11 is expressed in monocytes and macrophages (Offenhauser et al., 2011; zur Stadt et al., 2005), Syntaxin11 is also expressed in NK cells (Dabrazhynetskaya et al., 2012). In our study, we show that Syntaxin11 is

expressed in CD8^{+} cells and its expression is upregulated 3 folds upon stimulation which we confirmed with qRT-PCR (Figure 7). This result is consistent with studies on other immune cells which also show specific upregulation of certain SNAREs upon cell activation (Murray et al., 2005). Since, it is known that, mutations in Syntaxin11 results in defective degranulation, as previously shown in FHL-4 patient samples (Bryceson et al., 2007). We began our study with the degranulation assay which is an indirect measure of LG exocytosis. CTLs were treated with Syntaxin11 specific siRNA to knock down endogenous Syntaxin11 expression. We found that, Syntaxin11 knockdown led to a 76 % (Figure 9 C) reduction in LAMP1a degranulation in CTLs.

We confirmed these results using an independent approach to test the ability of CTLs for target cell cytotoxicity. Based on previous observations (Bryceson et al., 2007; D'Orlando et al., 2012), Syntaxin11 involvement in cytotoxicity is evident and over expression of Syntaxin11 in NK cells led to significant increase in the killing of the NK-sensitive tumor targets, 721 and K562 cells. Decreased expression of Syntaxin11 (knockdown studies using siRNA) reduced cytotoxicity in NK cells (Arneson et al., 2007).

We observed a severe defect in the ability of CTLs to kill target cells after Syntaxin11 expression was reduced, in contrast to control siRNA treated CTLs (Figure 10). This effect is specific for Syntaxin11 knockdown.

Based on our results showing defective LAMP1a degranulation and target cell cytotoxicity in CTLs that were knocked down for Syntaxin11, we used TIRFM to specifically look at the behavior of the LGs at the PM (Pattu et al., 2011).

The observation that loss of Syntaxin11 leads to FHL-4 led to speculation about a role for Syntaxin11 in CTLs and NK cells. However, the lack of appropriate high resolution techniques, has limited the progress in identifying the site where Syntaxin11 functions. We show that there are observable changes in LG behavior in real time, using evanescent wave microscopy (TIRFM) (Pattu et al., 2011). TIRFM allows us to visualize the events prior to fusion at the plasma membrane such as docking and priming, in addition to fusion.

Our TIRFM experiments in CTLs using Syntaxin11 siRNA, reveal a dramatic reduction in the fusion of LGs in CTLs. This result is in agreement with the results of LAMP1a degranulation and target cell cytotoxicity assay (Figure 9, 10). Further analysis revealed

that the LGs are unable to fuse at the IS, mainly because of defect in LG docking as confirmed by the dwell time analysis of LGs (Figure 12 B). The LGs failed to fuse at the IS in CTLs which are knocked down for Syntaxin11 (Figure 11 B).

4.3 Syntaxin11, a target SNARE for the fusion of LGs

Based on our findings we confirm that Syntaxin11 is not involved in LG maturation steps or in endosomal maturation. Syntaxin11 has been reported to be localized to TGN (Trans-Golgi network) and late endosomes in Hela cells (Tang et al., 1998a; Valdez et al., 1999), TGN and Cis-Golgi complex (Prekeris et al., 2000), specific tertiary granules in neutrophils (Xie et al., 2009), the plasma membrane in NK cells and CTLs (Arneson et al., 2007), growth hormone (GH) containing granules in GH producing cell line MtT/S cells (Kawashima et al., 2010), post Golgi in normal rat kidney cells (NRK cells) (Advani et al., 1998), plasma membrane in macrophages (Zhang et al., 2008), localized to mannose 6- phosphate receptor (M6PR) intracellular compartments, Rab27a positive vesicles and cytotoxic granules in NK cells (Dabrazhynetskaya et al., 2012), late endosomes and lysosomes in macrophages (Offenhauser et al., 2011).

Based on the functional studies in FHL-4 patient samples (zur Stadt et al., 2005), Syntaxin11 KO mouse (D'Orlando et al., 2012) and localization studies, it was proposed that Syntaxin11 mediates the fusion between late endosomes and lysosomes in macrophages (Offenhauser et al., 2011) and M6PR positive vesicles containing Rab27a and cytotoxic granules in NK cells (Dabrazhynetskaya et al., 2012). A role for Syntaxin11 in platelet secretion (Ye et al., 2012) and LG secretion in CTLs has been reported (Arneson et al., 2007; Bryceson et al., 2007; D'Orlando et al., 2012). Syntaxin11 has been proposed as the t-SNARE on the plasma membrane for the fusion of LGs at the IS (de Saint Basile et al., 2010; Hong, 2005).

A functional SNARE complex includes four SNARE helical bundles contributed by three cognate SNARE partners, typically Syntaxin, SNAP and synaptobrevin (Section 1.8 and 1.10). Members of the Syntaxin family belong to the prototype family of SNARE proteins, which have a characteristic trans-membrane domain at the carboxy-terminal end for anchoring to the plasma membrane attached to a coiled-coil domain by a short

linker. There are 15 members of the Syntaxin family in the human genome (Teng et al 2001).

The striking reduction of LG fusion (Figure 11) and dwell time (Figure 12) after knock down of Syntaxin11 provoked us to look at the association between LGs and Syntaxin11. To do so, we overexpressed CTLs with mCherry-Syntaxin11 along with the LG marker; Granzyme B-TFP and imaged them in TIRFM. We saw a strong overlap between Syntaxin11 clusters and LGs at the TIRF plane (at the IS).

Similar clusters of Syntaxin1A, the t-SNARE for synaptic vesicle fusion in neurons, have been reported in neurons. Other detailed studies of Syntaxin clusters at the plasma membrane or in cell free (in-vitro) systems have shown the interaction between Syntaxin and single secretory granules by dual color TIRFM in other cell types (Bar-On et al., 2009; Barg et al., 2010). Barg et al., (2010) showed that Syntaxin-GFP assembled in clusters at sites where single granules had docked at the plasma membrane. These clusters were intermittently present at granule sites, as Syntaxin molecules assembled and disassembled in a coordinated fashion. The clusters facilitated exocytosis and disassembled once exocytosis was complete. Syntaxin cluster formation defines an intermediate step in exocytosis. Further this Syntaxin clustering is mediated by electrostatic interactions with the strongly anionic lipid phosphatidylinositol-4, 5 - bisphosphate (PIP2) (van den Bogaart et al., 2009). Apart from Syntaxin1 A, clustering of other Syntaxins like Syntaxin3 and 4 have been reported in other cells (Low et al., 2006).

In agreement with the findings described above and based on our results, it is clear that in CTLs Syntaxin11 has a tendency to form clusters at the membrane, thus creating hotspots for the arriving LGs to fuse at the plasma membrane (Figure 14, 25 B and 25 C). Moreover, these findings provide clear evidence that Syntaxin11 functions as the only t-SNARE for LG fusion at the IS. These findings are supported by analysis of the average fluorescence intensity over time for both the Syntaxin11 clusters and the LGs at the IS (Figure 16). The fluorescence of Syntaxin11 always remained higher than that of the LGs at the IS. This phenomenon is in agreement with other reports that demonstrate a typical t-SNARE behavior on the PM (Bar-On et al., 2009; Barg et al., 2010). In our TIRF experiments with Syntaxin11 and LGs, as described in figure 14, we observed a strong overlap between the Syntaxin11 clusters and LGs, but, due to the

very narrow time window or time gap between the Syntaxin11 and LGs arrival, it was not possible to differentiate between the arrival of Syntaxin11 and LGs at the IS. We suggest that Syntaxin11 is the t-SNARE for lytic granule fusion. If this is true, Syntaxin11 should arrive at the IS prior to the arrival of LGs. We turned to live cell imaging to address the question of the arrival timing of Syntaxin11 and LGs at the IS. We used CTLs overexpressing TFP-Syntaxin11 and the LG marker Granzyme B-mCherry and imaged the cell before, during and after target cell contact. The pattern of distribution for Syntaxin11 positive compartments is completely different from those of LGs and TCR positive compartments. Interestingly, Syntaxin11 expression is abundant and exclusively in the polarizing end of the CTL i.e. uropods while the LGs are observed in the trailing part of the cell. Once the resting CTL recognizes its target cell, the CTL reorients itself completely towards the target cell. Immediately after target cell contact, Syntaxin11 positive cargo vesicles are delivered to the IS. Since, Syntaxin11 is the t-SNARE for LG fusion, it is expected to be delivered to the IS before LGs. After the CTL establishes firm contact with the target cell, the final step of LG polarization to the IS and fusion occur. The lethal hit occurs at the sites where the Syntaxin11 has accumulated. We observed the same phenomenon by both TIRFM on antibody coated glass coverslips (Figure 14) and by live imaging with target cells (Figure17).

4.4 In which compartments does Syntaxin11 reside?

Rab11a positive recycling endosomal compartments are known for their role in trafficking of Munc13-4 to the IS. We examined the association between Rab11a and the Syntaxin11 positive compartments. In our colocalization analysis, we observed a partial overlap of Syntaxin11 with Rab11a; Mander's colocalization coefficient = 0.8 ± 0.006 and of Rab11a with Syntaxin11; Mander's colocalization coefficient = 0.2 ± 0.006). Imaging in TIRFM showed a strong correlation between Rab11a and Syntaxin11 in TIRFM (Figure 20), this overlap was seen only in the Rab11a positive vesicles seen early in the experiment, providing evidence that these vesicles bring the Syntaxin11 molecules to the IS (Figure 25 A).

There was a strong overlap of fluorescence (Figure 22), but the fluorescence signal of Syntaxin11 remained constant throughout the acquisition in contrast to Rab11a, which showed an exponential increase. This is in line with the role of recycling endosomes in

delivery of components required for IS formation, the fluorescent signal of Syntaxin11 remains unchanged throughout the acquisition. This can be explained by the limited number of t-SNAREs that are delivered to the IS. The t-SNARE availability could control the number of LG fusion events per target cell.


4.5 Relevance of TCR/CD3 association with Syntaxin11 and the IS

We have defined the vesicles positive for both Syntaxin11 and Rab11a. Recycling TCR/CD3 complexes are an essential part of recycling endosomes and behave similarly to Rab11a positive recycling endosomes. The *TCR* gene has different subunits; TCR alpha, beta, gamma and delta. In thymus, T lymphocytes are classified based on which TCR complex they express on their surface. CD8$^+$ cells found in the thymus are either TCR alpha-beta cells or TCR gamma-delta cells (Correale et al., 1997). Similarly, CD3 occurs in different subunits, also called chains (gamma, delta- and epsilon-chain) (Clevers et al., 1988; Kearse et al., 1995).

We performed TIRF experiments using CTLs transfected with CD3e along with the Syntaxin11 and Rab11a. Interestingly, we found a significant amount of colocalization between intracellular CD3e positive compartments and Syntaxin11 compartments (Mander's colocalization; CD3e to Syntaxin11 = 0.8, Syntaxin11 overlapping CD3e = 0.8). Since Rab11a shows partial overlap with CD3e (Mander's colocalization; CD3e to Rab11a = 0.72; n=8, Rab11a overlapping CD3e = 0.17; n=8), this is in accordance with our results depicting a partial overlap between Syntaxin11 and Rab11a compartments. Therefore, based on our results, we conclude that a subpopulation of Rab11a containing recycling endosomes that contains TCR/CD3e/Syntaxin11, delivers the Syntaxin11 to the IS as depicted in the figure below (Figure 25 A).

Based on our results obtained in this study, we postulate a model that depicts the involvement of Rab11a recycling endosomes in bringing TCR/CD3 complexes along with Syntaxin11 to the IS (Figure 25 A). This results in the formation of Syntaxin11 clusters, hotspots for SNARE dependent LG fusion (Figure 25 B and C).

C
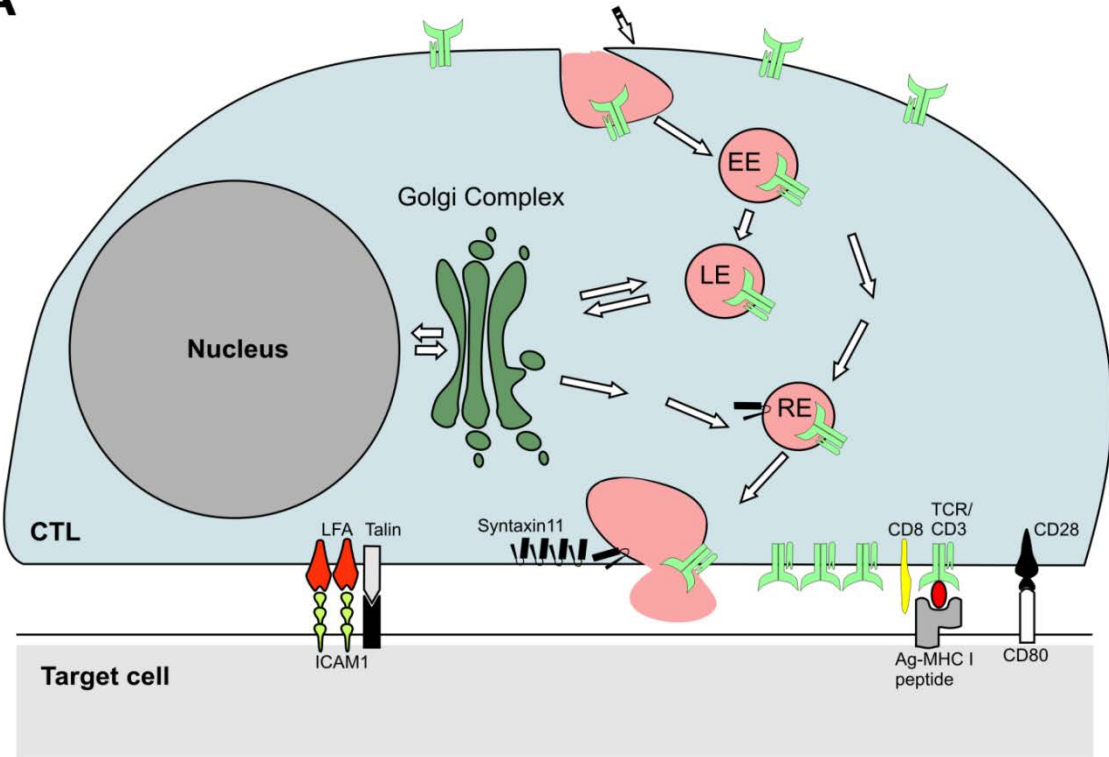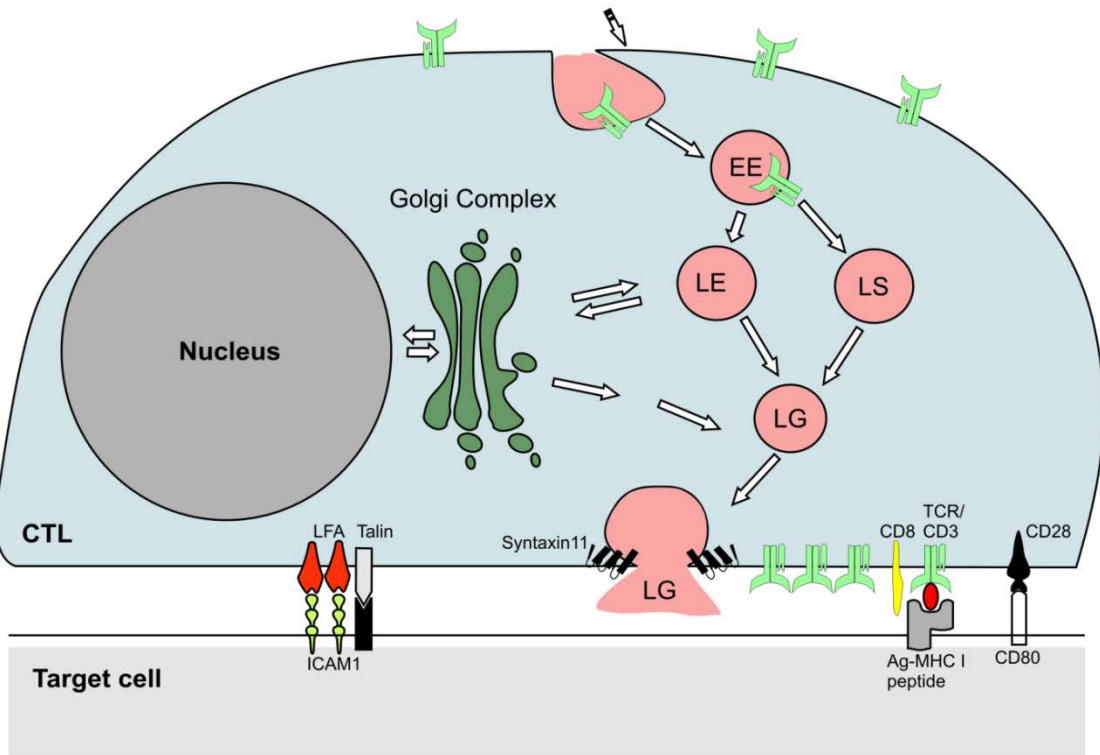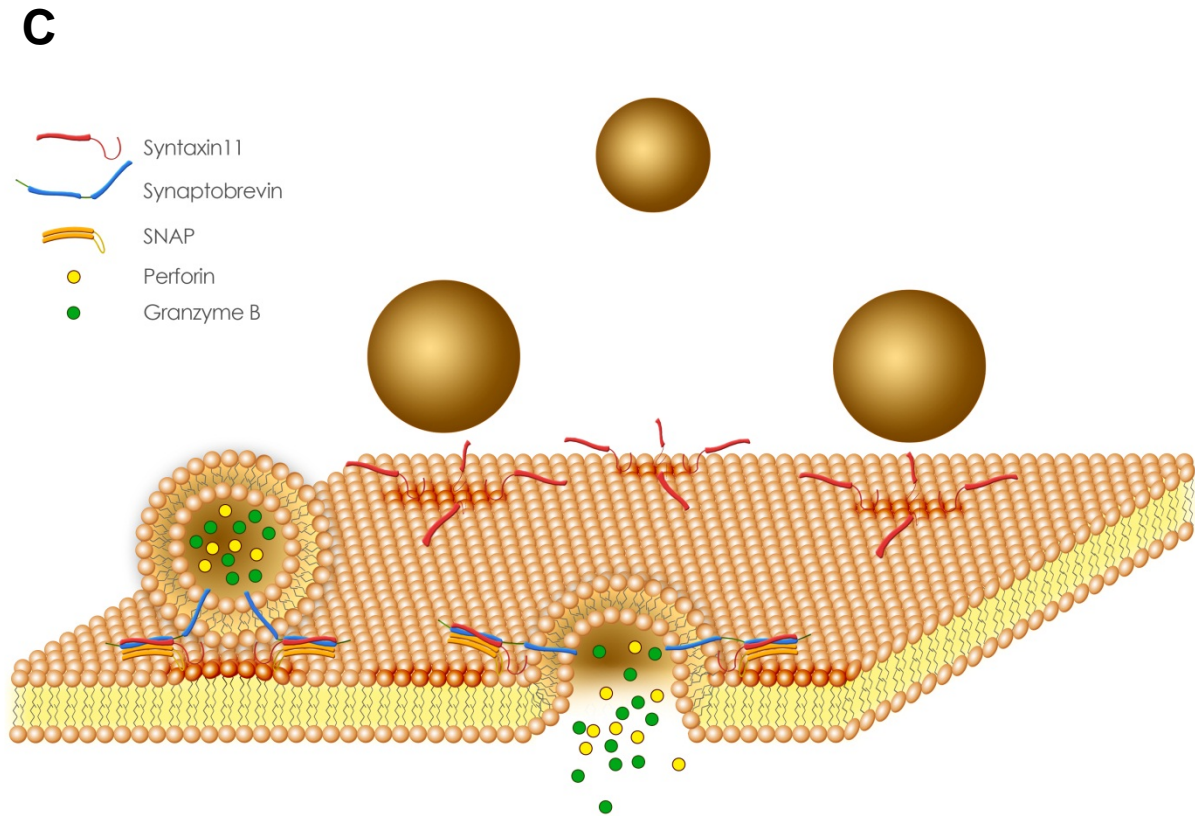
Figure 25: The fusion of LGs at the hotspots containing Syntaxin11 clusters

(A) TCR/CD3 containing endosomes fuse with Syntaxin11 containing recycling endosomes via early endosomes (EE) and late endosomes (LE).They are then delivered to the IS, thus stabilizing the IS for LGs arrival. (B) LGs dock, prime and fuse at the hotspots that contain Syntaxin11 clusters (t-SNARE). through either from lysosomes (LS) or from LEs, arrives at the hotspots containing Syntaxin11 clusters (t-SNARE) for fusion at the IS. (C) Syntaxin11 along with cognate SNARE partners, Synaptobrevin (blue) and SNAP (yellow) mediates the final fusion of LGs at the immunological synapse.

5. OUTLOOK

Elucidation of the function of Syntaxin11 in LG fusion at the IS, furthers our understanding of CTL function. Though a number of questions remain, the pivotal role of Syntaxin11 in T cells provides a potential target for future therapy, including the possibility of gene therapy replacement of Syntaxin11.

As discussed above Syntaxin11 has already received much attention in T cells, in mouse models of FHL-4, knockout of Syntaxin11 does not reproduce the lethality or phenocopy of FHL-4, unless Syntaxin11 KO mice are challenged with viral infections. It is likely that this difference is due to the lack of pathogen challenge in mouse models. This possibility should be addressed. In addition, the possibility of redundancy and/or promiscuity of various Syntaxins in CTLs must also be addressed.

Based on all the facts discussed above and in line with Bryceson et al (2007), we speculate that the severity of FHL-4 is much less when compared to FHL-2 and 3. Reconstitution of FHL-4 defects by substituting with recombinant IL-2 could be because there are some redundant SNARE proteins which compensate for Syntaxin11 function or that IL-2 stimulation induces a Syntaxin11 independent lytic granule degranulation pathway.

6. SUMMARY

We elucidate the molecular mechanism of lytic granule fusion in CTLs by identifying the Syntaxin11 as a t-SNARE for LG exocytosis. We knockdown the expression of Syntaxin11 in CTLs and showed that there is a strong reduction in LG fusion at the IS that is accompanied by a reduction in the dwell time of LGs at the plasma membrane. In agreement with the reported phenotype in FHL-4 and Syntaxin11 KO mice, we showed that CTLs treated with Syntaxin11 siRNA show reduced degranulation. In addition, these CTLs fail to kill target cells. Using high resolution microscopic techniques we show that Syntaxin11 moves from in intracellular compartments along with recycling TCRs, to the IS, in Rab11a positive recycling endosomes. The trafficking of Syntaxin11 along with TCRs clearly demonstrates that LG polarization towards the IS is a completely independent process that occurs after recycling endosomes have built a functional IS by bringing in all the essential early components for IS formation. Therefore, TCR-CD3 complexes, which strengthen the IS and the t-SNARE, Syntaxin11, which docks arriving LGs, polarize to the IS prior to LGs delivery.

Thus, we show that Syntaxin11 is not involved in the maturation steps of LGs or of any other intracellular compartment. This disproves all earlier reports indicating an involvement of Syntaxin11 in LG maturation steps. This conclusion is supported by TIRFM, fusion analysis and dwell time analysis, in which we show that there is no significant change in the number of LGs at the IS.

Our study gives new insights into the mechanisms of CTL mediated cytotoxicity. Our results answer the molecular basis of FHL-4, a genetic disorder resulting in a defect in CTL function, caused by mutations in Syntaxin11.

7. LITERATURE

Abbas, A. K., Lichtman, A. H., (2007). Basics of immunology. 3rd Edition, Saunders ELSEVIER.

Advani, R. J., Bae, H. R., Bock, J. B., Chao, D. S., Doung, Y. C., Prekeris, R., Yoo, J. S. and Scheller, R. H. (1998). Seven novel mammalian SNARE proteins localize to distinct membrane compartments. *J Biol Chem 273*, 10317-10324.

Andersen, M. H., Schrama, D., Thor Straten, P. and Becker, J. C. (2006) Cytotoxic T cells. *J Invest Dermatol 12,* 32-41.

Arneson, L. N., Brickshawana, A., Segovis, C. M., Schoon, R. A., Dick, C. J. and Leibson, P. J. (2007). Cutting edge: Syntaxin 11 regulates lymphocyte-mediated secretion and cytotoxicity. *J Immunol 179,* 3397-3401.

Baetz, K., Isaaz, S. and Griffiths, G. M. (1995). Loss of cytotoxic T lymphocyte function in Chediak-Higashi syndrome arises from a secretory defect that prevents lytic granule exocytosis. *J Immunol 154*, 6122-6131.

Bar-On, D., Gutman, M., Mezer, A., Ashery, U., Lang, T. and Nachliel, E. (2009). Evaluation of the heterogeneous reactivity of the Syntaxin molecules on the inner leaflet of the plasma membrane. *J Neurosci 29,* 12292-12301.

Barg, S., Knowles, M. K., Chen, X., Midorikawa, M. and Almers, W. (2010). Syntaxin clusters assemble reversibly at sites of secretory granules in live cells. *Proc Natl Acad Sci U S A 107,* 20804-20809.

Barnard, R. J., Morgan, A. and Burgoyne, R. D. (1996). Domains of alpha-SNAP required for the stimulation of exocytosis and for N-ethylmalemide-sensitive fusion protein (NSF) binding and activation. *Mol Biol Cell 7,* 693-701.

Barry, M., and Bleackley, C. (2002). Cytotoxic T lymphocytes: all roads lead to death. *Nat Rev Immunol 2,* 401-9.

Becherer, U., Medart, MR., Schirra, C., Krause, E., Stevens, D., and Rettig, J. (2012). Regulated exocytosis in chromaffin cells and cytotoxic T lymphocytes: how similar are they? *Cell Calcium 52*, 303-12.

Bennett, M. K., Garcia-Arraras, J. E., Elferink, L. A., Peterson, K., Fleming, A. M., Hazuka, C. D. and Scheller, R. H. (1993). The Syntaxin family of vesicular transport receptors. *Cell 74,* 863-873.

Billadeau, D. D., Nolz, J. C. and Gomez, T. S. (2007). Regulation of T-cell activation by the cytoskeleton. *Nat Rev Immunol 7*, 131-143.

Bock, J. B., Matern, H. T., Peden, A. A. and Scheller, R. H. (2001). A genomic perspective on membrane compartment organization. *Nature 409*, 839-841.

Bogaart, G., Meyenberg, K., Risselada, H. J., Amin, H., Diederichsen, U. and Jahn, R. (2009). Membrane protein sequestering by ionic protein-lipid interactions. *Nature 479*, 552-555.

Boswell, K. L., James, D. J., Esquibel, J. M., Bruinsma, S., Shirakawa, R., Horiuchi, H. and Martin, T. F. (2012). Munc13-4 reconstitutes calcium-dependent SNARE-mediated membrane fusion. *J Cell Biol 197,* 301-312.

Bousso, E. A. R. (2004). Dynamic Behavior of T Cells and Thymocytes in Lymphoid Organs as Revealed by Two-Photon Microscopy. *Immunity 3,* 349-55

Bromley, S. K. and Dustin, M. L. (2002). Stimulation of naïve T-cell adhesion and IS formation by chemokine-dependent and -independent mechanisms. *Immunology 106*, 289-298.

Brose, N., Hofmann, K., Hata, Y. and Sudhof, T. C. (1995). Mammalian homologues of Caenorhabditis elegans unc-13 gene define novel family of C2-domain proteins. *J Biol Chem 270*, 25273-25280.

Bryceson, Y. T., Rudd, E., Zheng, C., Edner, J., Ma, D., Wood, S. M., *et al.* (2007). Defective cytotoxic lymphocyte degranulation in Syntaxin-11 deficient familial hemophagocytic lymphohistiocytosis 4 (FHL4) patients. *Blood 110,* 1906-1915.

Cemerski, S. and Shaw, A. (2006). Immune synapses in T-cell activation. *Curr Opin Immunol 18,* 298-304.

Cetica, V., Santoro, A., Gilmour, K. C., Sieni, E., Beutel, K., Pende, D., Marcenaro, S., Koch, F., Grieve, S., Wheeler, R*., et al.* (2010). STXBP2 mutations in children with familial haemophagocytic lymphohistiocytosis type 5. *J Med Genet 47,* 595-600.

Chen, Y. A. and Scheller, R. H. (2001). SNARE-mediated membrane fusion. *Nat Rev Mol Cell Biol 2,* 98-106.

Clevers, H., Alarcon, B., Wileman, T. and Terhorst, C. (1988). The T cell receptor/CD3 complex: a dynamic protein ensemble. *Annu Rev Immunol 6,* 629-662.

Correale, J., Rojany, M. and Weiner, L. P. (1997). Human CD8+ TCR-alpha beta(+) and TCR-gamma delta(+) cells modulate autologous autoreactive neuroantigen-specific CD4+ T-cells by different mechanisms. *J Neuroimmunol 80,* 47-64.

Cote, M., Menager, M. M., Burgess, A., Mahlaoui, N., Picard, C., Schaffner, C., *et al.* (2009). Munc18-2 deficiency causes familial hemophagocytic lymphohistiocytosis type 5 and impairs cytotoxic granule exocytosis in patient NK cells. *J Clin Invest 119,* 3765-3773.

D'Orlando, O., Zhao, F., Kasper, B., Orinska, Z., Muller, J., Hermans-Borgmeyer, I., *et al.* (2012). Syntaxin 11 is required for NK and CD8(+) T-cell cytotoxicity and neutrophil degranulation. *Eur J Immunol. 43,* 194-208

Dabrazhynetskaya, A., Ma, J., Guerreiro-Cacais, A. O., Arany, Z., Rudd, E., Henter, J. I, *et al.* (2012). Syntaxin 11 marks a distinct intracellular compartment recruited to the IS of NK cells to colocalize with cytotoxic granules. *J Cell Mol Med 16,* 129-141.

Danielian, S., Basile, N., Rocco, C., Prieto, E., Rossi, J., Barsotti, D., *et al.* (2010). Novel Syntaxin 11 gene (STX11) mutation in three Argentinean patients with hemophagocytic lymphohistiocytosis. *J Clin Immunol 30,* 330-337.

de Saint Basile, G., Menasche, G. and Fischer, A. (2010). Molecular mechanisms of biogenesis and exocytosis of cytotoxic granules. *Nat Rev Immunol 10,* 568-579.

Delon, J., Kaibuchi, K. and Germain, R. N. (2001). Exclusion of CD43 from the IS is mediated by phosphorylation-regulated relocation of the cytoskeletal adaptor moesin. *Immunity 15,* 691-701.

Eisenbarth, S. C. and Flavell, R. A. (2009). Innate instruction of adaptive immunity revisited: the inflammasome. *EMBO Mol Med 1,* 92-98.

Elstak, E. D., Neeft, M., Nehme, N. T., Callebaut, I., de Saint Basile, G. and van der Sluijs, P. (2012). Munc13-4*rab27 complex tethers secretory lysosomes at the plasma membrane. *Commun Integr Biol 5,* 64-67.

Elstak, E. D., Neeft, M., Nehme, N. T., Voortman, J., Cheung, M., Goodarzifard, M., *et al.* (2011). The Munc13-4-rab27 complex is specifically required for tethering secretory lysosomes at the plasma membrane. Blood *118*, 1570-1578.

Finetti, F. and Baldari. (2009). Intraflagellar transport is required for polarized recycling of the TCR/CD3 complex to the immune synapse. Nat Cell Biol.11, 1332-1339.

Fais, S. and Malorni, W. (2003). Leukocyte uropod formation and membrane/cytoskeleton linkage in immune interactions. *J Leukoc Biol 73*, 556-563.

Fasshauer, D., Eliason, W. K., Brunger, A. T. and Jahn, R. (1998a). Identification of a minimal core of the synaptic SNARE complex sufficient for reversible assembly and disassembly. *Biochemistry 37,* 10354-10362.

Fasshauer, D., Sutton, R. B., Brunger, A. T. and Jahn, R. (1998b). Conserved structural features of the synaptic fusion complex: SNARE proteins reclassified as Q- and R-SNAREs. *Proc Natl Acad Sci U S A 95,* 15781-15786.

Feldmann, J., Callebaut, I., Raposo, G., Certain, S., Bacq, D., Dumont, C., *et al.* (2003). Munc13-4 is essential for cytolytic granules fusion and is mutated in a form of familial hemophagocytic lymphohistiocytosis (FHL3). *Cell 115,* 461-473.

Feldmann, J., Le Deist, F., Ouachee-Chardin, M., Certain, S., Alexander, S., Quartier, P., *et al.* (2002). Functional consequences of perforin gene mutations in 22 patients with familial haemophagocytic lymphohistiocytosis. *Br J Haematol 117,* 965-972.

Gay, D., Sekaly, R., Talle, MA., Godfrey, M., Long, E,. Goldstein, G., *et al.* (1987). Functional interaction between human T-cell protein CD4 and the major histocompatibility complex HLA-DR antigen. *Nature. 328*:626-9.

Garvin, SE., Koretzky, GA., and Jordan, MS. (2009). T Cell Activation. *Annu Rev Immunol. 27*:591-619

Geisler, C. (2004). TCR trafficking in resting and stimulated T cells. *Crit Rev Immunol 24,* 67-86.

Goldsby, R. A., Kindt, T. L., (2000). Kuby Immunology. 4th Edition, W H Freeman & Co (Sd).

Hahn, S., Gehri, R,. and Erb, P. (1995). Mechanism and biological significance of CD4-mediated cytotoxicity. *Immunol Rev 146*, 57-79.

Hatsuzawa, K., Hirose, H., Tani, K., Yamamoto, A., Scheller, R. H. and Tagaya, M. (2000). Syntaxin 18, a SNAP receptor that functions in the endoplasmic reticulum, intermediate compartment and cis-Golgi vesicle trafficking. *J Biol Chem 275*, 13713-13720.

Hayashi, T., McMahon, H., Yamasaki, S., Binz, T., Hata, Y., Sudhof, T. C. and Niemann, H. (1994). Synaptic vesicle membrane fusion complex: action of clostridial neurotoxins on assembly. *Embo J 13,* 5051-5061.

Helgason, C. D., Prendergast, J. A., Berke, G. and Bleackley, R. C. (1992). Culture hybridomas are cytolytic in the absence of cytotoxic cell proteinases and perforin. *Eur J Immunol.* 22, 3187–3190

Henter, J. I., Arico, M., Elinder, G., Imashuku, S. and Janka, G. (1998). Familial hemophagocytic lymphohistiocytosis. Primary hemophagocytic lymphohistiocytosis. *Hematol Oncol Clin North Am 12,* 417-433.

Hong, W. (2005). Cytotoxic T lymphocyte exocytosis: bring on the SNAREs! *Trends Cell Biol 15,* 644-650.

Horne, A., Ramme, K. G., Rudd, E., Zheng, C., Wali, Y., al-Lamki, Z., *et al.* (2008). Characterization of PRF1, STX11 and UNC13D genotype-phenotype correlations in familial hemophagocytic lymphohistiocytosis. Br J Haematol *143*, 75-83.

Huppa, J. B. and Davis, M. M. (2003). T-cell-antigen recognition and the IS. *Nat Rev Immunol 3,* 973-983.

Hurez, V., Saparov, A., Tousson, A., Fuller, M. J., Kubo, T., Oliver, J., *et al.* (2003). Restricted clonal expression of IL-2 by naïve T cells reflects differential dynamic interactions with dendritic cells. *J Exp Med 198,* 123-132.

Jahn, R., Lang, T. and Sudhof, T. C. (2003). Membrane fusion. *Cell 112,* 519-533.

Janka, G. E. (1983). Familial hemophagocytic lymphohistiocytosis. *Eur J Pediatr 140,* 221-230.

Janka, G. E. (2007). Familial and acquired hemophagocytic lymphohistiocytosis. *Eur J Pediatr 166,* 95-109.

Jenkins, M. R., Tsun, A., Stinchcombe, J. C. and Griffiths, G. M. (2009). The strength of T cell receptor signal controls the polarization of cytotoxic machinery to the IS. *Immunity 31,* 621-631.

Jewell, J. L., Oh, E. and Thurmond, D. C. (2010). Exocytosis mechanisms underlying insulin release and glucose uptake: conserved roles for Munc18c and Syntaxin 4. *Am J Physiol Regul Integr Comp Physiol 298,* R517-531.

Kawashima, R., Ikematsu, K., Abe, Y., Sato, M., Tsuruya, S., Nakasono, I., *et al*, (2010). Effect of glucocorticoid on the biosynthesis of growth hormone-containing secretory granules in pituitary cells. *Biochem Biophys Res Commun 400,* 225-229.

Kearse, K. P., Roberts, J. L. and Singer, A. (1995). TCR alpha-CD3 delta epsilon association is the initial step in alpha beta dimer formation in murine T cells and is limiting in immature CD4+ CD8+ thymocytes. *Immunity 2,* 391-399.

Kennedy, M. J., Davison, I. G., Robinson, C. G. and Ehlers, M. D. (2010). Syntaxin-4 defines a domain for activity-dependent exocytosis in dendritic spines. Cell *141*, 524-535.

Kesavan, J., Borisovska, M. and Bruns, D. (2007). v-SNARE actions during Ca(2+)-triggered exocytosis. *Cell 131,* 351-363.

Krammer, P. H. (2000). CD95's deadly mission in the immune system. *Nature 12,* 789-95.

Kummerow, C., Junker, C., Kruse, K., Rieger, H., Quintana, A. and Hoth, M. (2009). The IScontrols local and global calcium signals in T lymphocytes. *Immunol Rev, 231.*132-47.

Li, W., Zhang, Q., Oiso, N., Novak, E. K., Gautam, R., O'Brien, E. P., *et al.* (2003). Hermansky-Pudlak syndrome type 7 (HPS-7) results from mutant dysbindin, a member of the biogenesis of lysosome-related organelles complex 1 (BLOC-1). *Nat Genet 35*, 84-89.

Logan, M. R., Odemuyiwa, S. O. and Moqbel, R. (2003). Understanding exocytosis in immune and inflammatory cells: the molecular basis of mediator secretion. *J Allergy Clin Immunol 111,* 923-932.

Lopez, J. A. and Voskoboinik, I. (2013). Deciphering the syntax of cytotoxic lymphocyte degranulation. *Eur J Immunol 43,* 46-49.

Low, S. H., Vasanji, A., Nanduri, J., He, M., Sharma, N., Koo, M., Drazba, J. and Weimbs, T. (2006). Syntaxins 3 and 4 are concentrated in separate clusters on the plasma membrane before the establishment of cell polarity. *Mol Biol Cell 17,* 977-989.

Lowin, B., Beermann, F., Schmidt, A. and Tschopp, J. (1994). A null mutation in the perforin gene impairs cytolytic T lymphocyte- and natural killer cell-mediated cytotoxicity. *Proc Natl Acad Sci U S A 91,* 11571-11575.

Macartney, C. A., Weitzman, S., Wood, S. M., Bansal, D., Steele, M., Meeths, M., *et al.* (2011). Unusual functional manifestations of a novel STX11 frameshift mutation in two infants with familial hemophagocytic lymphohistiocytosis type 4 (FHL4). *Pediatr Blood Cancer 56,* 654-657.

Marsh, R. A., Satake, N., Biroschak, J., Jacobs, T., Johnson, J., Jordan, M. B., *et al.* (2010). STX11 mutations and clinical phenotypes of familial hemophagocytic lymphohistiocytosis in North America. *Pediatr Blood Cancer 55,* 134-140.

Menager, M. M., Menasche, G., Romao, M., Knapnougel, P., Ho, C. H., Garfa., *et al.* (2007). Secretory cytotoxic granule maturation and exocytosis require the effector protein hMunc13-4. *Nat Immunol 8,* 257-267.

Menasche, G., Pastural, E., Feldmann, J., Certain, S., Ersoy, F., Dupuis, S., *et al.* (2000). Mutations in RAB27A cause Griscelli syndrome associated with haemophagocytic syndrome. *Nat Genet 25,* 173-176.

Mentlik, K. B., Sanborn, E. L., Holzbaur, a. and Orange, J. S. (2010). Rapid Lytic Granule Convergence to the MTOC in Natural Killer Cells Is Dependent on Dynein But Not Cytolytic Commitment. *Mol Biol Cell. 21:*2241-56

Muppirala, M., Gupta, V. and Swarup, G. (2011). Syntaxin 17 cycles between the ER and ERGIC and is required to maintain the architecture of ERGIC and Golgi. *Biol Cell 103*, 333-350.

Murray, R. Z., Wylie, F. G., Khromykh, T., Hume, D. A. and Stow, J. L. (2005). Syntaxin 6 and Vti1b form a novel SNARE complex, which is up-regulated in activated macrophages to facilitate exocytosis of tumor necrosis Factor-alpha. *J Biol Chem 280,* 10478-10483.

Nagata, S. (1996). Fas-mediated apoptosis. *Adv Exp Med Biol 406,* 119-124.

Neeft, M., Wieffer, M., de Jong, A. S., Negroiu, G., Metz, C. H., van Loon, A., *et al.* (2005). Munc13-4 is an effector of rab27a and controls secretion of lysosomes in hematopoietic cells. *Mol Biol Cell 16,* 731-741.

O'Keefe, J. P. and Gajewski, T. F. (2005). Cutting edge: cytotoxic granule polarization and cytolysis can occur without central supramolecular activation cluster formation in CD8+ effector T cells. *J Immunol 175,* 5581-5585.

Offenhauser, C., Lei, N., Roy, S., Collins, B. M., Stow, J. L. and Murray, R. Z. (2011). Syntaxin 11 binds Vti1b and regulates late endosome to lysosome fusion in macrophages. *Traffic 12,* 762-773.

Ogawa, M. (1993). Differentiation and Proliferation of Hematopoietic Stem Cells. Blood *81,* 2844-53.

Orange, J. S. (2008). Formation and function of the lytic NK‑cell IS. *Nat Rev Immunol 8,* 713–725.

Orkin, S. H. (2000). Diversification of haematopoetic stem cells to specific lineages. *Nat Rev Genetics 1,* 57-64.

Osugi, Y., Hara, J., Tagawa, S., Takai, K., Hosoi, G., Matsuda, Y., *et al.* (1997). Cytokine production regulating Th1 and Th2 cytokines in hemophagocytic lymphohistiocytosis. *Blood 89,* 4100-4103.

Pattu, V., Qu, B., Marshall, M., Becherer, U., Junker, C., Matti, U., Schwarz, E. C., Krause, E., Hoth, M. and Rettig, J. (2011). Syntaxin7 is required for lytic granule release from cytotoxic T lymphocytes. *Traffic 7,* 890-901

Peter, ME. and Krammert, PH. (1998). Mechanisms of CD95 (APO-1/Fas)-mediated apoptosis. *Current Opinion in Immunology. 10:*545-51.

Prekeris, R., Klumperman, J. and Scheller, R. H. (2000). Syntaxin 11 is an atypical SNARE abundant in the immune system. *Eur J Cell Biol 79,* 771-780.

Prekeris, R., Yang, B., Oorschot, V., Klumperman, J. and Scheller, R. H. (1999). Differential roles of Syntaxin 7 and Syntaxin 8 in endosomal trafficking. *Mol Biol Cell 10,* 3891-3908.

Qu, B., Pattu, V., Junker, C., Schwarz, E. C., Bhat, S. S., Kummerow, C., *et al.* (2011). Docking of lytic granules at the IS in human CTL requires Vti1b-dependent pairing with CD3 endosomes. *J Immunol 186,* 6894-6904.

Ravichandran, V., Chawla, A. and Roche, P. A. (1996). Identification of a novel Syntaxin- and synaptobrevin/VAMP-binding protein, SNAP-23, expressed in non-neuronal tissues. *J Biol Chem 271,* 13300-13303.

Reiner, S. (2009). Decision making during the conception and career of CD4+ T cells. *Nat Rev Immunol 2,* 81-2.

Riento, K., Galli, T., Jansson, S., Ehnholm, C., Lehtonen, E. and Olkkonen, V. M. (1998). Interaction of Munc18-2 with Syntaxin 3 controls the association of apical SNAREs in epithelial cells. *J Cell Sci 111*, 2681-2688.

Risma, K. A., Frayer, R. W., Filipovich, A. H. and Sumegi, J. (2006). Aberrant maturation of mutant perforin underlies the clinical diversity of hemophagocytic lymphohistiocytosis. *J Clin Invest 116,* 182-192.

Rudd, E., Ericson, K., Zheng, C., Uysal, Z., Ozkan, A., Gurgey, A., *et al.* (2006). Spectrum and clinical implications of Syntaxin 11 gene mutations in familial haemophagocytic lymphohistiocytosis: association with disease-free remissions and haematopoietic malignancies. *J Med Genet 43,* e14.

Schmid, P. J., Ho, C. H., Diana, J., Pivert, G., Lehuen, A. and Geissmann, F., *et al.* (2008). A Griscelli syndrome type 2 murine model of hemophagocytic lymphohistiocytosis (HLH). *Eur J Immunol 38,* 3219-3225.

Schneider, E. M., Lorenz, I., Muller-Rosenberger, M., Steinbach, G., Kron, M. and Janka-Schaub, G. E. (2002). Hemophagocytic lymphohistiocytosis is associated with deficiencies of cellular cytolysis but normal expression of transcripts relevant to killer-cell-induced apoptosis. *Blood 100,* 2891-2898.

Seabra, M. C. and Wasmeier, C. (2004). Controlling the location and activation of Rab GTPases. *Curr Opin Cell Biol 16,* 451-457.

Shiffman, D., Rowland, C. M., Louie, J. Z., Luke, M. M., Bare, L. A., Bolonick, J. I., *et al.* (2006). Gene variants of VAMP8 and HNRPUL1 are associated with early-onset myocardial infarction. *Arterioscler Thromb Vasc Biol 26,* 1613-1618.

Sieber, J. J., Willig, K. I., Heintzmann, R., Hell, S. W. and Lang, T. (2006). The SNARE motif is essential for the formation of Syntaxin clusters in the plasma membrane. *Biophys J 90,* 2843-2851.

Sollner, T., Bennett, M. K., Whiteheart, S. W., Scheller, R. H. and Rothman, J. E. (1993). A protein assembly-disassembly pathway in vitro that may correspond to sequential steps of synaptic vesicle docking, activation and fusion. *Cell 75,* 409-418.

Stenmark, H. (2009). Rab GTPases as coordinators of vesicle traffic. *Nat Rev Mol Cell Biol 10,* 513-525.

Stow, J. L., Mander'son, A. P. and Murray, R. Z. (2006). SNAREing immunity: the role of SNAREs in the immune system. *Nat Rev Immunol 6,* 919-929.

Sutton, R. B., Fasshauer, D., Jahn, R. and Brunger, A. T. (1998). Crystal structure of a SNARE complex involved in synaptic exocytosis at 2.4 A resolution. *Nature 395,* 347-353.

Takada, K. and Jameson, S. C. (2009). Naïve T cell homeostasis: from awareness of space to a sense of place. *Nat Rev Immunol 9,* 823-832

Tanchot, B. R. (1995). The peripheral T cell repertoire: independent homeostatic regulation of virgin and activated CD8 T cells. *Eur J Immunol. 25:*2127-36.

Tang, B. L., Low, D. Y. and Hong, W. (1998a). Syntaxin 11: a member of the Syntaxin family without a carboxyl terminal transmembrane domain. *Biochem Biophys Res Commun 245,* 627-632.

Tang, B. L., Low, D. Y., Lee, S. S., Tan, A. E. and Hong, W. (1998b). Molecular cloning and localization of human Syntaxin 16, a member of the Syntaxin family of SNARE proteins. *Biochem Biophys Res Commun 242,* 673-679.

Teng, F. Y., Wang, Y. and Tang, B. L. (2001). The Syntaxins. *Genome Biol, REVIEWS* 3012.

Tipping, P. G. (2006). Toll-Like Receptors: The Interface between Innate and Adaptive Immunity. *Journal of the American Society of Nephrology 7,* 1769-1771.

Valdez, A. C., Cabaniols, J. P., Brown, M. J. and Roche, P. A. (1999). Syntaxin 11 is associated with SNAP-23 on late endosomes and the trans-Golgi network. *J Cell Sci 112,* 845-854.

Voskoboinik, I., Smyth, M. J. and Trapani, J. A. (2006). Perforin-mediated target-cell death and immune homeostasis. *Nat Rev Immunol 6,* 940-952.

Wang, Y., Tai, G., Lu, L., Johannes, L., Hong, W. and Tang, B. L. (2005). Trans-Golgi network Syntaxin 10 functions distinctly from Syntaxins 6 and 16. *Mol Membr Biol 22,* 313-325.

Wong, S. H., Xu, Y., Zhang, T. and Hong, W. (1998). Syntaxin 7, a novel Syntaxin member associated with the early endosomal compartment. *J Biol Chem 273,* 375-380.

Xie, L. X., de la Iglesia-Vicente, J., Fang, Y. X. and Mollinedo, F. (2009). Expression and subcellular localization of Syntaxin 11 in human neutrophils. *Inflamm Res 58,* 407-412.

Ye, S., Karim, Z. A., Al Hawas, R., Pessin, J. E., Filipovich, A. H. and Whiteheart, S. W. (2012.) Syntaxin-11, but not Syntaxin-2 or Syntaxin-4, is required for platelet secretion. *Blood 120,* 2484-2492.

Zhang, B. and Ginsburg, D., (2003). Getting secretory granules ready for prime time. *Cell 115,* 372-373.

Zhang, K., Filipovich, A. H., Johnson, J., Marsh, R. A. and Villanueva, J. (1993). Hemophagocytic Lymphohistiocytosis, Familial. *Bookshelf* ID: NBK1444

Zhang, S., Ma, D., Wang, X., Celkan, T., Nordenskjold, M., Henter, J. I., Fadeel, B. and Zheng, C. (2008). Syntaxin-11 is expressed in primary human monocytes/macrophages and acts as a negative regulator of macrophage engulfment of apoptotic cells and IgG-opsonized target cells. *Br J Haematol 142,* 469-479.

Zhizhuo, H., Junmei, X., Yuelin, S., Qiang, Q., Chunyan, L., Zhengde, X. and Kunling, S. (2012). Screening the PRF1, UNC13D, STX11, SH2D1A, XIAP and ITK gene mutations in Chinese children with Epstein-Barr virus-associated hemophagocytic lymphohistiocytosis. *Pediatr Blood Cancer 58,* 410-414.

Zur Stadt, U., Beutel, K., Kolberg, S., Schneppenheim, R., Kabisch, H., Janka, G. and Hennies, H. C. (2006). Mutation spectrum in children with primary hemophagocytic lymphohistiocytosis: molecular and functional analyses of PRF1, UNC13D, STX11 and RAB27A. *Hum Mutat 27,* 62-68.

zur Stadt, U., Rohr, J., Seifert, W., Koch, F., Grieve, S., Pagel, J., Strauss, J., Kasper, B., Nurnberg, G., Becker, C.*, et al.* (2009). Familial hemophagocytic lymphohistiocytosis type 5 (FHL-5) is caused by mutations in Munc18-2 and impaired binding to Syntaxin 11. *Am J Hum Genet 85,* 482-492.

zur Stadt, U., Schmidt, S., Kasper, B., Beutel, K., Diler, A. S., Henter, J. I., Kabisch, H., Schneppenheim, R., Nurnberg, P., Janka, G. and Hennies, H. C. (2005). Linkage of familial hemophagocytic lymphohistiocytosis (FHL) type-4 to chromosome 6q24 and identification of mutations in Syntaxin 11. *Hum Mol Genet 14,* 827-834.

8. CURRICULUM VITAE

Personal information

Name: Mahantappa Halimani

Date of birth: 1st June 1983

Place of birth: Chinamagera, India

Marital status: Single

Education

2005   Master degree in Biotechnology at Gulbarga University, India

2003   Bachelor degree in Chemistry Botany and Zoology at Gulbarga University, India

Research experience

July 2009-current   PhD at University of Saarland, under the supervision of Prof Jens Rettig, Physiologisches Institut.

2007-2009   Research associate CSIR Lab Institute of Genomics and Integrative Biology (IGIB), Delhi, India

2005-2007   Trainee and Quality Control manager at Cryostem Cell Pvt Ltd, Bangalore, India.

9. PUBLICATIONS

Published:

1. Matti U*, Pattu V*, **Halimani M**, Schirra C, Krause E, Liu Y, Weins L, Chang HF, Guzman R, Olausson J, Freichel M, Schmitz F, Pasche M, Becherer U, Bruns D & Rettig J. Synaptobrevin2 is the v-SNARE required for cytotoxic T lymphocyte lytic granule fusion. *Nat. Commun.* 4: 1439 doi: 10.1038/ncomms2467 (2013). PMID: 23385584
   *equal contribution

2. Bargaje R, Gupta S, Sarkeshik A, Park R, Xu T, Sarkar M, **Halimani M**, Roy SS, Yates J, Pillai B. Identification of Novel Targets for miR-29a Using miRNA Proteomics. *PLoS One.* 2012; 7(8):e43243. Epub 2012 Aug 27.PMID: 22952654

3. Pattu V*, Qu B*, Weins L, Shruthi SB, Marshall M, **Halimani M**, Schwarz EC, Rettig J, Hoth M. SNARE protein expression and localization in human cytotoxic T lymphocytes. *European Journal of Immunology.* 2012 Feb; 42(2):470-475. PMID: 22120889
   *equal contribution

4. **Halimani M,** Chandran P, Kashyap S, Jadhav V. M, Prasad LV, Hotha S, Maiti S. Dendritic Effect of Ligand-Coated Nanoparticles: Enhanced Apoptotic Activity of Silica−Berberine Nanoconjugates.
   Langmuir 2009 25 (4), 2339-2347. PMID: 19146398.

5. Ghosh T, Soni K, Scaria V, **Halimani M**, Chaitali B, Pillai B.MicroRNA mediated up regulation of an alternatively polyadenylated variant of the mouse cytoplasmic ß-actin gene. *Nucleic Acids Res* (2008).*1-15.* PMID: 18835850.

6. **Halimani M**, Banik A, Shivshankar J, Rao S G A. The Stem Cells in the Umbilical cord blood is not related to the volume and nucleated cell count. *Indian J Biotechnology.* 2008 (*7), 547-549*

Communicated:

1. **Halimani M,** Pattu V, Chang HF, Matti U, Becherer U, Krause E, Hoth M & Rettig J. Syntaxin11 serves as a t-SNARE for the final fusion step of lytic granules in human cytotoxic T lymphocytes. Feb 2013, Under Revision in *Blood.*

2. Hugo S, Dembla D, Peglow M, **Halimani M**, Matti U, Rieger H, Rettig J, Becherer U. Deciphering dead-end docking of large dense core vesicles in chromaffin cells. In preparation for submission to *JBC* in Feb 2013.

3. Marshall MR, Pattu V, **Halimani M**, Maier-Peuschel, Tschernig T, M, Hoth M, Rettig J. VAMP8 is the v-SNARE mediating recycling endosome fusion in CD3/CD28 mediated granule exocytosis of T lymphocytes. In submission to *Nat Immunology.*

4. Dudenhöffer-Pfeifer M, Marshall MR, **Halimani M**, Schirra C, Stevens D, Sester M, Planz O, , Hoth M, Krause E, Rettig J. Different Munc13 isoforms function in lytic granule release from cytotoxic T lymphocytes. Revise and resubmit in *Traffic Journal.*